

COMPUTER AIDED ANALYSIS AND MODELLING

OF WIRE DRAWING

A MASTER'S THESIS

in

MECHANICAL ENGINEERING

MIDDLE EAST TECHNICAL UNIVERSITY

T. C.
Yükseköğretim Kurulu
Dokümantasyon Merkezi

By

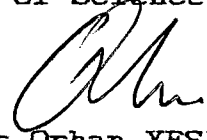
CIHAT AKSOY

SEPTEMBER 1987

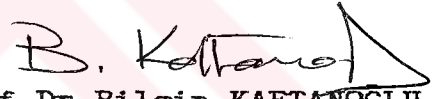
Approval of the Graduate School of Natural and Applied Sciences.


Prof. Dr. Halim DOĞRUSÖZ
Director

I certify that this thesis satisfies all the requirements as a thesis for the degree of Master of Science in Mechanical Engineering.


Prof. Dr. Orhan YESİN
Chairman of the Department

We certify that we have read this thesis and that in our opinion it is fully adequate, in scope and quality as a thesis for the degree of Master of Science in Mechanical Engineering.


Prof. Dr. Bilgin KAFTANOĞLU
Supervisor

Examining Committee in Charge:

Assoc. Prof. Dr. Metin Akkök (Chairman)



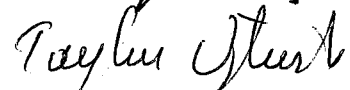
Prof. Dr. Bilgin Kaftanoğlu



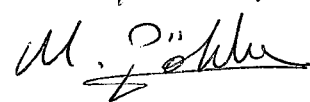
Assoc. Prof. Dr. Orhan Yıldırım



Assoc. Prof. Dr. Tayfur Öztürk



Asst. Prof. Dr. Mustafa Gökler



ABSTRACT

COMPUTER AIDED ANALYSIS AND MODELLING OF WIRE-DRAWING

Cihat Aksoy

M.S. in Mechanical Engineering

Supervisor: Prof. Dr. Bilgin Kaftanoglu

September 1987, 160 Pages

In connection with the formability of metals, the process of wire-drawing has been the subject of extensive theoretical and experimental investigations. An exact theory of wire-drawing has not yet been realized and all the theories make some assumptions about the deformation and the extent of the plastic region. In the complete solution of the problem the stresses and the mode of deformation must be compatible, as yet, no axisymmetric problems have been exactly solved.

This thesis is concerned with the development of the theory for wire-drawing and presents a further development for the analysis and modelling of the process. Since the deformation is not homogenous and extra work is expended in distortions which do not contribute to the final reduction in diameter, i.e., as redundant deformation, in the modelling technique the effects of the shearing in the entire plastic region is included.

Governing plasticity equations plus the material behaviour and the mode of deformations are all inherently non-linear in form. These lead to a mathematical problems which is rather intractable for an analytical solution. This makes the use of numerical methods to be inevitable. A numerical algorithm is developed to determine the plastic stresses and resulting deformations in the drawing region. It consists of a finite difference technique which solves the

plasticity equations to compute the space variation of the stresses and strains. The problem is treated as a three-dimensional stress-strain case for an anisotropic and strain-hardening material model.

Detailed description of the development of the theory and the algorithm for the numerical method of solution are presented. The analytical solution is also obtained by using Sachs, Siebel and Whitton equations, to compare with the numerical solution.



Key Words: Wire-drawing, plastic deformation, numerical solution

ÖZET

TEL-ÇEKME İŞLEMİNİN BİLGİSAYAR YARDIMIYLA ANALİZİ VE MODELLEŞTİRİLMESİ

Cihat Aksoy

Master tezi; Mak. Müh. Bölümü

Tez Yöneticisi: Prof. Dr. Bilgin Kaftanoğlu

Eylül 1987 , 160 Sayfa

Malzemelerin şekillendirilmesi yöntemlerinden tel-çekme işlemi, birçok teorik ve deneysel araştırmaya konu olmuştur. Geliştirilen tüm teorilerde plastik bölgedeki şekil değiştirmeler konusunda birtakım varsayımlar yapılmış ve tam bir teori henüz geliştirilmemiştir. Problemin tamamlanmış çözümünde gerilimler ve şekil değiştirmeler birbirleriyle uyumlu olmalıdırlar ki; henüz aksel simetrik böylesi problemler çözümlenmemiştir.

Bu tez, tel-çekme işlemine ilişkin teorisinin geliştirilmesini konu almakta ve işlemin yeni bir model oluşturularak analizi için ileri bir adım teşkil etmektedir. Model oluşturulurken; plastik bölgedeki tüm şekil değiştirmelerin aynı olmaması, fazladan iş harcanmasını gerektiren ve tel çapının azaltılmasına herhangi bir faydası olmayan şekil değiştirmelerin (redundant deformation) bulunması nedeniyle kayma birim-şekil değiştirmeler de dikkate alınmıştır.

Plastisite denklemleri, malzeme davranışları ve plastik şekil değiştirmeler doğrusal olmayan bir yapıya sahiptirler. Bu yapıya sahip matematiksel bir problemin ise analitik çözümünü kontrol etmek mümkün değildir. Bu durumda sayısal çözüm metodlarının kullanımı kaçınılmazdır.

Bu çalışmada da çekme bölgesindeki plastik gerilim ve şekil değiştirmelerin bulunması için sayısal bir çözüm

geliştirilmiştir. Sayısal çözüm, sonlu farklar yöntemini kullanmakta ve plastisite denklemleri aracılığı ile tel-çekme bölgesindeki gerilme ve birim şekil değiştirmeleri konuma bağlı olarak incelemektedir. Problem üç boyutlu bir gerilme problemi olarak ele alınmış, izotropik olmayan ve şekil değiştirme ile pekleşen bir malzeme modeli kullanılmıştır.

Bu tezde, tel-çekme işlemi için geliştirilen teori, çözüm yöntemleri ve elde edilen bulgular anlatılmakta, ayrıca karşılaştırma amacı ile Sachs, Siebel ve Whitton denklemleri kullanılarak analitik çözüm elde edilmektedir.

Anahtar kelimeler: Tel çekme, plastik şekil-değiştirme,
sayısal çözüm

ACKNOWLEDGEMENT

I am sincerely thankful in many respects to my Supervisor Prof. Dr. Bilgin Kaftanoglu. His great experience, deep insight and knowledge, together with friendly comments and very kind personality comprised the only source of encouragement for me during my desperate instants throughout my studies. His advice and discussions on my studies were invaluable and indispensable for the completion of this work. Without his kind help and many hours of overtime that he willingly spent, the thesis could not be finalized as it appears now, therefore I am dedicating this thesis to Prof. Dr. Bilgin Kaftanoglu alone and would like to express my thanks here once more...

TABLE OF CONTENTS

	<u>Page</u>
ABSTRACT	iii
OZET	v
ACKNOWLEDGEMENT	vii
TABLE OF CONTENTS	viii
LIST OF TABLES	xi
LIST OF FIGURES	xii
NOMENCLATURE	xiv
CHAPTER	
I. INTRODUCTION	1
1.1. Wire-Drawing Die	2
1.2. Lubrication in Wire-Drawing Process	4
1.3. Industrial Applications	6
II. SURVEY OF LITERATURE	8
2.1 Historical Background of Plasticity Theory	8
2.1.1. Theoretical Studies	8
2.1.2. Experimental Studies	10
2.1.3. Progress in Methods of Solutions	11
2.2. Investigations on Wire-Drawing	15
2.2.1. Theoretical and Experimental Studies	15

	<u>Page</u>
III.OBJECT OF PRESENT INVESTIGATION	25
IV.THEORY	27
4.1. Basic Equations of Plasticity	27
4.1.1. Plastic Yield Criteria	28
4.1.2. Definition of Plastic Strains	31
4.1.3. Constancy of Volume	37
4.1.4. Plastic Flow Rule for Anisotropic Material	38
4.1.5. Generalized Stress and Strain Relations for Anisotropic Work-Hardening material	42
4.1.6. Laws of material hardening	43
4.1.7. Stress equations of equilibrium in curvilinear coordinates	46
4.2. Analytical Analysis of Wire-Drawing Process	59
4.2.1. Derivation of Equations	62
4.3. Numerical Solution of the Drawing region	68
4.3.1. Boundary conditions	68
4.3.2. Formulation of the problem	70
V.DESCRPTION OF THE COMPUTER PROGRAM FOR THE NUMERICAL SOLUTION	84
5.1. Computer Algorithm	84
5.2. Sample Solution	93
5.3. Program Properties	94
VI.DESCRPTION OF THE COMPUTER PROGRAM FOR THE ANALYTICAL SOLUTION	96
6.1. Computer Algorithm	96

	<u>Page</u>
6.2. Sample Solution	98
VII. RESULTS AND DISCUSSIONS	99
7.1. Numerical results	99
7.2. Discussions	99
VIII. CONCLUSIONS	102
LIST OF REFERENCES	104
APPENDICES	111
A. Polynomial fit to discrete nodal points	112
B. Binary chopping and inverse interpolation method to determine the root of a function	116
C. Numerical integration	120
D. The numerical solution of ordinary differantial equation	123
E. Sample numerical and graphical outputs for analytical solution	124
F. Sample numerical and graphical outputs for numerical solution	

LIST OF TABLES

<u>Table</u>	<u>Page</u>
1.1 Typical values of coefficient of friction in Wire-Drawing	5
4.1 Normal and shear stresses acting on faces of a three dimensional curvilinear element	56



LIST OF FIGURES

<u>Figure no.</u>	<u>Page</u>
1.1 Notation in a wire-drawing process	7
4.1 An elastically deforming element under pure shear	33
4.2 Plastic, incremental shear strain nomenclature for a largely deforming grid element	35
4.3 A curvilinear element in two dimension (plain stress)	47
4.4 A curvilinear element in three dimensions	49
4.5 Stress nomenclature for a three dimensional curvilinear element	54
4.6 Radius of curvature and stress nomenclature for a deforming element in wire-drawing process	57
4.7 Variation of mean die pressure with reduction	61
4.8 Variation of drawing force with reduction	61
4.9 Sketch of wire drawing showing forces applied to strips of infinitesimal length	62
4.10 External forces acting during wire-drawing	65
4.11 Solution along a pair of α and β -lines for the unknown point A	74
4.12 Computer program layout for axial symmetry line	79
5.1 Sign convention for radius of curvature along a β -line	86
5.2 Computer program layout for numerical solution	92
6.1 Computer program layout for analytical solution	97
B.1 Determination of the root of a function	116
E.1 Drawing stress, mean die pressure, splitting force and drawing force versus reduction in area diagrams	127
E.2 Drawing stress versus reduction in area graphics	128
E.3 Drawing force versus reduction in area	129
E.4 Mean die pressure versus reduction in area	130
E.5 Splitting force versus reduction in area	131
F.1 Original grid lines along α and β lines	141

<u>Figure no</u>	<u>Page</u>
F.2 Grid lines after deformation	142
F.3 Drawing stress along α -direction	143
F.4 Radial stress along α -direction	144
F.5 Circumferantal stress along α -direction	145
F.6 Shear stress along α -direction	146
F.7 Drawing stress along β -direction	147
F.8 Radial stress along β -direction	148
F.9 Circumferantal stress along β -direction	149
F.10 Shear stress along β -direction	150
F.11 Drawing strain along α -direction	151
F.12 Radial strain along α -direction	152
F.13 Circumferantal strain along α -direction	153
F.14 Shear strain along α -direction	154
F.15 Drawing strain along β -direction	155
F.16 Radial strain along β -direction	156
F.17 Circumferantal strain along β -direction	157
F.18 Shear strain along β -direction	158
F.19 Drawing force along α -direction	159
F.20 Die splitting force along α -direction	160

NOMENCLATURE

<u>Symbol</u>	<u>Meaning</u>
A	Proportional factor in Swift's strain hardening law, cross-sectional area.
B	Pre-strain in Swift's strain-hardening law.
c	Any constant.
D	Diameter.
du, dv	Incremental trial displacements imposed to a nodal point along x and y axes respectively.
$d\lambda, \delta\lambda$	Proportionality factor of the plastic flow rule.
E	Young's moduli of elasticity.
e	Engineering strain.
e_L	Lagrangian strain.
e_E	Eulerian strain.
F	Force.
G	Modulus of rigidity.
I_1, I_2, I_3	Invariants of the stress tensor P

<u>Symbol</u>	<u>Meaning</u>
i	Step number along the row of grid matrix (x-direction)
J	Step number along the column of grid matrix (y-direction)
K	Stress ratio ($P_{\beta\beta} / P_{\alpha\alpha}$)
k	Yield constant.
L, l	Length.
MN	Number of grid nodes in x-direction.
NG	Number of grid nodes in x-direction.
NS	Index of deformation stage.
n	Exponent of strain-hardening rule.
P	Normal stress component, Principal stress.
\bar{P}	Equivalent stress.
p	Hydrostatic stress ($1/3 P_{ii}$)
R	Coefficient of anisotropy.
r	Radius of curvature.
S	Slope of a curvilinear line at a given point.

<u>Symbol</u>	<u>Meaning</u>
SS	Slope of a straight line.
W	Work done per unit volume.
ω	Rigid body rotation.
X	Stress ratio ($P_{\beta\beta} / P_{\alpha\alpha}$)
x	Axis of an orthogonal rectangular coordinate system fixed in space.
Y	Yield stress.
y	Axis of an orthogonal rectangular coordinate system fixed in space
Z	Stress ratio ($P_{\beta\alpha} / P_{\alpha\alpha}$)

<u>Superscripts</u>	<u>Meaning</u>
e	Elastic
p	Plastic.
*	Variation associated with time
.	Time rate of change of a variable ($d.../dt$)
~	Average.
^	Unit value of a variable.

<u>Subscripts</u>	<u>Meaning</u>
f	Final.
i, j	Row, column in grid matrix.
i, j, k	Direction code along x(α) and y(β) direction, indices for tensorial notation of a variable.
n	Normal.
o	Original.
p	Plastic.
t	Total.

<u>Greek Symbols</u>	<u>Meaning</u>
α	Die-cone angle
α, β, γ	Curvilinear co-ordinates in x-y plane.
γ	Shear strain(Engineering)
μ	Coefficient of friction.
δ	Suffix for incremental variations.
Δ	Suffix for small variations.
ϵ	Logarithmic strain.
$\bar{\epsilon}$	Equivalent strain.

<u>Greek Symbols</u>	<u>Meaning</u>
τ	Shear stress component
ρ	Radius of curvature.
θ	Angle of twist.
ϕ	Angle of rotation, angle on Mohr circle { $\tan^{-1}(P_{\beta\beta} / P_{\beta\alpha})$ }.
ψ	Shear angle at one side of the deformed element, angle of spin.

CHAPTER I

INTRODUCTION

Wire-drawing is the process whereby wire is progressively reduced in cross-section by pulling it through dies to produce a wire of a specified size and shape. Circular wire is most often drawn. The reduction is achieved by using a die with a tapered bore.

The pull on the wire at exit from the die, and the pressure developed between the wire and conical surface of the die (the "nip" of the die) are sufficient together to stress the metal so that it is plastic within the confines of the die.

The reduction in size per pass is limited by the amount of pull that can be applied without breaking the wire, so that many passes have usually made. The drawing process starts from "wire rod" conventionally at 5 S.W.G. (5.220 mm) but lately the trend has been to thicker rod up to 5/16 in (7.94 mm) diameter. Wire as fine as 0.0004 in. (0.11 mm) in diameter is drawn. The reduction of cross-sectional area per pass is generally within 10-45 percent where percentage reduction is defined as $(1 - A_2/A_1) \times 100$, A_1 being the initial A_2 the final cross sectional area of the wire, with 15-25 percent prevalent in the drawing of the fine wires, and 20-45 percent preferred for the coarser sizes. The progressive reductions are usually made in tandem on "multi-hole" wire drawing machines which may have from 5 to 21 dies. The pull for each die is supplied by a rotating capstan, which may also serve as a storage drum to reconcile the output from one die with the input to the next [1]. For example, the manufacture of 0.001 in diameter copper wire from 1/4 in. hot rolled rod may involve some fifty consecutive passes. Drawing speeds range from 100 to 8000 ft/min, depending on size and metal and the particular pass of a continuous machine [2]. Since wire drawing is a cold-forming process, an intermediate anneal is often required before the

final diameter is reached. Controlled atmosphere furnaces are common equipment in a wire-drawing plant. The hardness and ductility of the finished wire are controlled by the amount of reduction effected from the last recrystallization anneal to final product. Final heat treatment and coating can be given to the wire if desired [3]. In the early days the shaping and hardening of the dies, and the choice of successive passes to give maximum reduction without annealing or breaking the wire were closely-guarded secrets. Later these practical limitations became translated into the standard wire gauges. Modern practice enables the same reductions to be achieved in fewer passes, owing to improvements in quality of the wire, hardness and accuracy of dies and reduction in friction [1].

1.1 Wire Drawing Die

The total die angle can have values between 5° and 25° and the length of the cylindrical portion varies from nil to two wire diameters. A total die angle of less than 15° has been considered safe against the defect even with the lightest reductions [4]. The use of a bearing (short cylindrical extension of the die cone) has been recommended. The single pass wire drawing tests give evidence of the two stages (crack nucleation and crack propagation) of any ductile fracture with high values for the die angles and slight reductions internal axial defects were developed but fracture did not occur. Fracture took place when the die angle exceeded 24° and for intermediate reductions. Without back tension a draft of 33% reduction and $\Delta=2.6$ (ratio of the circular arc spanning the midpoints of the die face to the length of contact between wire and die) did not produce fracture; it was reasoned that nucleation was not possible due to the low hydrostatic tension. When the same draft was done under back-tension the wire fractured because nucleation was then possible.

In industrial practice, the die has a trumpet-shaped bore, but since the curvature near the working surface is small, this may be simplified here into a conical portion which serves to deform the wire and a cylindrical portion which is meant to preserve the size of the bore in the face of wear. Different materials are used for dies [3]. For the larger dimensions, economic considerations dictate the use of hardened tool steels. Medium sizes are made of carbides. For the very small sizes ultimate hardness and wear resistance are required, and diamond dies are used. Diamond, the hardest known material, is one hundred times as hard as aluminium and twenty-six times as hard as steel; its use dates from 1819, when its advantages for the drawing of wire first became known [5]. Diamond dies are now used almost exclusively for the drawing of fine wire, while heavier gauge round and shaped wire is generally drawn with tungsten carbide tools. Refractory materials are becoming more common as they are made tougher, more resistant to breakage, and less expensive. Also, dies of steel can now be lined with hard refractory material on the working faces to combine the wear resistance of the lining with the toughness of the steel support and with minimum use of the more expensive refractory. Thus larger and larger diameters can benefit from the advantages of refractory materials. Refractory materials of higher and higher hardness and wear resistance qualities are being developed. Since they are cheaper than diamonds, they are used for still smaller and smaller diameters. After a die has been worn on its conical face, it is ground or polished to restore its geometry and smoothness for further use. As the cylindrical portion is worn, the die is ground and polished, increasing the size to the next diameter, and used again. Quite specialized equipment is used in the production and maintenance of drawing dies. (Figure. 1.1)

1.2 Lubrication in Wire-Drawing Process

The two main problems in controlling the wire drawing process are removing the heat developed by plastic deformation and friction, and wear of the dies, which effects size and shape. Lubrication is therefore important. Traditionally the two principal methods are "wet" and "dry" drawing, which differ as regards preparation of wire, lubrication, and design of machine. In wet drawing, the entire drawing apparatus is usually submerged in a bath of liquid or and the wire is allowed to slip on the drawing capstans [2] [6]. In dry drawing, soap powders, picked up by the moving wire from a container placed ahead of the die, are commonly employed as lubricants, and the capstans are lapped by the wire a sufficient number of times to ensure that no tangential slip occurs. Fine wires, i. e. below, say, $1/32$ in. in diameter, are invariably drawn wet, and so is copper and its alloys in all sizes. The dry method is prevalent in the drawing of most other metals and alloys, from rod to intermediate sizes (though much aluminium wire is still drawn with liquid lubricants.) ferrous alloys, notably the harder ones, are usually precoated with soft metals or with inorganic compounds, such as zinc phosphates, oxalates, or ferrous hydroxides; when they are to be dry drawn, they are also given a wash of lime borax, or one or two other alkaline substances, reputedly to facilitate the pick-up of the soap powder (whence the term "lubricant carrier"). (Table.1.1).

In the production of bar, rod and wire products, surface removal is an important final step [7]. From the time that an ingot of steel is poured, all subsequent processing tends to produce two basic deleterious conditions : decarburization and surface flaws. Decarburization results from repeated reheatings that the semi-finished product is subjected to during processing. If one wants to take advantage of the beneficial work-hardening associated with cold drawing, it corrects the

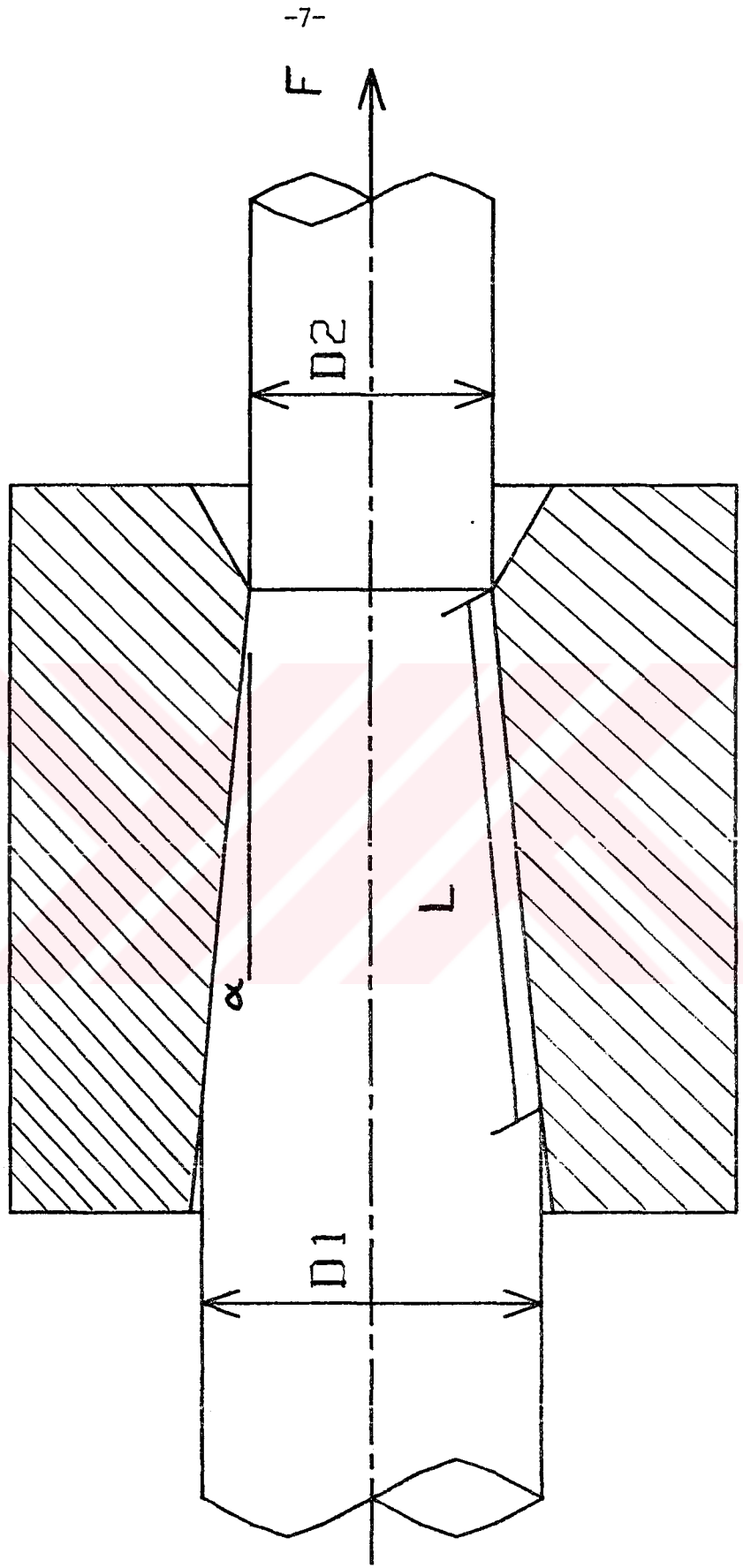
MATERIAL	U.T.S. (kg/cm ²)	COATING	LUBRICANT	DIE MATERIAL	SPEED (m/min)	NO. OF PASSES WITHOUT RELUBRI	μ
Copper	Soft	None	Castor oil	Diamond	5	---	0.10
				Carbide	"	---	0.10
				Steel	"	---	0.15
Copper	20	None	Sodium stear	Steel	6	1	0.02-0.03
			Sodium soap	Carbide	3.5	---	0.03-0.06
Brass	Annealed	None	R.O.D. emulsion	"	"	---	0.06-0.08
			Oil dag	"	"	---	0.09-0.10
Mild steel	Hard	Lime	Calcium stearate	Carbide	200	---	0.025
					2000	---	0.015
0.5% C Steel Patented	70 70 120	Lime " "	Grease Sodium soap "	Carbide " "	100	---	0.04
					"	---	0.02
					"	9	0.10
	70 150	Lime "	Graphite "	Carbide "	100	---	0.03
					"	13	0.13

TABLE.1.1.-Typical values of coefficient of friction (μ) in Wire-Drawing [2]

decarburization defects. The main functions of wire-drawing is to produce wire of specified size with a good surface finish.

1.3 Industrial Applications

Nowadays extremely large quantities of wire are drawn from all the metals and metal alloys used in industry and the articles made from wire range from the humble paperclip to the highly sophisticated equipment used in satellites. It is in fact impossible to imagine the modern world without wire. Copper may be cited as a typical example: in Western Germany approximately 400 000 tonnes of copper wire are produced and fabricated every year; the sphere of application ranges from the generation and distribution of electrical energy to transport and the transmission of communication and the smallest domestic appliances. Production ranges from overhead wire weighing up to 1100 kg per km for electrified railways to superfine wire 0.01 mm diameter weighing only just over 1 kg per 1400 km and destined for the manufacture of electronic components.



WIRE DRAWING DIE

Figure. 1.1. Notation in a wire-drawing process

CHAPTER I I

SURVEY OF LITERATURE

2.1 Historical Background of Placticity Theory

The theories of elasticity and plasticity describe the mechanics of deformation of most engineering solids. Both theories, as applied to metals and alloys, are based on experimental studies of the relations between stress and strain in a polycrystalline aggregate under simple loading conditions. Thus they are of a phenomenological nature on the macroscopic scale and, as yet, owe little to a knowledge of the structure of a metal. Swaging and drawing processes were already known and widely used in 16th. century. Other processes such as extrusion, rolling, metal machining, sheet and tube drawing which generally need more energy than a single person can supply, emerged as a consequence of the industrial innovations of the 19th century.

2.1.1. Theoretical Studies

Scientific studies in the theory of plasticity may justly be regarded as having started in 1864. In that year Tresca [1], [8] published a preliminary account of experiments on punching and extrusion, which led him to state that metals yield when the maximum shear stress attains a critical value. A similar criteria for the yielding of plastic solids has been previously proposed by Coulomb in 1773. Tresca's yield criteria was first applied by St. Venant in 1870 to determine the stresses in partly plastic cylinders subjected to torsion or bending. He set up a system of five governing stress-strain relationships for a two dimensional flow and claimed that the directions of maximum rate of shear strain coincide with the

directions of maximum shear stresses. Levy adapted St. Venant's conception of an ideal plastic material, and proposed three dimensional relationships among the components of stress and plastic strain increments in 1871. This rule was re-discovered by Von-Mises in 1913 and these relationships are now recalled as the "Levy-Mises" equations. The most satisfactory yield criterion was proposed by Von Mises in 1913. It was based on pure mathematics and was further interpreted by Hencky some years later. In 1921 Prandtl showed that the nature of the two-dimensional plasticity problem is hyperbolic. The general theory, covering also Prandtl's special solution was supplied by Hencky in 1923. He also discovered simple geometrical properties of the field of slip lines for the condition of plane plastic strain.

Theory of plasticity was first effectively applied in 1925 to industrial processes by Karman who analysed the state of stress in rolling by an elementary method. Siebel, and soon afterwards Sachs suggested similar theories for wire-drawing. Reuss allowed the elastic component of strain to appear in Levy-Mises equations in 1930. Work-hardening of materials under plastic deformation was firstly incorporated with these equations by Prandtl and then by Schmidt in 1932. Thus, by the end of 1932 the general theory was obtained for an isotropic material at ordinary temperatures. Theories describing anisotropic behaviour have been proposed by Jackson [9], [10] [11], Hill [12] and Dorn [13]. Much of this work was produced between 1939 and 1945. Sokolovsky analysed various practical problems in plastic deformation of metals and also wrote an appraisal about the studies being made in Russia [9]. Prager [14] re-formulated the stress-strain laws of the mathematical theory of plasticity. Geiringer [15] gave some recent results for ideally plastic bodies. Drucker [16] introduced the limit analysis and compared the stress-strain relations with experimental data [17]. Shapiro [18] analysed the propagation

of disturbances in in non-linear plastic media. Rebinder [19], Freudenthal [20] and Hodge [21] gave seperately, the recent mathematical analysis of theory of plasticity. Hopkins [22] introduced the dynamical analysis of non-linear problems in non-linear plastic media.

2.1.2. Experimental Studies

Fundamental tests such as the uni-axial tension test and plain strain compression test were developed to asses the basics of plastic-flow rule and to obtain basic information for the formability of materials [23] [24] [25]. Such tests gave useful information also about other properties such as material anisotropy. The variation of tensile stress with orientation had been studied earlier by Cook, Palmer and Smith [25] had studied it for brass. Additional experimental information was supplied by Baldwin and et. al. [26] for copper, and by Klinger [27] for aluminium. Recently Mellor [28] gave a detailed appraisal on this subject. He found that the coefficient of anisotropy R , remains constant at a particular orientantion at all stages of the deformation. Fundamental tests were also made to asses the hardening behaviour of plastic materials, Ludwig proposed a strain hardening law based upon his extensive experimental research. He related the equivalent stress to equivalent strain by a simple power formula. Similar suggestions were made by Voce [29] and Swift [30].

In full scale tests, it is a common practice to engrave a suitable grid to the part of the measure the plastic strains after the deformation. Using square grids scribed on the blank and then determining the resulting change in unit area of the grid elements after the blank had been pressed in to the desired shape. Keeler [31] firstly introduced the concept of "Forming limit diagrams" in 1965. Three years later, He [32]

claimed that his proposal of using a grid system which consisted of circles with small diameters gave very satisfactory results in full scale testing of sheet metals. Alexander [33] adapted a suitable method of engraving and measuring grids in experimental plasticity. In certain industrial applications such as rolling, the grid can be integrated in the material. For sheet metals, the general experience is to engrave the grid lines on the material surface. There are various definitions of strain in the literature: Goodwin [34] calculated the major strains by measuring the change in length of the axes of the so formed ellipses after the deformation of originally circular grid elements.

2.1.3. Progress in Methods of Solutions

Analytical solutions of certain simple problems have been suggested by many authors: Complete solutions for symmetrically loaded circular plates were given by Hopkins and Prager [35], Sawczuk considered a circular orthotropic plate using linearized yield conditions. Analytical solutions related with industrial processes is not so easy to obtain and has not yet been developed completely. Markov [36] introduced the variational principles to the theory of plasticity in 1947. Variational principles were later used in finite element solutions for certain industrial processes, since governing plasticity equations are non-linear and usually the material properties are also non-linear together with the physical boundary conditions. This makes much more difficult to achieve a complete analytical solution for complex industrial processes.

Numerical solutions: With the advantages offered by computers, numerical formulations of the continuum which were suggested long before thus effectively entered into practice.

Although numerical solutions are considered to be approximate solutions, very accurate results can be obtained for most of the engineering problems.

Successful applications began in early fifties, first with the analysis of linear steady problems [37]. Relevant continuum equations either in the form of differential or integral simultaneous equations were solved. The method principally consists of decomposing the medium into a fine mesh of grids and is termed as "Finite Difference Method". In practice, symmetrical and rather uniform problems can be solved in cartesian or cylindrical co-ordinates. Lee, Mallet and Keeing [38] gave an updated appraisal in relation with the finite difference applications in press-shop operations. Spancer [39] developed the methodology for axially symmetric plastic flow problems.

Before finite element methods entered into the field of numerical solutions, there was only one competing numerical technique namely the Rayleigh-Ritz-Galerkin method. This is a general procedure for obtaining approximate solutions of problems expressed in variational form. This method offers a more suitable algorithm and methodology for practical problems. Martin [40] dealt with structures with large deflections and obtain a solution for a linear, rectangular plate bending problem loaded in compression at all edges. Wolf [41] attempted to derive a generalized finite element analysis of linear theory of elasticity. Gurkok and Akay [42] developed a generalized finite element analysis program for linear, plane, axi-symmetric solid elasticity problems. Agyris and et. al. [43] proposed new techniques to handle static, geometrically and material non-linear problems. Yamada and et. al. [44] used the Prandtl-Reuss equations in plasticity theory and treated the elastic-plastic problems in a piecewise approach. Lee and Kobayashi solved the axisymmetric flat punch indentation problem by making an analogy with the

solution of elasticity. Bruce and Welch [45] developed a three dimensional finite element program to predict the large and inelastic deformations of automobile structures. Hibbitt and at.al. [46] firstly formulated an algorithm for problems of large strain and large displacements. Stricklin analysed stiffened shells of revolution and Backlund solved the stretch-forming problem for a steel strip clamped at its ends. In spite of these attempts, no complete solution has been achieved yet in the analysis of non-linear plasticity problems. Perzyna [47] recently suggested a new method which is known as the "flow approach" or simply "viscoplasticity" where an analogy between the plastic flow in the deforming material and the flow of a fluid of non-newtonian kind is made.

Slip-line field analysis: Prandtl's consideration of the indentation of a semi-infinite block using slip-line field was perhaps the first attempt for a practical problem. Nadai adapted this solution to consider the crushing of blunt edges in 1921. Henky stated the well known equations in 1923. Geiringer firstly formulated the velocity equations. Russian scientists such as Tomlenov and Unshov made various contributions to the slip-line theory and its applications. Hill and Tupper [63] introduced the subject to practical problems by applying the slip-line method to wire-drawing. Today, slip-line field solutions are used in many practical problems including many forming processes such as compression between parallel or inclined dies and indentation. Ho and Brewer [49] suggested a slip-line field solution for machining with discontinuous chips. Johnson analysed and formulated the extrusion problem through wedged shaped dies. Tomlenov [59] explained the plastic flow in the deforming sheet metals with complex shapes.

Johnson and Sowerby [51] gave a detailed appraisal on the industrial applications of slip line field solutions. In spite of the merits of slip-line solutions they do not predict the onset of plastic instabilities and the solutions are rather confined to steady state problems with field geometry.



2.2 Investigations on Wire-Drawing

2.2.1 Theoretical and Experimental Studies

There is an abundant literature on wire-drawing, but until recently, the predominant concern has been with the relationships of drawing force and power on the various conditions of a rod passing through a die. [52]

One of the earliest articles is that of Smith in 1887. Except for Musiol's work in 1900 no discussion appears on wire-drawing until that Lewis [53] [54] in 1915, and then later in 1933 and 1938, where he attempted to relate power used with the dimensions and properties of the wire by empirical factors. Except for Elder's [55] extension of Lewis's work to include strain hardening, little occurs in American literature up to 1944 regarding wire-drawing, especially forces in dies. Following 1944, one finds several articles on the theory of wire-drawing in American and English literature.

In England, Alkins and Cartwright investigated relative reductions of concentric copper tubular layers built on a solid core. Alkins reports tests conducted on 0.435 in. diameter annealed copper rod and found that when the reduction is affected by successive drafts, the tensile strengths attained for any given reduction of the original area are lower, the lighter the drafting, that is, the more numerous the stages by which the reduction is carried out. Dies with a straight taper of 5° were lubricated with vegetable oil when the short rods were pulled. Up to 15 percent nominal reduction of area, the sequence had no effect on a plot of nominal tensile strength versus reduction of area; from a reduction of area at 15 percent and beyond there was no longer a linear relationship and the tensile strengths were higher for single drafts than five successive drafts. It was lowest for nine successive drafts. No "reverse" sequence was investigated. Alkins concluded that

there was a fundamental difference between reductions by cold-drawing of less than 15 percent and those which exceed this amount.

Thompson and Francis [56],[57],[58],[59],[60] give an account of the drawing of nonferrous wires approximately 0.08 in. diameter. Several conclusions were drawn from tests on aluminium, copper, bronze 70:30 brass, 7 percent nickel-brass, and 20 percent nickel-brass. They have shown that the force necessary to draw wire is proportional to the reduction of area and for ferrous metals this proportionality extends to a reduction of about 30 percent, after which the necessary pull increases less rapidly. For nonferrous metals, the linearity of the curves remains up to a reduction of 50 to 60 percent. This same relation has been found also by Giraud and Brown. In various graphs of drawing force versus reduction of area, they show that the experimental points fall on a straight line which will cut the force axes at some finite value. This seems to indicate that a certain force is required for no reduction of area. Thompson and Francis [57] [58] also show that a reduction in the drawing force is obtained if a back-tension of a considerable magnitude is applied.

Lewis in a discussion of a foregoing paper comments that the coefficient of friction is irregular in the first draft and higher while the film is being established than in subsequent drafts.

Several investigators have attempted to analyze the wire-drawing problem from a mathematical standpoint. Probably the first work of this kind was done by Sachs (1927) [61]. He obtained expressions for the force necessary to draw a wire through a given die and for the pressure stress distribution along the die as the wire is being drawn. Sachs computed friction coefficient from a knowledge of the ideal drawing stress, actual drawing stress, value of yield strength and the die dimensions. His basic equation was one of the statics,

summing forces along the rod axis. Die angles of 2, 4, 8, 16 and 32 degree were investigated. All dies had an average value of about 0.08 for the friction coefficient. Horsburgh has developed similar expressions which are comparable with those of Sachs. The theory has presented by Sachs will appear as a special case of the present development.

Korber and Eichinger improved on Sachs work by considering the direction of the greatest principal strains as directed toward the die-cone vertex, as well as Davis and Dokos [56] who considered strain hardening effects. They also work out equations for sheet drawing, so that their theory can be tested by comparing it with the rigorous Hill-Tupper-Green analysis. One finds that the Korber-Eichinger analysis grossly overestimates redundant deformation in the absence of friction and also exaggerates the attenuating effect of friction.

The force required to draw a wire through a die depends upon several factors, the two most important of which are the friction of the wire on the walls of the die and the resistance of the die wire to plastic deformation. The latter factor will depend upon the stress-strain relations of the wire. In most previous mathematical treatments, the material to be drawn was assumed to be ideally plastic. An ideally plastic material has a finite yield point at which the material flows continuously without any increase in the applied stress. Unlike previous mathematical treatments where the metals were assumed to be ideally plastic, Davis and Dokos considered the strain hardening of the wire being drawn and the mathematical expressions used have been adjusted to take care of the large strains encountered in the process of wire-drawing.

Lunt and MacLellan [62] and MacLellan [63] have discussed and generalized the theory originated by Sachs. The split-die technique suggested by MacLellan (1952, 1953) was used to ascertain the mean die pressure. The die was in two halves and the forces tending to separate the two halves was measured

concurrently with the drawing force, then the mean coefficient of friction and the mean die pressure can be calculated directly from measurement, without recourse to wire-drawing theory [6]. In the past the coefficient of friction has been treated as a parameter which could be adjusted to give the best correlation between theory and experiment. Its derivation from experiment is therefore an important development. The measurement of the splitting force presents some difficulty, for the die halves must remain in contact during the experiment; otherwise fins are formed on the wire which vitiates the prescribed conditions of drawing [64]. Though he did not succeed in getting good results by this method, reputedly because of penetration of lubricant into the "split". The effect of cylindrical extension on the pull has been calculated by MacLellan, on the assumption that there is no transverse variation in the longitudinal stresses at the die exit, that the wire remains in contact with the bore throughout, and that in the cylindrical extension it is in a state of incipient plastic flow. His tests of the formula were inconclusive owing to uncertainty about the magnitude of the friction and the precise length of the cylindrical extension.

Wistreich [2], obtained reasonable data adapting Maclellan's experimental technique. The most detailed investigation into the mechanics of wire-drawing has been carried out by Wistreich (1955). The investigation was limited to the slow drawing of round wire, without back-pull, through dies with bores in the shape of truncated cones. Wistreich has reported an extensive experimental study to determinate the effects of reduction and cone angle on drawing stress. In his investigation, Wistreich used mainly light drawn electrolytic copper wire, since it was easy to lubricate well and did not cause rapid wear of the steel dies. Also the material in this condition does not work-harden rapidly and it is a good approximation in any theory to take account of the work-

hardening by assuming a mean yield stress. As a result of other experiments, it was concluded that the deformation is independent of the properties of the metal except in the case of annealed wire drawn with very light reductions. The lubricant was sodium stearate, special care being taken to apply it evenly and so minimize frictional variations. The value of coefficient of friction under these conditions averaged 0.02 to 0.03 and it did not vary significantly with die pressure. Majors (1955), in his tests, measured the coefficient of friction directly for the drawing of steel rods, and obtained much higher values, ranging from 0.08 to 0.2. For certain combinations of the die angle and reduction, the die pressure greatly exceeded the values of yield stress. It was also established from further tests that, other things being equal, the greater the friction, the lower the die pressure.

Split dies were used for the drawing stress, and the drawing force and the separation force exerted on the two halves of the die were measured [3]. The measurement of the splitting force presented some difficulty, since the die halves must remain in contact during the experiment, or fins will form on the wire. Wistrieck was able to obtain a measure of the splitting force at all points during the draw. The tests were terminated after appreciable separation (0.003 to 0.005 in), and the drawn wire was gauged in the plane normal to that of separation by means of a fiducial micrometer. This procedure, while workable, requires sophisticated equipment and is difficult to carry out accurately.

Yang used a similar "split-die" technique for measuring friction coefficient in the drawing of pure aluminium and zinc wires. His method, however, was to enclose a split die in a die plate with a curved opening near the periphery. Into this curved opening he then placed a thin ring of aluminium alloy on which four vertical strain gauges were attached and used to

measure the separating force. Yang believes that the split die opened in his tests to a much smaller gap than in Wistreich's test. Reasonably good results were obtained. The effect of the land or parallel portion in the die on the coefficient of friction was indicated in the results. Its importance was emphasized. A theoretical equation of the drawing stress with the effect of land considered was derived. Using the coefficient of friction obtained by the split-die method, drawing stresses were calculated from the derived equation. A comparison the theoretical and experimental drawing stresses was made. It was concluded that including the land in the analysis of wire-drawing is important and further research in analysing the shear deformation must be pursued in order to get a close agreement between theoretical analysis and experimental results [65].

According to Shield's theory, the material is assumed to be non-work-hardening, and the frictional drag between die and wire is taken as constant [1]. The plastic region within the die is bounded by spherical surfaces at the entry and exit sections, the material within moving in the direction of the virtual apex of the die. This analysis ignores the redundant shear at entry and exit, so that it may be in error for small passes and large die angles. The sudden change of motion from entirely axial to partly radial at entry and back again to entirely axial at exit is assumed to take place by shear at these sections only, so that all redundant shear is concentrated in these inlet and exit boundaries, and the reduction in cross-section is then looked upon as a homogeneous extension. The die pressure exceeds the yield stress near the die inlet and falls progressively toward the outlet, at a rate decreasing with distance from inlet. The longitudinal stresses vary laterally as well as longitudinally; the transverse variation is roughly parabolic, with a maximum on the axis. Shear stresses are present throughout the plastic

region and increase progressively from nil on the axis to μq at the interface. Close to the inlet, the longitudinal stresses are compressive in the outer layers of the wire. Shield's numerical data are of little practical value in wire-drawing so long as it is not known within what range of die geometries the end effects are insignificant.

In Hill-Tugger-Green theory of sheet drawing, the problem treated is that of the two-dimensional (plane strain) analogue of wire drawing. Solutions have been obtained for a wide range of die angles and reductions, without and with friction, for a non-work-hardening solid obeying the Von Mises yield criterion and rigid within the elastic range of loading. A method has also been devised for extending the use of the data for the pull to metals that work-harden. The effect of dimensional change, internal distortion, and friction, are not additive, and the stress and motion of a particle within the sheet is a function not only of its distance from the die inlet but also of the reduction, die angle, and friction between sheet and die. Redundant deformation contributes significantly to the work done. Boundaries of the region of plastic deformation are cusp-shaped and the material flows in a markedly uneven manner. As a consequence, plane cross-sections of the original sheet are distorted by passage through the die. The mean die pressure may exceed the yield stress up to about two and a half times, locally, it never exceeds the inlet value, but otherwise it follows a variety of courses, each of which is associated with a well-defined range of die geometries. The effect of work-hardening on the pull can be allowed for, according to Hill & Tupper, by assuming that the mean strain imparted by drawing depends only on the parameters so far considered and not on the hardening characteristics of the metal.

Siebel (1947) has proposed a theory of wire-drawing in which he assumes that the effects of homogeneous deformation, friction and non-useful distortion are additive. He assumes that the

plastic region within the die is bounded by spherical caps with centres at the virtual apex of the cone. As the wire enters and leaves the die it is sheared instantaneously along these surfaces and within the die the metal moves towards the virtual apex of the cone. The stress distribution is, generally, which shows several striking similarities with the results of Shield's rigorous analysis, notably, a transverse variation of the longitudinal stresses with a maximum on the axis of the wire, and an inlet die pressure in excess of the yield stress together with a compressive longitudinal surface stress at die entry. Siebel and Huhne have shown, by means of engraved models, the strain distribution and the distortion of the individual cross sections of the material as it passes through the die. Thompson and Barton [66] have carried out photoelastic tests of various shaped dies. Although their tests were two-dimensional in character, they indicate clearly the directions of the principal stresses. How completely this method and the one used by Siebel and Huhne agree with the conditions actually occurring in the wire-drawing process is somewhat questionable. However, it can be stated that, for the smaller angles of reduction, the distortion of the cross-sectional planes will be less and that, for a mathematical treatment, it will be convenient to assume that the original cross sections remain planes. Siebel [3] has pointed out that if hard wire with little remanent ductility is drawn through a die with a large value of Δ , the drawing stress on the axis of the wire may exceed the cohesive strength of the metal, even though the unit pull is below the yield stress on the drawing wire; consequently, the wire may repeatedly fracture at the centre and yet continue to be drawn.

Whitton (1958) has compared the drawing forces based on the theories (Sachs, Siebel) with experimental values obtained by Wistreich. A coefficient of friction 0.025 was adapted and relevant values of mean yield stress were taken from the same

experimental source. The mean yield stress is taken as the average of the values before and after drawing. It will be noticed that the Sachs equation gives good correlation for a die of semi-angle 2.29° but that for a die of semi-angle 15.5° it under-estimates the drawing force, especially at low reductions. This is, of course, because the Sachs equation does not allow for the non-useful distortion, the effect of which increases with increasing die angle, and which is attenuated by increasing reduction. On the other hand, the Siebel equation overestimates the redundant shearing and therefore the drawing force, and is only in good agreement with experiment at low values of reduction. In an attempt to get closer correlation with the experimental results, Whitton devised an empirical formula.

The expenditure of redundant work and the creation of redundant strain in wire and bar drawing has been the subject of later papers. In Caddell and Atkins's study (1968), values of the redundant work factor in rod drawing were determined experimentally for four metals over a wide range of variables; none of the metals were strain hardened prior to drawing. The method of superposition of stress-strain curves before and after drawing was used, and an expression for the redundant work factor was found to be related to the strain hardening characteristics of the metal being drawn. Use of this factor was made to predict certain mechanical properties of the drawn metals; these agreed quite well with the values measured experimentally.

Siebel's (1947) and Korber and Eichinger's (1940) formulae can be recommended for rough calculations over the entire range of die geometries commonly employed in wire-drawing. If the reduction exceeds $8\alpha/(1+0.04\alpha)$ percent, the formula Sachs (1927) is suitable for hard-drawn wires, the formula of Davis and Dokos (1944) for annealed wires.

The only trustworthy formula for calculating the mean die pressure is that based on Siebel's(1947) theory. However, in practice, it is more convenient to calculate it from a knowledge or estimate of drawing force and coefficient of friction.



CHAPTER III

OBJECT OF PRESENT INVESTIGATION

An exact theory of wire drawing has not yet been realized and all the theories make arbitrary assumptions about the deformation and the extent of the plastic region. In the complete solution of the problem the stresses and the mode of deformation must be compatible, as yet, no axisymmetric problems have been solved.

An interactive procedure on the computer is developed for the modelling of the wire-drawing process through an axisymmetrical die. Material model is such that strain-hardening, plastic anisotropy can be incorporated. The user can enter the geometrical, material and process parameters on an interactive basis. Then the developed algorithm including the material model and the integration of the differential equations will calculate the pressure distributions on the die and the drawing force. These results can also be displayed graphically on the screen.

Present study on its own, is believed to be an initiation and innovation in this field with respect to the philosophy of approach, method of solutions and the results obtained. It was found out that a complete assessment of the problem is only possible if different aspects of investigations are realized. These are: theoretical analysis, experimental research and method of solutions.

The governing plasticity equations plus the material behaviour and the mode of deformations are all inherently non-linear in form. This lead to mathematical problem which is rather intractable for an analytical solution. This conclusion is not surprising since similar situations often arise in connection with much more simple linear problems. This makes the use of numerical methods to be inevitable.

Finite element techniques seem to be more popular due to their flexibility and adaptability to complex shapes. There appears no complete variational formulation of the wire-drawing problem and seem to be unachievable in the near future. As a consequence, finite difference techniques seem to be the only alternative for a numerical solution.

The analytical solution is also obtained to compare with the numerical solution for the wire-drawing process.

The object of thesis is to develop a more realistic model of wire-drawing process. In previous analysis the redundant shear is ignored and deformation within the plastic region is treated as homogenous and all redundant deformation is concentrated on the inlet and outlet boundaries of the region. In general, the deformations is not homogenous; plane sections do not remain plane on passing through the die, and extra work is expended in distortions which do not contribute to the final reduction in diameter, i. e., as redundant deformation. The modelling technique for wire-drawing allows for observation of effects of the shearing in the entire plastic region. The proposed method incorporates the strain-hardening and plastic anisotropy properties of the wire material and also allows for optimization of the process such that for a given reduction, the die profile can be optimized with different materials and frictional conditions.

CHAPTER IV

THEORY

Plasticity can be defined as "the property which enables a material to be deformed continuously and permanently without rupture during the applications of stresses exceeding those necessary to cause yielding of the material". In plasticity, the deformations are large and permanent and these current deformations depend upon the previous deformations or in other words; the strain history. The plasticity theory is most commonly applied to metals. The nature of plastic deformation is attributed to the sliding of atoms over each other and moving away towards less stressed regions in the material. Such movement can occur in oblique planes to the principal stress directions and only with a shear type of strain. Due to material continuity the plastic deformation takes place at constant volume. There are two important contradictions to the ideal material model. These are:

- i;- Material hardens during the course of plastic deformation.
- ii;- Isotropy of the material may be destroyed after large deformations.

4.1. Basic Equations of Plasticity

The plastic deformation of an element must obey and satisfy the laws of plastic flow, equilibrium of forces, time and spaces compatibility, hardening law, imposed boundary conditions and geometrical restrictions [8]. Since large plastic deformations are involved, elastic strains are usually neglected. The general relation between stress and strain must contain:

1. The elastic stress-strain relations
2. The stress condition (yield criterion) which indicates onset of plastic flow.
3. The plastic stress-strain or stress-strain increment relations.

4.1.1 Plastic Yield Criteria

The state of stress at a point in material is uniquely determined by three stress components in principal directions which are the roots of the following cubic equation [8]:

$$S^3 - I_1 S^2 - I_2 S - I_3 = 0 \quad (4.1)$$

The invariants of the stress tensor I_1, I_2 and I_3 are defined as: (independent of the direction of the axis chosen)

$$I_1 = P_{ii} \quad (4.2.a)$$

$$I_2 = 1/2 (P_{ij})^2 - 1/2 (P_{ii})^2 \quad (4.2.b)$$

$$I_3 = 1/3 P_{ij} P_{jk} P_{ki} - 1/2 P_{ij} P_{kk} + 1/6 (P_{ii})^3 \quad (4.2.c)$$

A possible yield criterion could be a symmetric function in stress:

$$f(I_1, I_2, I_3) = 0$$

For a wide of range materials, a yield function quadratic in stresses P_{ij} is satisfactory:

$$f(I_2) = 0$$

From the tensor notation for I_2 and for an orthogonal system of co-ordinates:

$$\begin{aligned} & \langle P_{xx} - P_{yy} \rangle^2 + \langle P_{yy} - P_{zz} \rangle^2 + \langle P_{zz} - P_{xx} \rangle^2 + 6 \langle P_{xy}^2 + P_{yz}^2 + P_{zx}^2 \rangle \\ & = 6k^2 = \bar{P}^2 \end{aligned} \quad (4.3)$$

This is Von-Mises yield criterion for a material point defined in a cartesian system of co-ordinates.

In terms of principal stresses P_1, P_2 and P_3 :

$$\langle P_1 - P_2 \rangle^2 + \langle P_2 - P_3 \rangle^2 + \langle P_3 - P_1 \rangle^2 = 6k^2 = \bar{P}^2 \quad (4.4)$$

\bar{P} is the equivalent stress for a uniaxial tensile stress state. The constant k can be easily interpreted in terms of yield strength Y in simple tension. ($P_2 = P_3 = 0, P_1 = Y = \bar{P}$)

$$2P_1^2 = 2\bar{P}^2 = 2Y^2 = 6k^2$$

solving for k

$$k = Y/\sqrt{3} \quad (4.5)$$

Considering a pure shear case ($P_2 = 0, P_1 = -P_3$)

$$P_1^2 + P_2^2 + 2P_1^2 = 6k^2$$

$$\text{Then: } P_1 = -P_3 = k = Y/\sqrt{3} \quad (4.6)$$

So k is the yield stress in pure shear.

An Anisotropic Yield Criterion: All metals exhibit anisotropy to a greater or lesser degree when deformed at room temperature, that is, the mechanical properties of the metal vary in different directions.

Theories describing anisotropic behaviour have been proposed by Jackson, Smith and Lankford (1948), Hill (1948) and Dorn (1949). The theory of Hill (1948-1950) will be used here to describe a state of simple orthotropic anisotropy, that is, there are three mutually orthogonal planes of symmetry at every point. The intersections of these planes are known as the principal axis of anisotropy. The yield criterion proposed by Hill when referred to these axis has the form

$$2f(P_{ij}) \equiv F(P_{yy} - P_{zz})^2 + G(P_{zz} - P_{xx})^2 + H(P_{xx} - P_{yy})^2 + 2LP_{yz}^2 + 2MP_{zx}^2 + 2NP_{xy}^2 = 1 \quad (4.7)$$

where F, G, H, L, M, N are parameters characteristics of the current state of anisotropy. It is assumed that there is no Bauschinger effect and that a hydrostatic stress does not influence yielding. The conditions for planar isotropy (rotational symmetry about the z-axis) are determined by noting that the above equation must remain invariant for arbitrary (x, y) axes of reference. It can be shown that

$$N = F + 2H = G + 2H, \quad L = M.$$

For complete isotropy

$$L = M = N = 3F = 3G = 3H$$

When anisotropy is vanishingly small the expression reduces to the Von Misses criterion [6].

4.1.2 Definitions of Plastic Strains

The study of strain is the study of the displacement of points in a body relative to one another when the body is deformed. It is not concerned with rigid body movements.

Plastic strains can be classified into two groups:

- i- Direct (normal) strains
- ii- Shear strains

The plastic strains are often evaluated using equations derived for a homogenous plastic strain field. This can be justified if the region of a non-homogenous strain field is subdivided into very small elements where in each of the element the plastic flow is "sufficiently homogenous". Consequently concept of incremental plastic strains is introduced [8].

Normal Strains: The current normal strains can be related to the original length for a homogenous strain field where the normal unit elongations are small enough to remain in the elastic range:

$$e_L^e = \frac{l_f - l_o}{l_o} \quad (4.8)$$

This is the well known Lagrangian (engineering) definition of elastic strain. A second definition is the Eulerian strain:

$$e_E^e = \frac{l_f - l_o}{l_f} \quad (4.9)$$

The tensorial definition of Lagrangian strain is:

$$e_{ii}^e = \frac{l_f - l_0}{2l_0} \quad (4.10)$$

To describe the plastic deformation, natural or logarithmic strain is used. Consider an element of original length of l_0 , strained in m steps to a final length of l_m . The increment of strain at the n th. step is:

$$\delta \epsilon^n = \frac{l_n - l_{n-1}}{l_{n-1}} = \frac{\delta l}{l_{n-1}} \quad (4.11)$$

in analogous to Langrangian definition.

The incremental steps should be further subdivided into j steps each:

$$\delta \epsilon^n = \sum_{k=1}^j \frac{\delta_1^k l}{l_{n-1}^k} \quad (4.12)$$

For the limiting case for infinitesimally small lengths

$$\delta \epsilon^n = \int_{l_{n-1}}^{l_n} \frac{dl}{l} = \ln \frac{l_n}{l_{n-1}} \quad (4.13)$$

Then the total strain that has taken up to the m .th. step of deformation process will be

$$\epsilon = \sum_{n=1}^m (\delta \epsilon^n) = \sum_{n=1}^m \ln \frac{l^n}{l^{n-1}} = \ln \frac{l_m}{l_0} \quad (4.14)$$

Plastic strain definition is approximately equal to Langrangian definition of elastic strain for diminishingly small magnitudes.

Shear Strains: An element with corners A, B, C and D as shown in Figure.4.1 assumes a new configurations after a certain distortion. The angular distortion at point A will be:

$$\gamma_{\alpha\beta} = \left(\frac{\delta u}{\delta \alpha} + \frac{\delta v}{\delta \beta} \right) \quad (4.15)$$

The deformation is called a shear deformation when the distortion takes place without any change in area. For infinitesimally small strains:

$$\tan \psi_{\alpha} \approx \psi_{\alpha} = du/d\alpha \approx \delta u/\delta \alpha \quad (4.16)$$

$$\tan \psi_{\beta} \approx \psi_{\beta} = dv/d\beta \approx \delta v/\delta \beta \quad (4.17)$$

A shear strain is considered to be positive if the current subtended angle B'A D' is less than the original one taking into account this sign convention:

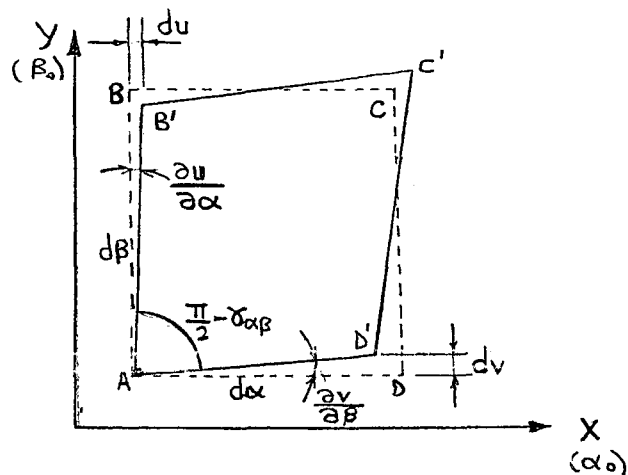


Figure.4.1 An elastically deforming element under pure shear

$$\gamma_{\alpha\beta} \approx \tan\psi_{\alpha} + \tan\psi_{\beta}$$

This is the engineering notation of the shear strain at point A. In this case the strain matrix consists of nine components in a three-dimensional co-ordinate system. This matrix includes the rigid body rotation components and therefore it is not symmetrical. If the components of rigid body rotation are not considered then the symmetric strain components in shear are obtained:

$$e_{\alpha\beta} = 1/2 (\delta u / \delta \alpha + \delta v / \delta \beta) \quad (4.18)$$

This is the tensor notation of the elastic shear strain. Comparing equations (4.15) and (4.18)

$$e_{\alpha\beta} = 1/2 \gamma_{\alpha\beta} \quad (4.19)$$

For large and arbitrary deformations, the strain field is not homogenous anymore and the sides of infinitesimal elements become curvilinear and oblique. Figure 4.2 shows one of the edges of such an element. Angle generated by anticlockwise rotation of the lines are taken to be positive.

Partial incremental plastic shear strains associated with the α and β -lines are defined as follows:

$$\delta\gamma_{\beta} = \tan \delta\psi_{\beta} \quad (4.20. a)$$

$$\delta\gamma_{\alpha} = \tan \delta\psi_{\alpha} \quad (4.20. b)$$

The total incremental plastic shear strain at point A is:

$$\left(\delta\gamma_{\beta\alpha} \right)_A^{n+1} = (\tan \delta\psi_{\beta} - \tan \delta\psi_{\alpha}) \quad (4.21)$$

In tensor notation, the incremental plastic shear strain will be:

$$\delta \epsilon_{Jk} = 1/2 (\tan \delta \psi_J - \tan \delta \psi_k) \quad (4.22)$$

The current slopes of α and β -lines at point A are:

$$S_{\alpha}^{n+1} \Big|_A = dy/dx \Big|_{A-B'} = \tan \psi_{\alpha}^{n+1} = \tan (\psi_{\alpha}^n + \delta \psi_{\alpha}) \quad (4.23)$$

where:

$$\tan (\psi_{\alpha}^n + \delta \psi_{\alpha}) = \frac{\tan \psi_{\alpha}^n + \tan (\delta \psi_{\alpha})}{1 - \tan \psi_{\alpha}^n \tan (\delta \psi_{\alpha})} \quad (4.24)$$

for relatively small incremental angle changes, the denominator of above equation is close to unity.

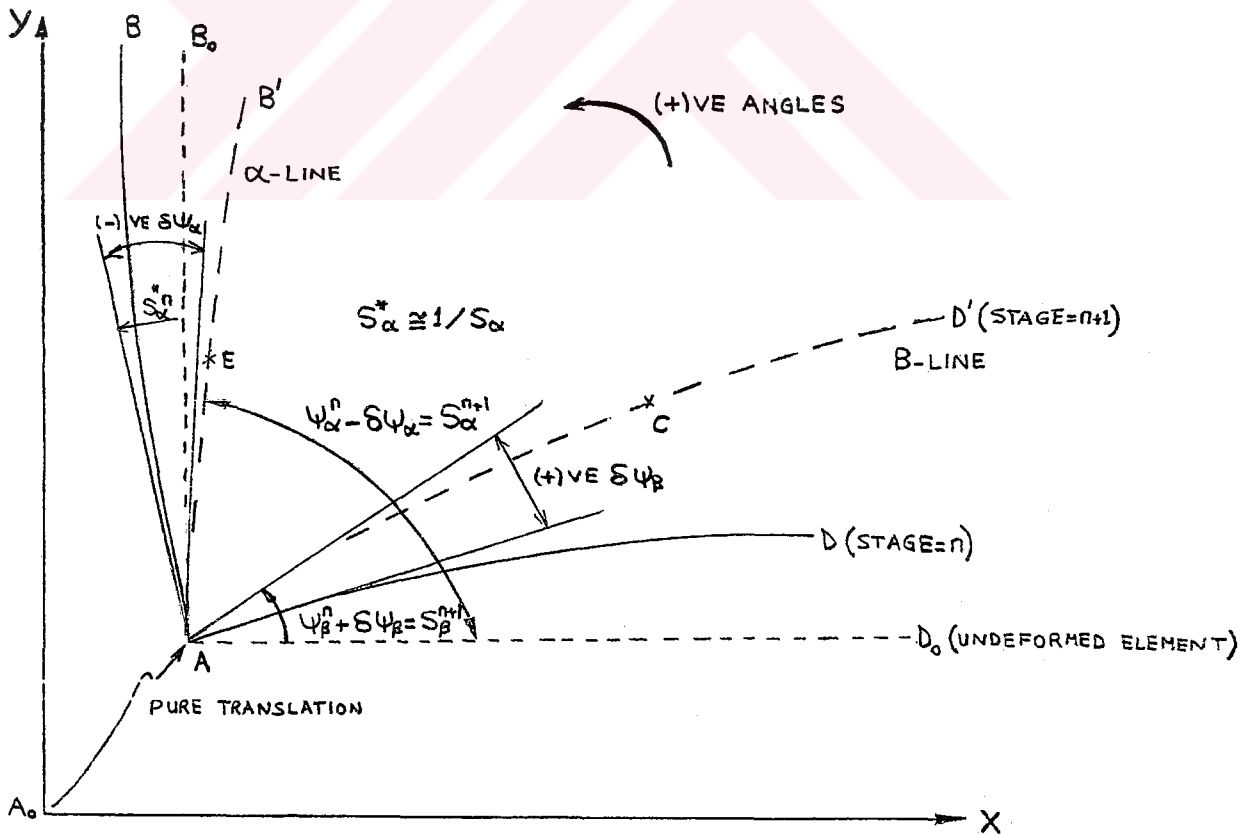


Figure.4.2 Plastic incremental shear strain nomenclature for a largely deforming grid element

Then:

$$S_{\alpha}^{n+1} \approx \tan \psi_{\alpha}^n + \tan(\delta\psi_{\alpha}) \quad (4.25)$$

using equation 4.23

$$\tan \psi_{\alpha}^n = S_{\alpha}^n \quad (4.26)$$

finally:

$$S_{\alpha}^{n+1} \approx S_{\alpha}^n + \tan(\delta\psi_{\alpha}) \quad (4.27)$$

and similarly: .

$$S_{\beta}^{n+1} \approx S_{\beta}^n + \tan(\delta\psi_{\beta}) \quad (4.28)$$

Inserting equations 4.27 and 4.28 into equation 4.22 :

$$\delta\epsilon_{Jk} \Big|_A^{n+1} = 1/2 [\langle S_J^{n+1} - S_J^n \rangle - \langle S_k^{n+1} - S_k^n \rangle] \Big|_{\substack{J \equiv \beta \\ k \equiv \alpha}} \quad (4.29)$$

It will be convenient to write above equation in the form of

$$\delta\epsilon_{\beta\alpha} \Big|_A^{n+1} = 1/2 [\langle S_{\beta}^{n+1} - S_{\beta}^n \rangle + \langle S_{\alpha}^{n+1} - S_{\alpha}^n \rangle] \quad (4.30)$$

where:

$$S_{\alpha}^{n+1} \Big|_A = dx/dy \Big|_{A-B}, \quad \text{and vice versa.} \quad (4.31)$$

Total shear strain will be direct sum of the incremental shear strains:

$$\epsilon_{\beta\alpha} \Big|_A^{n+1} \approx \sum_{n=0}^{n+1} \delta\epsilon_{\beta\alpha} \Big|_A^n$$

From equation 4.30

$$\epsilon_{\beta\alpha} \Big|_A^{n+1} \approx 1/2 \{ \langle S_{\beta}^{n+1} - S_{\beta}^0 \rangle + \langle S_{\alpha}^{n+1} - S_{\alpha}^0 \rangle \}$$

For an initially rectangular element with sides parallel to the co-ordinate axes:

$$\epsilon_{\beta\alpha} \Big|_A^{n+1} \approx 1/2 (S_{\beta}^{n+1} + S_{\alpha}^{n+1}) \quad (4.32)$$

For curvilinear lines, definitions of normal strains over the arc length becomes more complicated. Summing up the individual, infinitesimal, linear, plastic strains, one can obtain an average direct strain in association with the given arc length. Nevertheless, it can be suggested that this average strain takes place at the mid-point of the arc.

Then:

$$\delta\epsilon_{\beta\beta} \Big|_{A-D'}^{n+1} = \delta\epsilon_{\beta\beta} \Big|_C^{n+1} = \text{Ln}(\overline{A-D'} / \overline{A-D}) \quad (4.33)$$

$$\delta\epsilon_{\alpha\alpha} \Big|_{A-B'}^{n+1} = \delta\epsilon_{\alpha\alpha} \Big|_E^{n+1} = \text{Ln}(\overline{A-B'} / \overline{A-B}) \quad (4.34)$$

Constancy of Volume

Volume of metallic materials remain practically constant even after large plastic deformations :

$$\delta\epsilon_{\alpha\alpha} + \delta\epsilon_{\beta\beta} + \delta\epsilon_{\gamma\gamma} = 0 \quad (4.35)$$

Shear strain terms automatically drop out since shear strains do not create any change in volume. Equation (4.35) can be extended to total plastic strains:

$$\epsilon_{\alpha\alpha} + \epsilon_{\beta\beta} + \epsilon_{\gamma\gamma} = 0 \quad (4.36)$$

4.1.4 Plastic Flow Rule for Anisotropic Material

The incremental strains are derived by partially differentiating $f(P_{ij})$ with respect to P_{ij} . Since [6]

$$2f(P_{ij}) = F(P_{\alpha\alpha} - P_{\gamma\gamma})^2 + G(P_{\gamma\gamma} - P_{\alpha\alpha})^2 + H(P_{\alpha\alpha} - P_{\beta\beta})^2 + 2LP_{\beta\alpha}^2 + 2MP_{\gamma\alpha}^2 + 2NP_{\alpha\beta}^2$$

$$\delta f / \delta P_{\alpha\alpha} = G(P_{\alpha\alpha} - P_{\gamma\gamma}) + H(P_{\alpha\alpha} - P_{\beta\beta}) \quad (4.38)$$

and hence

$$\frac{d\epsilon_{\alpha\alpha}^p}{G(P_{\alpha\alpha} - P_{\gamma\gamma}) + H(P_{\alpha\alpha} - P_{\beta\beta})} = d\lambda \quad (4.39)$$

Where $d\lambda$ is constant of proportionality.

Similar expressions are obtained for the other components of the strain increment and can be written down as,

$$d\epsilon_{\alpha\alpha}^p = d\lambda [H(P_{\alpha\alpha} - P_{\beta\beta}) + G(P_{\alpha\alpha} - P_{\gamma\gamma})] \quad (4.40.a)$$

$$d\epsilon_{\beta\beta}^p = d\lambda [F(P_{\beta\beta} - P_{\gamma\gamma}) + H(P_{\beta\beta} - P_{\alpha\alpha})] \quad (4.40.b)$$

$$d\epsilon_{\gamma\gamma}^p = d\lambda [G(P_{\gamma\gamma} - P_{\alpha\alpha}) + F(P_{\gamma\gamma} - P_{\beta\beta})] \quad (4.40.c)$$

$$d\epsilon_{\beta\gamma}^p = d\lambda L P_{\beta\gamma} \quad (4.40.d)$$

$$d\epsilon_{\gamma\alpha}^p = d\lambda M P_{\gamma\alpha} \quad (4.40.e)$$

$$d\epsilon_{\alpha\beta}^p = d\lambda N P_{\alpha\beta} \quad (4.40.f)$$

These expressions of course satisfy the incompressibility condition $d\epsilon_{\alpha\alpha} + d\epsilon_{\beta\beta} + d\epsilon_{\gamma\gamma} = 0$.

For a material subjected to plane stress, with rotational symmetry about α -axis, so that [6]

$$H=G \quad \text{and} \quad F/G = F/H = R \quad (4.41)$$

equations (4.40.a), (4.40.b) and (4.40.c) reduce to

$$d\epsilon_{\alpha\alpha}^P = d\lambda G [(P_{\alpha\alpha} - P_{\beta\beta}) + (P_{\alpha\alpha} - P_{\gamma\gamma})] \quad (4.42.a)$$

$$d\epsilon_{\beta\beta}^P = d\lambda G [R(P_{\beta\beta} - P_{\gamma\gamma}) + (P_{\gamma\gamma} - P_{\alpha\alpha})] \quad (4.42.b)$$

$$d\epsilon_{\gamma\gamma}^P = d\lambda G [(P_{\gamma\gamma} - P_{\alpha\alpha}) + R(P_{\gamma\gamma} - P_{\beta\beta})] \quad (4.42.c)$$

If anisotropic material is subjected to forces in the plane of material, the (α, β) plane, then $P_{\alpha\gamma}$ and $P_{\gamma\beta}$ will be zero. [6]

$\delta\lambda$ is not a constant property of material, it varies from point to point within the plastically deforming material. Furthermore, it also varies with time for a given point. Due to this inconvenience, sometimes arbitrarily defined stress ratios are employed to eliminate $\delta\lambda$:

$$X = \frac{P_{\beta\beta}}{P_{\alpha\alpha}} \quad (4.43)$$

$$K = \frac{P_{\gamma\gamma}}{P_{\alpha\alpha}} \quad (4.44)$$

$$Z = \frac{P_{\beta\alpha}}{P_{\alpha\alpha}} \quad (4.45)$$

Using 4.42a, 4.42b & 4.42c

$$\frac{d\epsilon_{\alpha\alpha}}{d\epsilon_{\beta\beta}} = \frac{(1-X) + (1-K)}{R(X-K) + (X-1)} \quad (4.46)$$

$$\frac{d\epsilon_{\alpha\alpha}}{d\epsilon_{\gamma\gamma}} = \frac{(1-X) + (1-K)}{(K-1) + R(K-X)} \quad (4.47)$$

$$\frac{d\epsilon_{\alpha\alpha}}{d\gamma_{\beta\alpha}} = \frac{G}{N Z} [(1-X) + (1-K)] \quad (4.48)$$

It can be shown that:

$$R_{45^\circ} = \frac{2N - (F+G)}{2(F+G)} \text{ or } \frac{N}{G} = (R_{45^\circ} + 1/2) (1 + R_0/R_{90}) \quad (4.49)$$

R_0 , R_{45} and R_{90} indicate R-values along, at forty-five degrees and ninety degrees respectively to the direction of drawing. Assuming $R_0 \approx R_{90}$

$$\frac{N}{G} = 2R + 1 \quad (4.50)$$

Then the equation 4.48 becomes

$$\frac{d\epsilon_{\alpha\alpha}}{d\gamma_{\beta\alpha}} = \frac{1}{(2R+1)Z} [(1-X) + (1-K)]$$

By using 4.46 & 4.47:

$$K = X \frac{(\frac{d\epsilon_{\alpha\alpha}}{d\epsilon_{\beta\beta}}) + (\frac{d\epsilon_{\alpha\alpha}}{d\epsilon_{\gamma\gamma}})R + (\frac{d\epsilon_{\alpha\alpha}}{d\epsilon_{\beta\beta}})R}{(\frac{d\epsilon_{\alpha\alpha}}{d\epsilon_{\gamma\gamma}}) + (\frac{d\epsilon_{\alpha\alpha}}{d\epsilon_{\gamma\gamma}})R + (\frac{d\epsilon_{\alpha\alpha}}{d\epsilon_{\beta\beta}})R} + \frac{(\frac{d\epsilon_{\alpha\alpha}}{d\epsilon_{\gamma\gamma}}) - (\frac{d\epsilon_{\alpha\alpha}}{d\epsilon_{\beta\beta}})}{(\frac{d\epsilon_{\alpha\alpha}}{d\epsilon_{\gamma\gamma}})R + (\frac{d\epsilon_{\alpha\alpha}}{d\epsilon_{\beta\beta}})R + (\frac{d\epsilon_{\alpha\alpha}}{d\epsilon_{\gamma\gamma}})} \quad (4.51)$$

Let's take

$$\frac{d\epsilon_{\alpha\alpha}}{d\epsilon_{\beta\beta}} = P \quad ; \quad \frac{d\epsilon_{\alpha\alpha}}{d\epsilon_{\gamma\gamma}} = Q \quad ; \quad \frac{d\gamma_{\beta\alpha}}{d\epsilon_{\alpha\alpha}} = E$$

Then:

$$K = X \frac{P+QR+PR}{Q+QR+PR} + \frac{Q-P}{QR+PR+Q}$$

and take

$$\frac{P+QR+PR}{Q+QR+PR} = S \quad ; \quad \frac{Q-P}{QR+PR+Q} = T$$

$$K = XS + T \quad (4.52)$$

$P_{\beta\alpha} = P_{\beta\beta} \cdot \mu$ (at interface of wire and die)

$$P_{\beta\alpha} = X P_{\alpha\alpha} \mu$$

$$\Rightarrow \frac{P_{\beta\alpha}}{P_{\alpha\alpha}} = \mu X \Rightarrow Z = \mu X \quad (4.53)$$

Substituting the above equation into equation 4.48:

$$Z = E \frac{1}{2R+1} [(1-X) + (1-K)]$$

$$K = 2 - X[1 + (\mu/E)(2R+1)] \quad (4.54)$$

By using equation 4.52 equation 4.54:

$$X = \frac{2 + \frac{P-Q}{Q+QR+PR}}{\left(\frac{P+QR+PR}{Q+QR+PR}\right) + \left(1 + \frac{\mu}{E} (2R+1)\right)} \quad (4.55. a)$$

$$K=XS+T \quad (4.55. b)$$

$$Z=\mu X \quad (4.55. c)$$

4.1.5. Generalized Stress and Strain Relations for Anisotropic Work Hardening Material

Hill (1950) has proposed that the equivalent stress should be defined as [6]

$$\bar{P} = \sqrt{3/2} \left[\frac{F(P_{\beta\beta} - P_{\gamma\gamma})^2 + G(P_{\gamma\gamma} - P_{\alpha\alpha})^2 + H(P_{\alpha\alpha} - P_{\beta\beta})^2 + 2NP_{\beta\alpha}^2 + 2MP_{\gamma\alpha}^2 + 2LP_{\beta\gamma}^2}{F+G+H} \right]^{1/2} \quad (4.56)$$

where it is understood that only ratios of the anisotropic parameters, not the absolute values, will be considered. Since $P_{\alpha\gamma}$ and $P_{\gamma\beta}$ is equal to zero and there exists rotational symmetry about α -axis, so that

$$\bar{P} = \sqrt{3/2} \left[\frac{R(P_{\beta\beta} - P_{\gamma\gamma})^2 + (P_{\gamma\gamma} - P_{\alpha\alpha})^2 + (P_{\alpha\alpha} - P_{\beta\beta})^2 + 2NP_{\beta\alpha}^2}{2+R} \right]^{1/2} \quad (4.57)$$

The generalized strain increment, $d\bar{\epsilon}$, can be defined from

$$d\omega = \bar{P}d\bar{\epsilon} = d\lambda$$

as

$$d\bar{\epsilon} = \frac{d\lambda}{\bar{P}} = \sqrt{\frac{2}{3}} [F+G+H]^{1/2} \left[F \left(\frac{Gd\epsilon_{\beta\beta} - Hd\epsilon_{\gamma\gamma}}{FG+GH+HF} \right)^2 + G \left(\frac{Fd\epsilon_{\alpha\alpha} - Hd\epsilon_{\gamma\gamma}}{FG+GH+HF} \right)^2 + H \left(\frac{Fd\epsilon_{\alpha\alpha} - Gd\epsilon_{\beta\beta}}{FG+GH+HF} \right)^2 + \frac{2d\gamma_{\beta\alpha}^2}{N} \right]^{1/2} \quad (4.58)$$

Because of rotational symmetry, equation (4.58) reduces to:

$$d\bar{\epsilon} = \sqrt{\frac{2}{3}} \left[\frac{2+R}{(1+2R)^2} \left\{ (d\epsilon_{\gamma\gamma} - Rd\epsilon_{\alpha\alpha})^2 + (d\epsilon_{\beta\beta} - Rd\epsilon_{\alpha\alpha})^2 + R(d\epsilon_{\beta\beta} - d\epsilon_{\gamma\gamma})^2 \right\} \right]^{1/2} \quad (4.59)$$

4.1.6 Laws of Material Hardening

Plasticity theory assumes that the onset of plastic yield takes place either suddenly at zero strain (rigid-plastic material model) or from a finite elastic strain (elastic-plastic material model). After the initial yield, most of the materials harden upon further application of the deforming loads.

Work-hardening hypothesis: The current value of the yield stress \bar{P} is a function of the plastic work done per unit volume of the material, and independent of the strain history:

$$\bar{P} = f(\omega^p)$$

Strain-hardening hypothesis: In this hypothesis, hardening and thus the plastic work depends upon the strain history:

$$\bar{P} = f^*(\omega^p) = f^* \left(\int_0^{\bar{\epsilon}} \bar{P} d\bar{\epsilon}^* \right)$$

Above equation gives the functional relationship between \bar{P} and $\bar{\epsilon}$.

$$\bar{P} = \bar{f}^* \int_0^{\bar{\epsilon}} d\bar{\epsilon}^*$$

It would be convenient to express the function \bar{f}^* in a mathematical form. A mathematical form was first given by Ludwig:

$$\bar{P} = A \cdot \epsilon^n \quad 0 \leq n \leq 1$$

Constants A and n are the material properties to be determined from uniaxial tensile tests. It does not explicitly include the effects of strain-hardening rate and its variation with time. Voce suggested another equation:

$$\bar{P} = a + (b-a) \{1 - e^{-n\bar{\epsilon}}\}$$

This equation is too complicated for numerical analysis. Swift proposed a simpler but equivalently comprehensive formula for isotropic materials:

$$\bar{P} = A(B + \bar{\epsilon})^n \quad (4.60)$$

Here, B is the amount of pre-strain. Exponent n determines the rate of strain-hardening with respect to the equivalent strain. Coefficient A has the units of stress.

A form of expression proposed by Prager is

$$P = Y \tanh(E\epsilon/Y)$$

By using Swift's Law and equations 4.57 & 4.59

$$\begin{aligned}
 & \sqrt{3/2} \left[\frac{R(XP_{\alpha\alpha} - KP_{\alpha\alpha})^2 + (KP_{\alpha\alpha} - P_{\alpha\alpha})^2 + (P_{\alpha\alpha} - XP_{\alpha\alpha})^2 + 2NZ^2 P_{\alpha\beta}^2}{2+R} \right]^{1/2} \\
 &= A \left[\sqrt{2/3} \left[\left(\frac{2+R}{1+2R} \right)^2 \left\{ (d\epsilon_{\gamma\gamma} - Rd\epsilon_{\alpha\alpha})^2 + (d\epsilon_{\beta\beta} - Rd\epsilon_{\alpha\alpha})^2 + \right. \right. \right. \\
 & \quad \left. \left. \left. + R(d\epsilon_{\beta\beta} - d\epsilon_{\gamma\gamma})^2 \right\} \right]^{1/2} + B \right]^n \\
 & \sqrt{3/2} P_{\alpha\alpha} \left[(R(X-K)^2 + (K-1)^2 + (1-X)^2 + 2NZ^2) / (2+R) \right]^{1/2} \\
 &= A \left[\sqrt{2/3} \left[\left(\frac{2+R}{1+2R} \right)^2 \left\{ (d\epsilon_{\gamma\gamma} - Rd\epsilon_{\alpha\alpha})^2 + (d\epsilon_{\beta\beta} - Rd\epsilon_{\alpha\alpha})^2 + \right. \right. \right. \\
 & \quad \left. \left. \left. + R(d\epsilon_{\beta\beta} - d\epsilon_{\gamma\gamma})^2 \right\} \right]^{1/2} + B \right]^n \\
 \Rightarrow P_{\alpha\alpha}^* &= \left[A \left[B + \sqrt{2/3} \left[\left(\frac{2+R}{1+2R} \right)^2 \left\{ (d\epsilon_{\gamma\gamma} - Rd\epsilon_{\alpha\alpha})^2 + (d\epsilon_{\beta\beta} - Rd\epsilon_{\alpha\alpha})^2 + \right. \right. \right. \right. \right. \\
 & \quad \left. \left. \left. + R(d\epsilon_{\beta\beta} - d\epsilon_{\gamma\gamma})^2 \right\} \right]^{1/2} \right]^n / \left[\sqrt{3/2} \left[(R(X-K)^2 + (K-1)^2 + (1-X)^2 + \right. \right. \right. \\
 & \quad \left. \left. \left. + 2NZ^2) / (2+R) \right] \right]^{1/2}
 \end{aligned}$$

(4.61)

4.1.7. Stress Equations of Equilibrium in Curvilinear Coordinates:

In plasticity problems, it is necessary to investigate the conditions that control the way in which the stresses vary in a discretized but finite field of plastic deformation. This can be appropriately achieved by considering the force equilibrium for every material element within the field. An orthogonal-curvilinear co-ordinate system may be suitable to analyse and formulate non axi-symmetric deformation problems provided only that the sides of the grid elements remain practically orthogonal to each other throughout the course of deformation [1].

The spherical and cylindrical coordinates can be shown to be special cases of general curvilinear coordinates in which the spaces coordinates are all curved and the curvature from one point to another is not necessarily constant. Curvilinear coordinates are useful also in some special elasticity problems, particularly for the stresses at the root of an elliptical notch.

The case of two dimensional curvilinear coordinates will first be dealt with.

Consider the small element ABCD cut off by neighbouring pairs of α and β lines which differ from each other by increments $+\Delta\alpha/2$ and $+\Delta\beta/2$ along the curvilinear axes at point O. The element has plane faces which are parallel to the xy plane and it is taken as of unit thickness normal to the plane [1]. (Figure .4.3)

Equilibrium equation for the α -direction :

$$\frac{\delta P_{\alpha\alpha}}{\delta\alpha} + \frac{\delta P_{\alpha\beta}}{\delta\beta} + \frac{P_{\alpha\alpha} - P_{\beta\beta}}{r_{\beta}} - \frac{2P_{\alpha\beta}}{r_{\alpha}} = 0 \quad (4.62)$$

for the β -direction

$$\frac{\delta P_{\beta\beta}}{\delta\beta} + \frac{\delta P_{\beta\alpha}}{\delta\alpha} + \frac{P_{\beta\beta} - P_{\alpha\alpha}}{r_\alpha} + \frac{2P_{\beta\alpha}}{r_\beta} = 0 \quad (4.63)$$

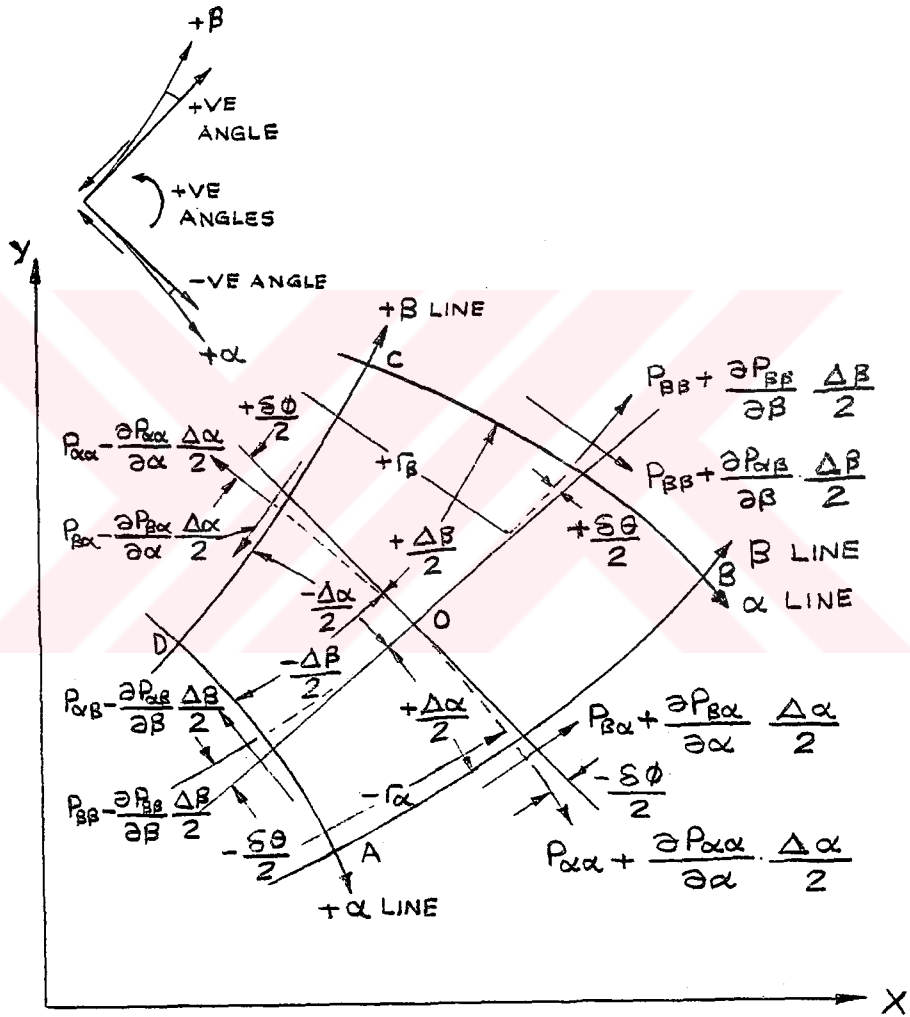


Figure.4.3.A curvilinear element in two dimension[1]

Curvilinear Coordinates in Three Dimensions :

Figure 4.4 shows the element formed, about the point O, of faces with side lengths $\Delta\alpha, \Delta\beta, \Delta\gamma$ through the curvilinear co-ordinates equidistant from O in the α, β and γ directions. The stresses acting on the faces of this element will in general be inclined at small angles to the co-ordinate directions at point O. They will be inclined not only parallel to a given plane as in that case, but also in the third orthogonal plane as well. It will be considered the equilibrium of forces in the α -direction at the point O. It is much easier if we take distances $+\Delta\alpha, +\Delta\beta$ and $+\Delta\gamma$ along the α, β and γ lines through the corner A. We must refer to the curvature of, for example, the α line at AB to both the β and γ directions, i.e. the α line has radius of curvature $r_{\alpha\beta}$ with respect to the $\alpha\beta$ plane at O and $r_{\alpha\gamma}$ with respect to the $\alpha\gamma$ plane.

The equilibrium in the α -direction will now be considered:

1) $AB = \Delta\alpha$, $AF = \Delta\beta$, $AD = \Delta\gamma$

2) CD is slightly longer than AB. The angle between the sides AD and BC, to a first approximation, is $\Delta\alpha/r_{\alpha\gamma}$ and the length of CD is therefore:

$$(r_{\alpha\gamma} + \Delta\gamma) (\Delta\alpha/r_{\alpha\gamma}) = \Delta\alpha + (\Delta\alpha\Delta\gamma/r_{\alpha\gamma}) \quad (4.64)$$

The mean length in the α -direction is therefore

$$\Delta\alpha + (\Delta\alpha\Delta\gamma/2r_{\alpha\gamma}) \quad (4.65)$$

3) the length of BC is similarly obtained from

$$\Delta\gamma / -r_{\gamma\alpha} (-r_{\gamma\alpha} + \Delta\alpha) = \Delta\gamma + (\Delta\gamma\Delta\alpha / -r_{\gamma\alpha}) \quad (4.66)$$

giving a mean length of

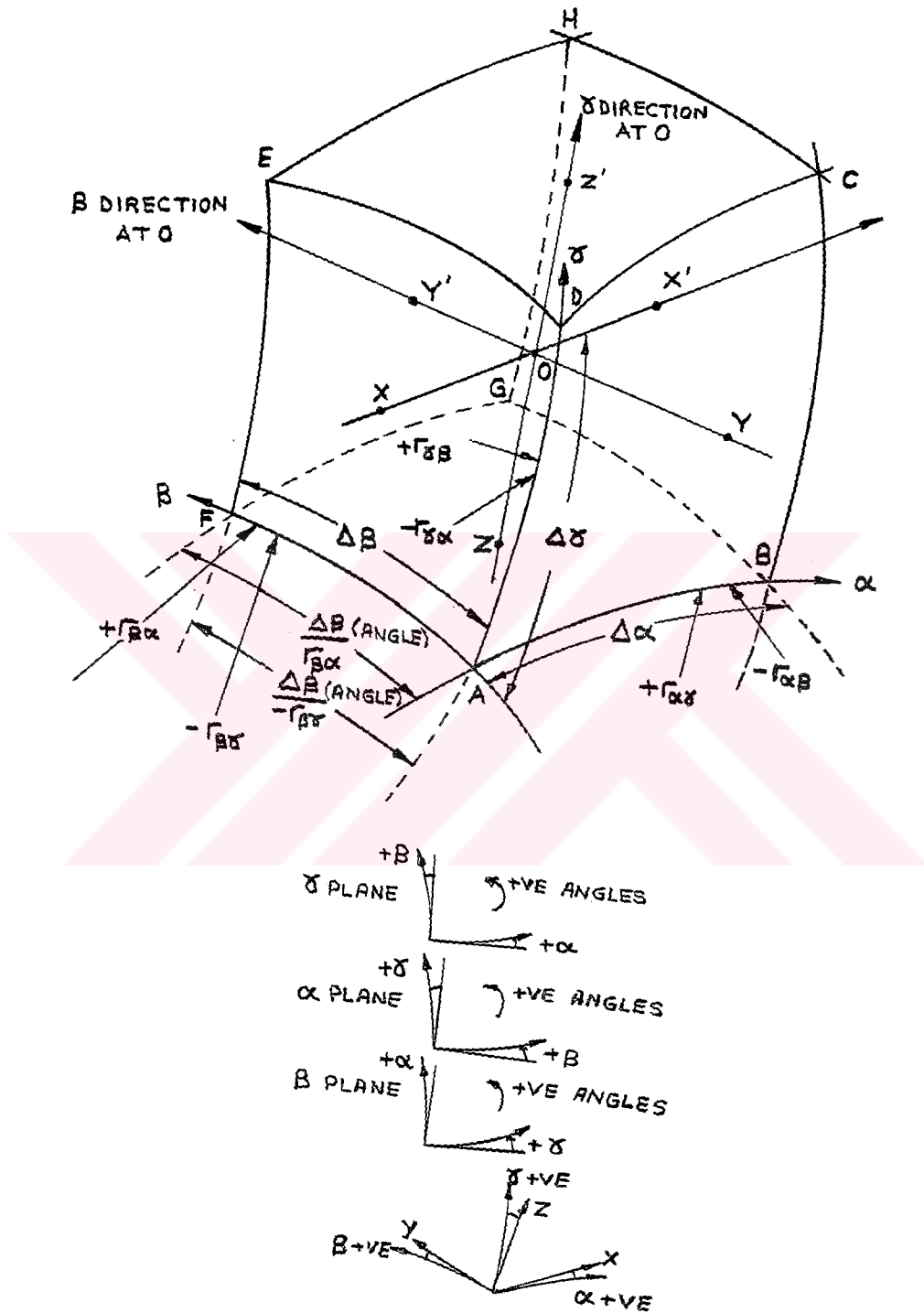


Figure.4.4 A curvilinear element in three dimensions[1]

$$\Delta\gamma - (\Delta\gamma\Delta\alpha/2r_{\gamma\alpha}) \quad (4.67)$$

4) The area of the face ABCD is therefore

$$\left(\Delta\alpha + \frac{\Delta\alpha\Delta\gamma}{2r_{\alpha\gamma}}\right) \left(\Delta\gamma - \frac{\Delta\gamma\Delta\alpha}{2r_{\gamma\alpha}}\right) = \Delta\alpha\Delta\gamma \left(1 + \frac{\Delta\gamma}{2r_{\alpha\gamma}} - \frac{\Delta\alpha}{2r_{\gamma\alpha}}\right) \quad (4.68)$$

5) The length $BG = \Delta\beta + (\Delta\beta\Delta\alpha/r_{\beta\alpha})$. (4.69)

6) For the length GH, there is an increase for both the β and γ directions. The side BC is longer than AD by

$$(\Delta\gamma/-r_{\gamma\alpha})\Delta\alpha \quad (4.70)$$

HG is longer than BC by

$$(\Delta\gamma/+r_{\gamma\beta})\Delta\beta \quad (4.71)$$

Finally

$$GH = \Delta\gamma - (\Delta\gamma\Delta\alpha)/r_{\gamma\alpha} + (\Delta\gamma\Delta\beta)/r_{\gamma\beta} \quad (4.72)$$

7) Accordingly CH, by cyclical permutation is

$$CH = \Delta\beta + (\Delta\beta\Delta\alpha/r_{\beta\alpha}) - (\Delta\beta\Delta\gamma/r_{\beta\gamma}) \quad (4.73)$$

8) The area of face, BCHG

= Mean height \times mean depth

$$= \left(\Delta\beta + \frac{\Delta\beta\Delta\alpha}{r_{\beta\alpha}} - \frac{\Delta\beta\Delta\gamma}{2r_{\beta\gamma}}\right) \left(\Delta\gamma - \frac{\Delta\gamma\Delta\alpha}{r_{\gamma\alpha}} + \frac{\Delta\gamma\Delta\beta}{2r_{\gamma\beta}}\right)$$

$$\text{Area} = \Delta\beta\Delta\gamma \left(1 - \frac{\Delta\alpha}{r_{\gamma\alpha}} + \frac{\Delta\alpha}{r_{\beta\alpha}} + \frac{\Delta\beta}{2r_{\gamma\beta}} - \frac{\Delta\gamma}{2r_{\beta\gamma}} \right) \quad (4.74)$$

The other areas can be obtained by cyclic permutations.

$$\text{Area AFED} = \Delta\beta\Delta\gamma \left(1 + \frac{\Delta\beta}{2r_{\gamma\beta}} - \frac{\Delta\gamma}{2r_{\beta\gamma}} \right) \quad (4.75)$$

$$\text{Area ABGH} = \Delta\alpha\Delta\beta \left(1 + \frac{\Delta\alpha}{2r_{\beta\alpha}} - \frac{\Delta\beta}{2r_{\alpha\beta}} \right) \quad (4.76)$$

$$\text{Area EFGH} = \Delta\alpha\Delta\gamma \left(1 + \frac{\Delta\beta}{r_{\gamma\beta}} - \frac{\Delta\beta}{r_{\alpha\beta}} - \frac{\Delta\alpha}{2r_{\gamma\alpha}} + \frac{\Delta\gamma}{2r_{\alpha\gamma}} \right) \quad (4.77)$$

$$\text{Area CDEH} = \Delta\alpha\Delta\beta \left(1 + \frac{\Delta\gamma}{r_{\alpha\gamma}} - \frac{\Delta\gamma}{r_{\beta\gamma}} + \frac{\Delta\alpha}{2r_{\beta\alpha}} - \frac{\Delta\beta}{2r_{\alpha\beta}} \right) \quad (4.78)$$

Next, resolve the stresses in the α direction at 0. There are three stresses on each face. The stress is $P_{\alpha\alpha}$ in the direction α at 0, and is

$$P_{\alpha\alpha} - \frac{\delta P_{\alpha\alpha}}{\delta\alpha} \frac{\Delta\alpha}{2} \quad (4.79)$$

at face AFED and

$$P_{\alpha\alpha} + \frac{\delta P_{\alpha\alpha}}{\delta\alpha} \frac{\Delta\alpha}{2} \quad (4.80)$$

at face BCHG (Figure.4.5).

For the forces, the stresses must be multiplied by the appropriate areas.

Force on ABCD in direction α

$$-\Delta\alpha\Delta\gamma \left(1 + \frac{\Delta\gamma}{2r_{\alpha\gamma}} - \frac{\Delta\alpha}{2r_{\gamma\alpha}}\right) \left\{ \left(P_{\beta\beta} - \frac{\delta P_{\beta\beta}}{\delta\beta} \frac{\Delta\beta}{2} \right) \frac{\Delta\beta}{2r_{\beta\alpha}} + \left(P_{\beta\alpha} - \frac{\delta P_{\beta\alpha}}{\delta\beta} \frac{\Delta\beta}{2} \right) \right\}$$

(4.81)

Neglecting second order of small quantities, this is

$$-\Delta\alpha\Delta\beta\Delta\gamma \left\{ \frac{P_{\beta\beta}}{2r_{\beta\alpha}} - \frac{1}{2} \frac{\delta P_{\beta\alpha}}{\delta\beta} + P_{\beta\alpha} \left(1 + \frac{\Delta\gamma}{2\Delta\beta r_{\alpha\gamma}} - \frac{\Delta\alpha}{2\Delta\beta r_{\gamma\alpha}}\right) \right\}$$

(4.82)

Force on BCHG

$$\Delta\beta\Delta\gamma \left(1 - \frac{\Delta\alpha}{r_{\gamma\alpha}} + \frac{\Delta\alpha}{r_{\beta\alpha}} + \frac{\Delta\beta}{2r_{\gamma\beta}} - \frac{\Delta\gamma}{2r_{\beta\gamma}}\right) \left\{ \left(P_{\alpha\alpha} + \frac{\Delta P_{\alpha\alpha}}{\delta\alpha} \frac{\Delta\alpha}{2} \right) + \frac{\Delta\alpha}{2r_{\alpha\gamma}} P_{\alpha\gamma} - \frac{\Delta\alpha}{2r_{\alpha\beta}} P_{\alpha\beta} \right\}$$

(4.83)

and neglecting second order of small quantities,

$$\Delta\alpha\Delta\beta\Delta\gamma \left\{ P_{\alpha\alpha} \left(1 - \frac{1}{r_{\gamma\alpha}} + \frac{1}{r_{\beta\alpha}} + \frac{\Delta\beta}{2\Delta\alpha r_{\gamma\beta}} - \frac{\Delta\gamma}{2\Delta\alpha r_{\beta\gamma}}\right) + 1/2 \frac{\delta P_{\alpha\alpha}}{\delta\alpha} + \frac{P_{\alpha\gamma}}{2r_{\alpha\gamma}} - \frac{P_{\alpha\beta}}{2r_{\alpha\beta}} \right\}$$

(4.84)

Force on AFED

$$-\Delta\beta\Delta\gamma \left(1 - \frac{\Delta\gamma}{2r_{\beta\gamma}} + \frac{\Delta\beta}{2r_{\gamma\beta}}\right) \left\{ \left(P_{\alpha\alpha} - \frac{\delta P_{\alpha\alpha}}{\delta\alpha} \frac{\Delta\alpha}{2} \right) - \frac{\Delta\alpha}{2r_{\alpha\gamma}} P_{\alpha\gamma} + \frac{\Delta\alpha}{2r_{\alpha\beta}} P_{\alpha\beta} \right\}$$

(4.85)

giving

$$-\Delta\alpha\Delta\beta\Delta\gamma \left\{ P_{\alpha\alpha} \left(1 - \frac{\Delta\gamma}{2\Delta\alpha r_{\beta\gamma}} + \frac{\Delta\beta}{2\Delta\alpha r_{\gamma\beta}}\right) - 1/2 \frac{\delta P_{\alpha\alpha}}{\delta\alpha} - \frac{P_{\alpha\gamma}}{2r_{\alpha\gamma}} + \frac{P_{\alpha\beta}}{2r_{\alpha\beta}} \right\}$$

(4.86)

Combining (4.84) and (4.86) gives

$$-\Delta\alpha\Delta\beta\Delta\gamma \left\{ P_{\alpha\alpha} \left(\frac{1}{r_{\gamma\alpha}} - \frac{1}{r_{\beta\alpha}} \right) - \frac{\delta P_{\alpha\alpha}}{\Delta\alpha} - \frac{P_{\alpha\gamma}}{r_{\alpha\gamma}} + \frac{P_{\alpha\beta}}{r_{\alpha\beta}} \right\} \quad (4.87)$$

Force on EFGH

$$-\Delta\alpha\Delta\gamma \left(1 + \frac{\Delta\beta}{r_{\gamma\beta}} - \frac{\Delta\beta}{r_{\alpha\beta}} - \frac{\Delta\alpha}{2r_{\gamma\alpha}} + \frac{\Delta\gamma}{r_{\alpha\gamma}} \right) \left\{ \left(P_{\beta\beta} + \frac{\delta P_{\beta\beta}}{\delta\beta} \frac{\Delta\beta}{2} \right) \frac{\Delta\beta}{2r_{\beta\alpha}} - \left(P_{\beta\alpha} + \frac{\delta P_{\beta\alpha}}{\delta\beta} \frac{\Delta\beta}{2} \right) \right\} \quad (4.88)$$

gives

$$-\Delta\alpha\Delta\beta\Delta\gamma \left\{ \frac{P}{2r_{\beta\alpha}} - \frac{1}{2} \frac{\delta P_{\beta\alpha}}{\delta\beta} - P_{\beta\alpha} - P_{\beta\alpha} \left(\frac{1}{r_{\gamma\beta}} - \frac{1}{r_{\alpha\beta}} \right) - P_{\beta\alpha} \frac{\Delta\gamma}{2\Delta\beta r_{\alpha\gamma}} + P_{\beta\alpha} \frac{\Delta\alpha}{2\Delta\beta r_{\gamma\alpha}} \right\} \quad (4.89)$$

Combining (4.82) and (4.89)

$$-\Delta\alpha\Delta\beta\Delta\gamma \left\{ \frac{P_{\beta\beta}}{r_{\beta\alpha}} - \frac{\delta P_{\beta\alpha}}{\delta\beta} - P_{\beta\alpha} \left(\frac{1}{r_{\delta\beta}} - \frac{1}{r_{\alpha\beta}} \right) \right\} \quad (4.90)$$

Force on ABGF

$$-\Delta\alpha\Delta\beta \left(1 - \frac{\Delta\beta}{2r_{\alpha\beta}} + \frac{\Delta\alpha}{2r_{\beta\alpha}} \right) \left\{ \frac{P_{\gamma\gamma}}{-2r} + P_{\gamma\alpha} - \frac{\delta P_{\gamma\alpha}}{\delta\gamma} \frac{\Delta\gamma}{2} \right\} -$$

$$-\Delta\alpha\Delta\beta\Delta\gamma \left\{ \frac{-P_{\gamma\gamma}}{2r_{\gamma\alpha}} + P_{\alpha\alpha} \left(1 - \frac{\Delta\beta}{2\Delta\gamma r_{\alpha\beta}} + \frac{\Delta\alpha}{2\Delta\gamma r_{\beta\alpha}} \right) - \frac{1}{2} \frac{\delta P_{\gamma\alpha}}{\delta\gamma} \right\} \quad (4.91)$$

Force on CDEH

$$-\Delta\alpha\Delta\beta \left(1 + \frac{\Delta\gamma}{r_{\alpha\gamma}} - \frac{\Delta\gamma}{r_{\beta\gamma}} + \frac{\Delta\alpha}{2r_{\beta\alpha}} - \frac{\Delta\beta}{2r_{\alpha\beta}} \right) \left\{ \frac{-\Delta\gamma}{2r_{\gamma\alpha}} P_{\gamma\gamma} - P_{\gamma\alpha} - \frac{\delta P_{\gamma\alpha}}{\delta\gamma} \frac{\Delta\gamma}{2} \right\}$$

Giving

$$-\Delta\alpha\Delta\beta\Delta\gamma \left\{ \frac{-P_{\gamma\gamma}}{2r_{\gamma\alpha}} - \frac{1}{2} \frac{\delta P_{\gamma\alpha}}{\delta\gamma} - P_{\gamma\alpha} \left(1 + \frac{1}{r_{\alpha\gamma}} - \frac{1}{r_{\beta\gamma}} + \frac{\Delta\alpha}{2\Delta\gamma r_{\beta\alpha}} - \frac{\Delta\beta}{2\Delta\gamma r_{\alpha\beta}} \right) \right\} \quad (4.93)$$

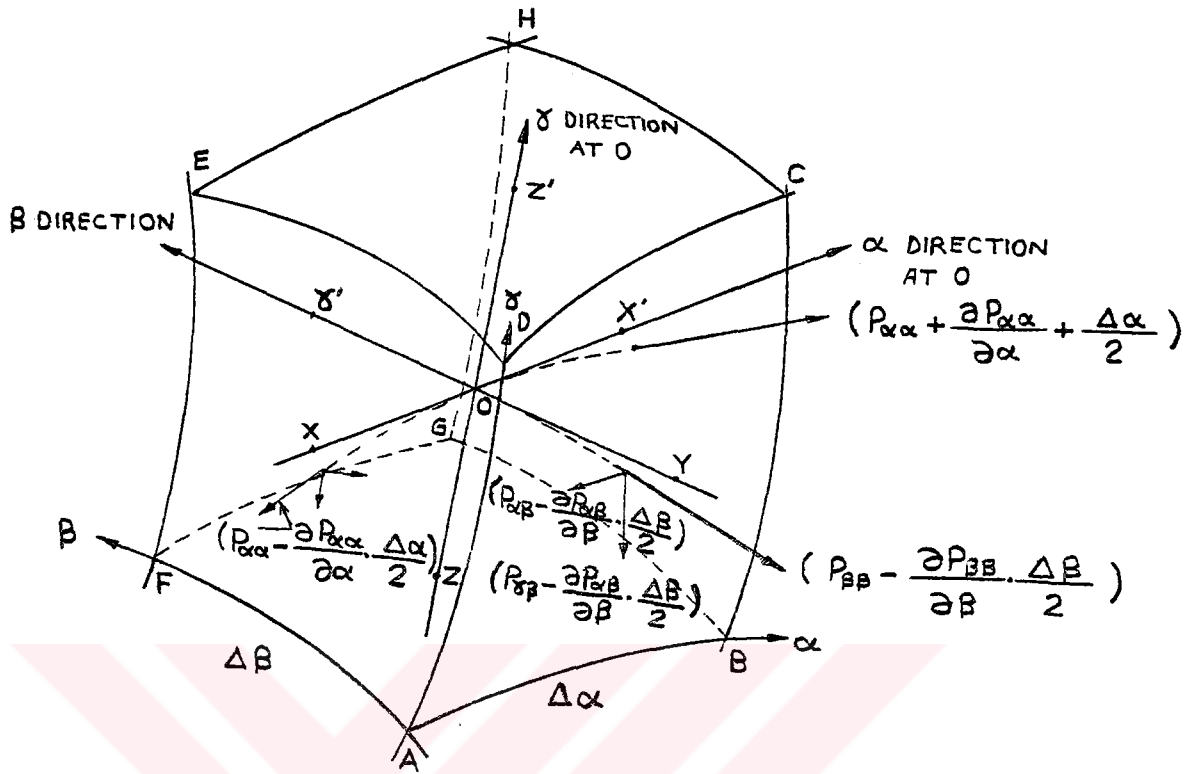


Figure.4.5 Stress nomenclature for a three dimensional curvilinear element[1]

Combining (4.91) and (4.93)

$$-\Delta\alpha\Delta\beta\Delta\gamma \left\{ \frac{P_{\gamma\gamma}}{r_{\gamma\alpha}} - \frac{\delta P_{\gamma\alpha}}{\delta\gamma} - P_{\gamma\alpha} \left(\frac{1}{r_{\alpha\gamma}} - \frac{1}{r_{\beta\gamma}} \right) \right\} \quad (4.94)$$

Finally combining (4.87), (4.90) and (4.94) and equating to zero the final equilibrium equations can be obtained and given in the following page.

The sign convention in equilibrium equation :

If the three curvilinear axes are chosen arbitrarily convex to one another at the origin, so that the areas of the faces of a curvilinear element increase in the positive directions of the axes, then with the convention used for

shear stress direction there will be a positive contribution to the force resolved in the direction of any axis, from each stress component. Thus, if the curvatures of the coordinate axes are such that the angles are positive, and the six radii of curvature of the three (convex to one another) axes denoted positive, then all terms in equilibrium equations will be zero.

If the sign convention for the angular displacement in the positive direction along an axis shown in the Figure. 4.4 is adapted, then three of the radii of curvature of the three (convex to another) axes become negative, namely $r_{\alpha\beta}$, $r_{\beta\gamma}$ and $r_{\gamma\alpha}$. Hence the negative signs between the terms in equilibrium equations.

Final Equilibrium Equations:

In the positive α -direction:

$$\frac{\delta P_{\alpha\alpha}}{\delta\alpha} + \frac{\delta P_{\beta\alpha}}{\delta\beta} + \frac{\delta P_{\gamma\alpha}}{\delta\gamma} + \frac{P_{\alpha\alpha} - P_{\beta\beta}}{r_{\beta\alpha}} - \frac{P_{\alpha\alpha} - P_{\gamma\gamma}}{r_{\gamma\alpha}} - P_{\alpha\beta} \left(\frac{2}{r_{\alpha\beta}} - \frac{1}{r_{\beta\gamma}} \right) + P_{\alpha\gamma} \left(\frac{2}{r_{\alpha\gamma}} - \frac{1}{r_{\beta\gamma}} \right) = 0 \quad (4.95)$$

In the positive β -direction:

$$\frac{\delta P_{\beta\beta}}{\delta\beta} + \frac{\delta P_{\beta\alpha}}{\delta\alpha} + \frac{\delta P_{\beta\gamma}}{\delta\gamma} + \frac{P_{\beta\beta} - P_{\gamma\gamma}}{r_{\gamma\beta}} - \frac{P_{\beta\beta} - P_{\alpha\alpha}}{r_{\alpha\beta}} - P_{\beta\alpha} \left(\frac{2}{r_{\beta\alpha}} - \frac{1}{r_{\alpha\gamma}} \right) + P_{\beta\gamma} \left(\frac{2}{r_{\beta\gamma}} - \frac{1}{r_{\alpha\gamma}} \right) = 0 \quad (4.96)$$

In the positive γ -direction:

$$\frac{\delta P_{\gamma\gamma}}{\delta\gamma} + \frac{\delta P_{\gamma\alpha}}{\delta\alpha} + \frac{\delta P_{\gamma\beta}}{\delta\beta} + \frac{P_{\gamma\gamma} - P_{\alpha\alpha}}{r_{\alpha\gamma}} - \frac{P_{\gamma\gamma} - P_{\beta\beta}}{r_{\beta\gamma}} - P_{\gamma\alpha} \left(\frac{2}{r_{\gamma\alpha}} - \frac{1}{r_{\beta\alpha}} \right) + P_{\gamma\beta} \left(\frac{2}{r_{\gamma\beta}} - \frac{1}{r_{\alpha\beta}} \right) = 0 \quad (4.97)$$

By using $P_{\alpha\gamma}=0$; $P_{\beta\gamma}=0$; $r_{\gamma\alpha} \rightarrow \infty$; $r_{\alpha\gamma} \rightarrow \infty$; $r_{\beta\gamma} \rightarrow \infty$
Equilibrium equations reduce to :

α -direction

$$\frac{\delta P_{\alpha\alpha}}{\delta\alpha} + \frac{\delta P_{\beta\alpha}}{\delta\beta} + \frac{P_{\alpha\alpha} - P_{\beta\beta}}{r_{\beta\alpha}} - \frac{P_{\alpha\alpha} - P_{\gamma\gamma}}{r_{\gamma\alpha}} - P_{\alpha\beta} \left(\frac{2}{r_{\alpha\beta}} - \frac{1}{r_{\beta\gamma}} \right) = 0 \quad (4.98)$$

FACE	NORMAL STRESS	SHEAR STRESS
AFED	$-(P_{\alpha\alpha} - \frac{\delta P_{\alpha\alpha}}{\delta\alpha} \frac{\Delta\alpha}{2})$	$(P_{\alpha\beta} - \frac{\delta P_{\alpha\beta}}{\delta\alpha} \frac{\Delta\alpha}{2}) (\frac{\Delta\alpha}{2});$ $(P_{\alpha\gamma} - \frac{\delta P_{\alpha\gamma}}{\delta\alpha} \frac{\Delta\alpha}{2}) (\frac{\Delta\alpha}{2});$ $-2r_{\alpha\beta}$ $2r_{\alpha\gamma}$
BCHG	$(P_{\alpha\alpha} + \frac{\delta P_{\alpha\alpha}}{\delta\alpha} \frac{\Delta\alpha}{2})$	$-(P_{\alpha\beta} + \frac{\delta P_{\alpha\beta}}{\delta\alpha} \frac{\Delta\alpha}{2}) (\frac{\Delta\alpha}{2});$ $(P_{\alpha\gamma} + \frac{\delta P_{\alpha\gamma}}{\delta\alpha} \frac{\Delta\alpha}{2}) (\frac{\Delta\alpha}{2});$ $-2r_{\alpha\beta}$ $2r_{\alpha\gamma}$
ABCD	$(P_{\beta\beta} - \frac{\delta P_{\beta\beta}}{\delta\beta} \frac{\Delta\beta}{2}) \frac{\Delta\beta}{2r_{\beta\alpha}}$	$0;$ $-(P_{\beta\alpha} - \frac{\delta P_{\beta\alpha}}{\delta\beta} \frac{\Delta\beta}{2})$
EFGH	$(P_{\beta\beta} + \frac{\delta P_{\beta\beta}}{\delta\beta} \frac{\Delta\beta}{2}) \frac{\Delta\beta}{2r_{\beta\alpha}}$	$0;$ $(P_{\beta\alpha} + \frac{\delta P_{\beta\alpha}}{\delta\beta} \frac{\Delta\beta}{2})$
ABGF	$-(P_{\gamma\gamma} - \frac{\delta P_{\gamma\gamma}}{\delta\gamma} \frac{\Delta\gamma}{2}) (\frac{\Delta\gamma}{2})$ $-2r_{\gamma\alpha}$	$-(P_{\gamma\alpha} - \frac{\delta P_{\gamma\alpha}}{\delta\gamma} \frac{\Delta\gamma}{2});$ 0
CDEF	$-(P_{\gamma\gamma} + \frac{\delta P_{\gamma\gamma}}{\delta\gamma} \frac{\Delta\gamma}{2}) (\frac{\Delta\gamma}{2})$ $-2r_{\gamma\alpha}$	$(P_{\gamma\alpha} + \frac{\delta P_{\gamma\alpha}}{\delta\gamma} \frac{\Delta\gamma}{2});$ 0

TABLE 4.1. Normal and shear stresses acting on forces of a three dimensional curvilinear element.[1]

β -direction:

$$\frac{\delta P_{\beta\beta}}{\delta\beta} + \frac{\delta P_{\beta\alpha}}{\delta\alpha} + \frac{P_{\beta\beta} - P_{\gamma\gamma}}{r_{\gamma\beta}} - \frac{P_{\beta\beta} - P_{\alpha\alpha}}{r_{\alpha\beta}} + P_{\beta\alpha} \left(\frac{2}{r_{\beta\alpha}} - \frac{1}{r_{\gamma\alpha}} \right) = 0 \quad (4.99)$$

γ -direction:

$$\frac{P_{\gamma\gamma} - P_{\alpha\alpha}}{r_{\alpha\gamma}} - \frac{P_{\gamma\gamma} - P_{\beta\beta}}{r_{\beta\gamma}} = 0 \quad (4.100)$$

$$K = \frac{r_{\beta\gamma} - X r_{\alpha\gamma}}{r_{\beta\gamma} - r_{\alpha\gamma}} \quad (4.101)$$

$$P_{\gamma\gamma} = P_{\alpha\alpha} K \quad ; \quad P_{\beta\beta} = P_{\alpha\alpha} X \quad (4.102)$$

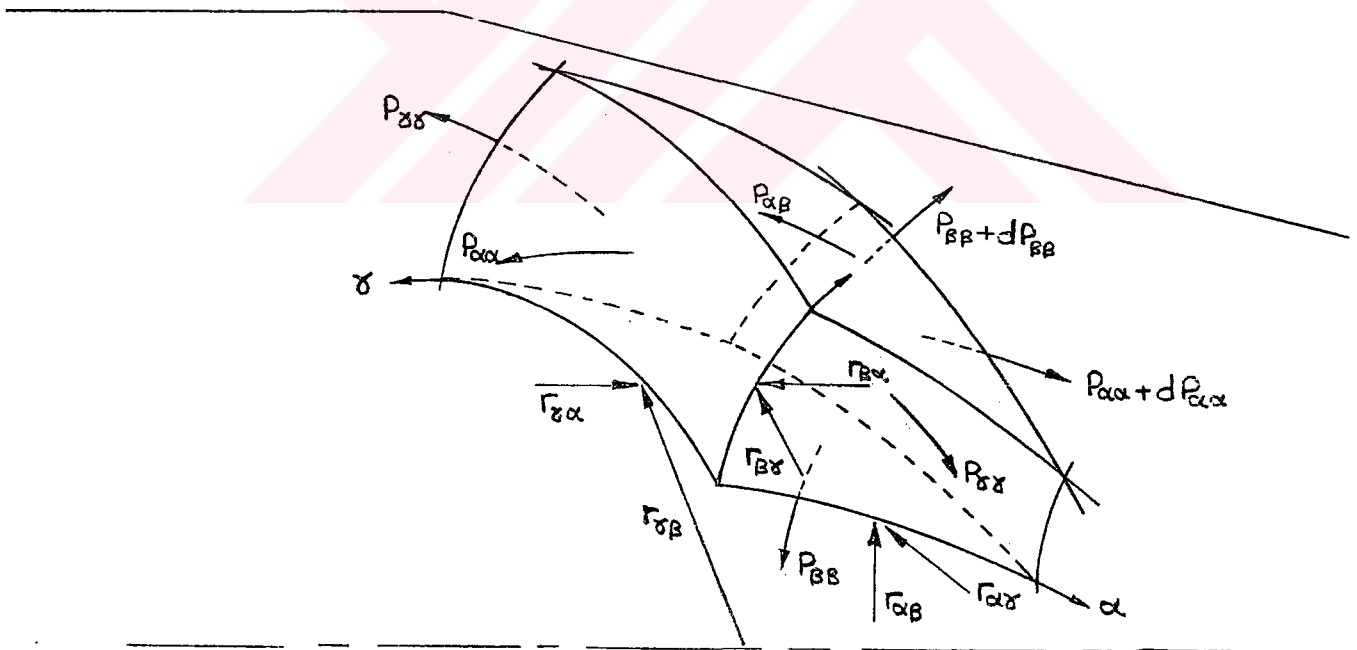


Figure.4.6 Radius of curvature and stress nomenclature for a deforming element in wire-drawing process

Final equilibrium equations:

α -Direction

$$\frac{\delta P_{\alpha\alpha}}{\delta\alpha} + \frac{\delta P_{\beta\alpha}}{\delta\beta} + \frac{P_{\alpha\alpha} - P_{\beta\beta}}{r_{\beta}} - P_{\alpha\beta} \left(\frac{2}{r_{\alpha}} - \frac{1}{r_{\gamma}} \right) = 0 \quad (4.103)$$

β -direction

$$\frac{\delta P_{\beta\beta}}{\delta\beta} + \frac{\delta P_{\beta\alpha}}{\delta\alpha} + \frac{P_{\beta\beta} - P_{\alpha\alpha}}{r_{\gamma}} - \frac{P_{\beta\beta} - P_{\alpha\alpha}}{r_{\alpha}} + P_{\beta\alpha} \left(\frac{2}{r_{\beta}} \right) = 0 \quad (4.104)$$



4.2 Analytical Analysis of Wire-Drawing Process

Certain basic relationships can be developed from energy considerations. The work done on the wire is expended in three ways:

- i/ In changing the wire dimensions.
- ii/ In redundant deformation that does not appear as a change in wire cross-section
- iii/ In overcoming friction.

In wire-drawing assumption of uniform stress throughout the wire leads to approximately correct values of drawing force for certain limited combinations of the die angle and reduction [6]. In general, the deformation is not homogenous; plane sections do not remain plane on passing through the die, and extra work is expended in distortions which do not contribute to the final reduction in diameter, i.e., as redundant deformation. If α is the semi-angle of the die cone, the area in contact with the die is $(A_1 - A_2) / \sin\alpha$ and for equilibrium, equating drawing force, P , and forces due to mean die pressure, q_m ,

$$P = (A_1 - A_2) (1 + \mu \cot\alpha) q_m \quad (4.105)$$

If D_1 is the initial diameter and D_2 the final diameter of the wire, the length of the wire in contact with the die $L = (D_1 - D_2) / 2 \sin\alpha$ and the splitting force S between the two halves of the die is given by

$$S = q_m ((D_1 + D_2) / 2) L (\cos\alpha - \mu \sin\alpha) \quad (4.106)$$

From equations (4.105) and (4.106)

$$\mu = \frac{1 - \pi(S/P) \tan\alpha}{\tan\alpha + \pi(S/P)} \quad (4.107)$$

and

$$q_m = \pi S / (A_1 - A_2) (\cot \alpha - \mu) \quad (4.108)$$

If it is assumed that the deformation is homogenous and that there is no friction between wire and die, then the work expended per unit volume in reducing the area of cross-section of the wire from A_1 to A_2 will be $Y_m \ln A_1/A_2$ where Y_m is the mean yield stress. The work done in the producing unit length of wire is then PA_2 and the work per unit volume is simply the drawing stress P . Therefore

$$P = Y_m \ln A_1/A_2 \quad (4.109)$$

This is the most efficient, or ideal, means of reducing the wire diameter and it gives the unattainable minimum value of the drawing stress.

The variation of the die pressure with percentage reduction is shown in Figure 4.7, for three different die angles [6].

The variation of drawing force with percentage reduction of area for the same three die angles is shown in Figure 9. It will be noticed that the curves do not pass through the origin when extrapolated. The explanation of this apparent intercept on the ordinate axis lies in the fact that for very light reductions the wire bulges prior to its entry to the die

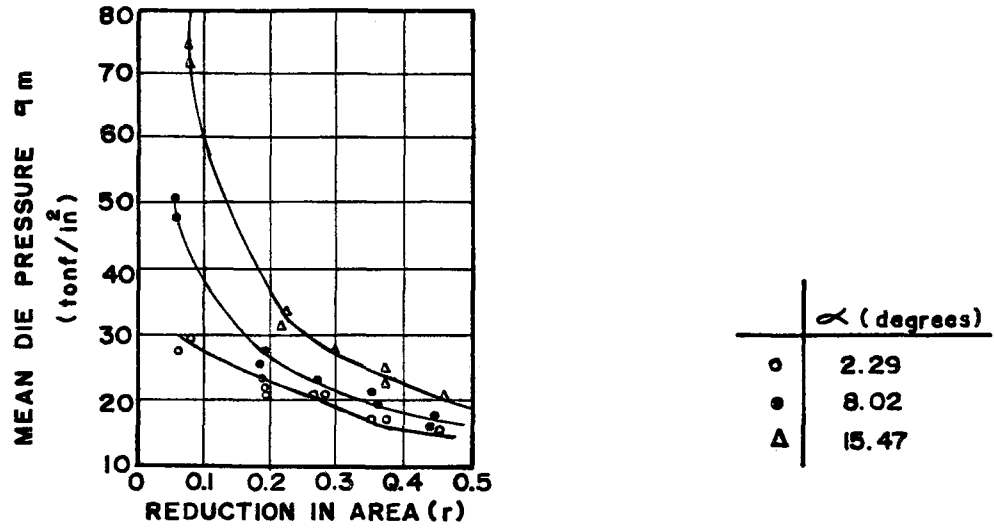


Figure.4.7. Variation of mean die pressure with reduction [6]

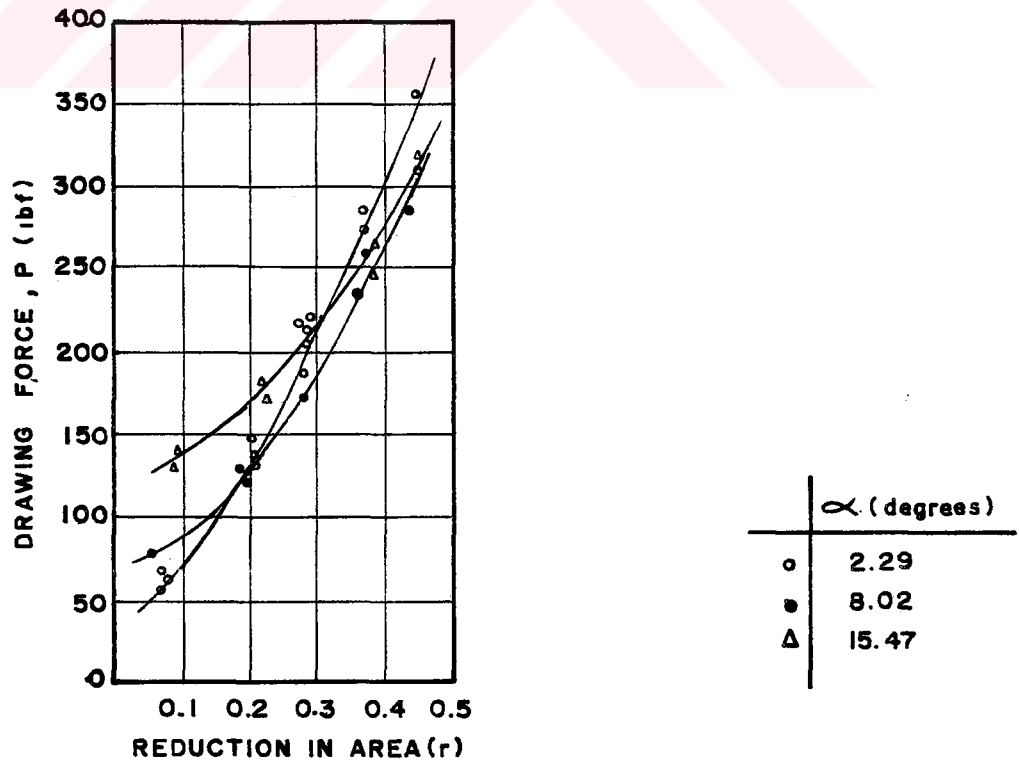
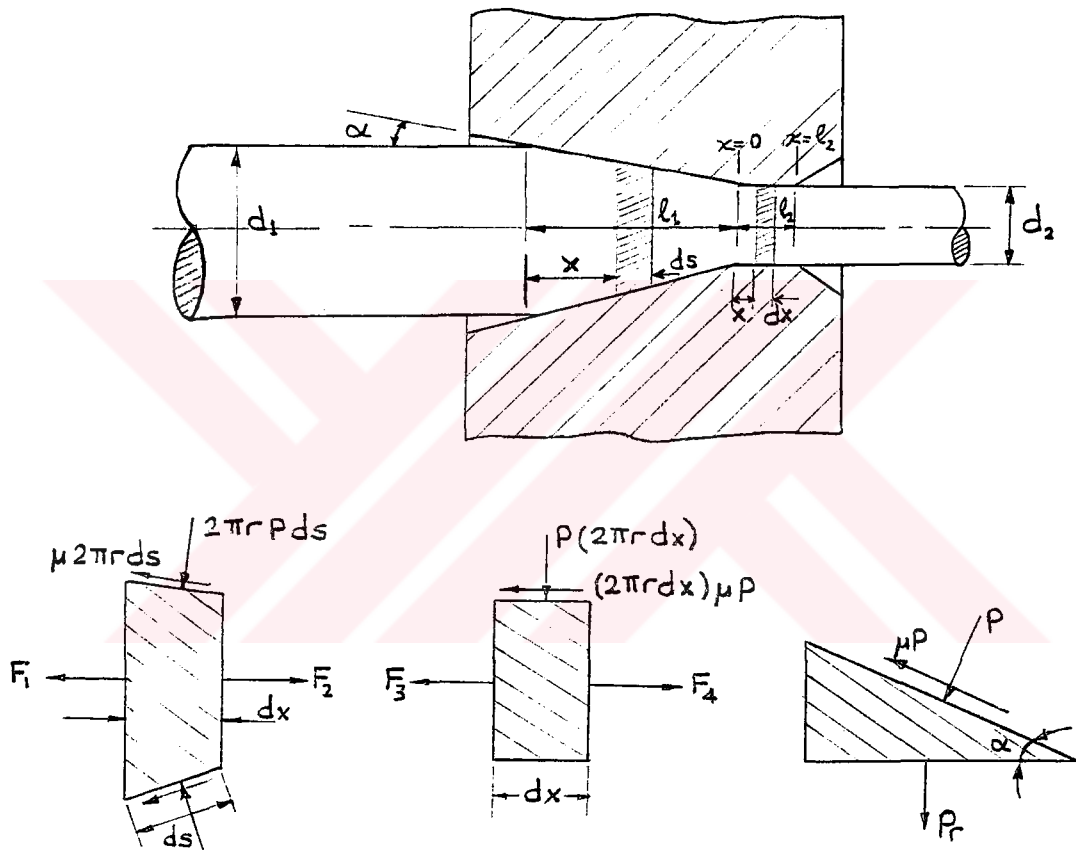


Figure.4.8. Variation of drawing force with reduction [6]

4.2.1 Derivation of Equations

Analysis for the first trial value of X



$$F_1 = P_X \cdot A$$

$$F_3 = P_X \cdot A_2$$

$$F_2 = P_X \cdot A + ((\delta / \delta x) (P_X \cdot A) dx) \quad F_4 = P_X \cdot A_2 + d(P_X \cdot A_2)$$

Figure.4.9 Sketch of wire-drawing showing forces applied to strips of infinitesimal length.[65]

P_x : Longitudinal (drawing stress)

P : Normal die pressure

P_r : Radial stress

An equilibrium of the longitudinal forces:

$$(\delta/\delta x)(P_x A)dx - 2\pi r P ds(\sin\alpha + \mu\cos\alpha) = 0 \quad (4.110)$$

where A is the cross-sectional area of the wire at point x .

[65]

$$dx/ds = \cos\alpha \quad \& \quad ds = dx/\cos\alpha \quad (4.111)$$

$$(\delta/\delta x)(P_x A) = 2\pi r P(\tan\alpha + \mu)$$

$$d(P_x A) = 2\pi r P(\tan\alpha + \mu)dx \quad (4.112)$$

$$A = \pi r^2 \quad \Rightarrow \quad dx = dA/2\pi r \tan\alpha \quad (4.113)$$

By substituting equation (4.113) into equation (4.112)

$$d(P_x A) = P(1 + \mu\cot\alpha)dA \quad (4.114)$$

Equilibrium of the transverse forces:

$$P_r = P(\mu\sin\alpha - \cos\alpha)(ds/dx) \quad (4.115)$$

or

$$P_r = P(\mu\tan\alpha - 1) \quad (4.116)$$

By substituting equation (4.116) into (4.114)

$$d(P_x A) = - \left(\frac{1 + \mu \cot \alpha}{1 - \mu \tan \alpha} \right) P_r dA \quad (4.117)$$

$$C = \frac{1 + \mu \cot \alpha}{1 - \mu \tan \alpha} \quad (4.118)$$

$$d(P_x A) = -C P_r dA \quad (4.119)$$

Differentiating equation (4.114)

$$A(dP_x/dA) + P_x = P(1 + \mu \cot \alpha) \quad (4.120)$$

A second equation for the stresses is given by the yield criterion of the material.

The Tresca yield criterion gives:

$$P_x - P = Y \quad (4.121)$$

The yield criterion adapted will be

$$P_x - P = mY \quad (4.122)$$

Where m is a constant obtained by the method of least squares to satisfy Von Mises' criterion. The stress, P , is obtained from the assumed yield criterion and substituted in the equilibrium equation 4.120, to give

$$\frac{dP_x}{P_x \mu \cot \alpha - mY(1 + \mu \cot \alpha)} = \frac{dA}{A} \quad (4.123)$$

Integrating:

$$\frac{1}{\mu \cot \alpha} \ln \{ P_x \mu \cot \alpha - mY(1 + \mu \cot \alpha) \} = \ln AK \quad (4.124)$$

or:
$$P_x \mu \cot \alpha - mY(1 + \mu \cot \alpha) = (AK)^{\mu \cot \alpha} \quad (4.125)$$

Where K is a constant obtained by knowing that
 at $A=A_0$ (die entry), $P_x=0$ (4.126)

$$\frac{P_x}{mY} = \left(1 + \frac{1}{\mu \cot \alpha}\right) \left\{1 - \left(\frac{A}{A_0}\right)^{\mu \cot \alpha}\right\} \quad (4.127)$$

$$C = \frac{P_x}{mY} \quad (4.128)$$

and

$$\frac{P}{mY} - \frac{P_x}{mY} - 1 = C - 1 \quad (4.129)$$

By introducing a stress ratio: $X = P/P_x$ (4.130)

$$X = \frac{C-1}{C} \quad \text{(This is used for the first trial value of X in numerical analysis.)} \quad (4.131)$$

This equation was derived by Sachs(1927) and in the analysis frictional force is taken into account [65]. So far, the non-useful work of distortion has not been taken into account.

Siebel's Theory: Siebel (1947) has proposed a theory of wire drawing in which he assumes that the effect of homogenous deformation, friction and non-useful distortion are additive. He assumes that the plastic region with the die is bounded by spherical caps with centres at the virtual apex of the cone.

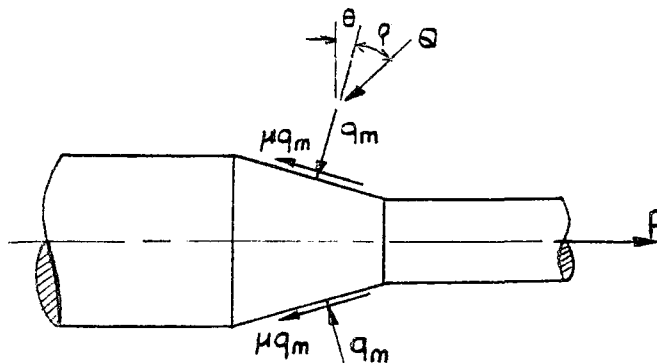


Figure. 4.10. External forces acting during wire-drawing [67]

As the wire enters and leaves the die it is sheared instantaneously along these surfaces and within the die the metal moves towards the virtual apex of the cone.

As shown in Figure.4.10.the force on the die element, Q , is inclined at an angle ρ to the normal to the die, where $\rho = \tan \mu$. Resolving these forces [67].

$$Q = P / (\sin(\theta + \rho)) \quad (4.132)$$

Siebel continues his analysis by saying that a fairly accurate picture of the drawing process can be obtained by imagining that the mean die pressure attains the yield stress of the material Y_m . Since the actual area of the die is $(A_1 - A_2) / \sin\theta$

$$Q = Y_m \frac{A_1 - A_2}{\sin\theta} \quad (4.133)$$

Substituting equation (4.133) into equation (4.132)

$$P = Y_m (A_1 - A_2) \frac{\sin(\theta + \rho)}{\sin\theta} \quad (4.134)$$

$$P \approx Y_m (A_1 - A_2) (1 + (\mu/\theta)) \quad (4.135)$$

Siebel then divides the energy of deformation into useful energy and lost energy. By analogy with the previous processes discussed the useful energy per unit volume is $Y_m \ln(A_1/A_2)$. It can be seen from equation (4.135), after realizing that $Y_m (A_1 - A_2) \approx Y_m A_2 \ln(A_1/A_2)$, that the energy lost due to friction is approximately $(\mu/\theta) Y_m \ln(A_1/A_2)$. The energy lost due to redundant working occurs mainly at entry and exit, and may be determined as follows. The material entering R_1 shears through an angle α , and it may be assumed that

$\alpha = (R/R_1)\theta$. The work done per unit volume in shearing through the angle α is $k\alpha = k(R/R_1)\theta$, where k is the yield shear stress.

For a small element of length dx entering the deformation zone the element of work done is $k(R/R_1)\theta 2\pi R dR dx$. Assuming the Tresca criterion, the total work in entering is therefore $2/3\pi k\theta R_1^2 dx$, and since the volume entering $\pi R_1^2 dx$, the redundant energy per unit volume in entering is $2/3k\theta$, or $(Y/3)\theta$. For both entry and exit redundant shearing the lost work is therefore $2/3Y_m\theta$. Summarizing, the total drawing stress is given by the sum of these terms:

$$P\alpha = Y_m \left[\left(1 + \frac{\mu}{\alpha}\right) \ln \frac{A_1}{A_2} + \frac{2}{3}\alpha \right] \quad (4.136)$$

The first term accounts for the homogenous deformation, the second the frictional component and the third the additional force required because of non-useful distortion.

Whitton empirical formula: Whitton (1958) has compared the drawing forces based on the above theories with experimental values obtained by Wistreich. In an attempt to get closer correlation with the experimental results, Whitton devised the following empirical formula [6]:

$$P = A_2 Y_m (1 + \cot(\alpha/\mu)) \left[1 - (A_2/A_1)^{\mu \cot \alpha} \right] + 2A_2 Y_m \alpha^2 (1-r)/3r \quad (4.137)$$

where r is the reduction of area $(A_1 - A_2)/A_1$. The final term is the extra drawing force for the non-useful distortion. The accuracy of the formula is within ± 10 percent for the experimental results.

4.3 Numerical Solution of The Drawing Region

In order to define the deformation variables as a function of space, an initially orthogonal, square grid is embedded in the material. As the deformation progresses, the grid elements turn into non-orthogonal curvilinear shape. It is necessary to follow this deformation pattern throughout the deformation sequence because of the history dependence of the plasticity laws.

Beginning from the original stage, to be able to solve the next deformation stage; associated boundary conditions have to be specified. Starting from these boundaries with known initial values, the solution can proceed in a stepwise algorithm. After the solution is completed, the next stage can be analysed similarly, provided that the boundary conditions are up-dated with respect to the new configuration.

4.3.1 Boundary Conditions

1 /Axial-symmetry line

A-Qualitative conditions:

i- Shear terms are zero along this line.

$$\delta\epsilon_{\alpha\beta} = \delta\epsilon_{\beta\alpha} = 0 \quad (4.138)$$

Similarly the total shear strain is zero:

$$ii- \epsilon_{\alpha\beta} = \epsilon_{\beta\alpha} = 0 \quad (4.139)$$

Consequently:

$$iii- P_{\alpha\beta} = P_{\beta\alpha} = 0 \quad (4.140)$$

$v = Y = 0$ for all points moving along this axial symmetry line, throughout the deformation stage. The slope of β -lines are identically zero at all stages of deformation due to geometrical symmetry. As a consequence, any associated variable has zero rate of change with respect to β -direction.

$$v = \delta / \delta \beta = 0 \quad (4.141)$$

and since $r_{\alpha\alpha} = \infty$

$$v = 1 / r_{\alpha\alpha} = 0 \quad (4.142)$$

B. Quantitative conditions:

Incremental strain in α -direction ($\delta \epsilon_{\alpha\alpha}$) is assumed at the beginning of numerical solution. The solution proceeds along the beta direction until the interface between die and wire is reached. At this final node along the beta direction, this assumed incremental strain is checked with the radius by comparing the coordinate of the node. If the coordinate of the node ($\text{Beta}(I, J)$) is not equal to the reduced radius, then iteration will continue by changing the incremental strain until $\text{Beta}(I, J)$ will equal to radius.

2 / Die inlet

The following deformation variables may be taken as known parameters:

$$\delta \epsilon_{\alpha\alpha}, \delta \epsilon_{\beta\beta}, \delta \epsilon_{\gamma\gamma}, P_{\alpha\alpha}, P_{\beta\beta}, P_{\gamma\gamma}, P_{\beta\alpha}$$

and taken to be equal zero. This is a free boundary.

3 / Boundary at the interface between wire and die.

$$P_{\alpha\beta} = P_{\beta\beta} \mu \quad (4.143)$$

μ =Coefficient of friction at the interface between wire & die.

4.3.2 Formulation of the problem

The following rules are used in formulation:

- 1-Material is anisotropic.
- 2-Material strain-hardens according to Swift's law.
- 3-Hill's generalized stress and strain relations for anisotropic work-hardening material is used.
- 4-Stress field is three dimensional.
- 5-The problem is three dimensional in strains.
- 6- α -axis is a principal direction.
- 7-The variation of incremental direct strains along the sides of any grid element are assumed to be linear.
- 8-Associated variations of stresses can be described by second-order polynomials for shear.
- 9-Deformed elements have non-orthogonal, curvilinear sides, each of these sides can be expressed in terms of second order polynomials.

The following boundary conditions are given at each increment of deformation.

i-Positions of the deformed grid elements in terms of their coordinates along the die-inlet. The associated total strains are also specified.

ii- $\epsilon_{\alpha\alpha}$ value along the axial-symmetry line is assumed and then checked.

These given conditions are sufficient to complete the numerical solution. By using the above mentioned rules and the boundary conditions, the relevant plasticity equations can be summarized as follows.

A-Generalized stress and strain relations for anisotropic work hardening material:

Hill's equivalent stress equation for anisotropic work-hardening material: (for rotational symmetry)

$$\bar{P} = \sqrt{3/2} [(R(P_{\beta\beta} - P_{\gamma\gamma})^2 + (P_{\gamma\gamma} - P_{\alpha\alpha})^2 + (P_{\alpha\alpha} - P_{\beta\beta})^2 + 2NP_{\beta\alpha}^2) / (2+R)]^{1/2} \quad (4.144)$$

and generalized strain increment equation:

$$d\bar{\epsilon} = \sqrt{2/3} [(2+R) / (1+2R)]^{1/2} [(d\epsilon_{\gamma\gamma} - Rd\epsilon_{\alpha\alpha})^2 + (d\epsilon_{\beta\beta} - Rd\epsilon_{\alpha\alpha})^2 + R(d\epsilon_{\beta\beta} - d\epsilon_{\gamma\gamma})^2]^{1/2} \quad (4.145)$$

The stress ratios as previously defined

$$X = P_{\beta\beta} / P_{\alpha\alpha} \quad (4.146)$$

$$K = P_{\gamma\gamma} / P_{\alpha\alpha} \quad (4.147)$$

$$Z = P_{\beta\alpha} / P_{\alpha\alpha} \quad (4.148)$$

B-From Plastic flow rule for anisotropic material:

$$K = X \frac{(d\epsilon_{\alpha\alpha} / d\epsilon_{\beta\beta}) + (d\epsilon_{\alpha\alpha} / d\epsilon_{\gamma\gamma})R + (d\epsilon_{\alpha\alpha} / d\epsilon_{\beta\beta})R}{(d\epsilon_{\alpha\alpha} / d\epsilon_{\gamma\gamma}) + (d\epsilon_{\alpha\alpha} / d\epsilon_{\gamma\gamma})R + (d\epsilon_{\alpha\alpha} / d\epsilon_{\beta\beta})R} + \frac{(d\epsilon_{\alpha\alpha} / d\epsilon_{\gamma\gamma}) - (d\epsilon_{\alpha\alpha} / d\epsilon_{\beta\beta})}{(d\epsilon_{\alpha\alpha} / d\epsilon_{\gamma\gamma})R + (d\epsilon_{\alpha\alpha} / d\epsilon_{\beta\beta})R + (d\epsilon_{\alpha\alpha} / d\epsilon_{\gamma\gamma})} \quad (4.149)$$

$$X = \frac{2 + ((d\epsilon_{\alpha\alpha} / d\epsilon_{\beta\beta}) - (d\epsilon_{\alpha\alpha} / d\epsilon_{\gamma\gamma})) / ((d\epsilon_{\alpha\alpha} / d\epsilon_{\gamma\gamma}) + (d\epsilon_{\alpha\alpha} / d\epsilon_{\gamma\gamma})R + (d\epsilon_{\alpha\alpha} / d\epsilon_{\beta\beta})R)}{(d\epsilon_{\alpha\alpha} / d\epsilon_{\beta\beta}) + (d\epsilon_{\alpha\alpha} / d\epsilon_{\gamma\gamma})R + (d\epsilon_{\alpha\alpha} / d\epsilon_{\beta\beta})R} + (1 + \frac{\mu}{(d\gamma_{\beta\alpha} / d\epsilon_{\alpha\alpha})} (2R+1)) \quad (4.150)$$

$$Z = X\mu \quad (4.151)$$

C-Constancy of volume:

$$\delta\epsilon_{\alpha\alpha} + \delta\epsilon_{\beta\beta} + \delta\epsilon_{\gamma\gamma} = 0 \quad (4.152)$$

Consequently:

$$\delta\gamma\gamma = -(\delta\epsilon_{\alpha\alpha} + \delta\epsilon_{\beta\beta}) \quad (4.153)$$

Using Swift Law:

$$\bar{P} = A(B + \bar{\epsilon})^n \quad (4.154)$$

$$P_{\alpha\alpha}^* = \frac{A \left[B + \sqrt{\frac{2+R}{3}} \left[\frac{2+R}{(1+2R)^2} \{ (d\epsilon_{\gamma\gamma} - R d\epsilon_{\alpha\alpha})^2 + (d\epsilon_{\beta\beta} - R d\epsilon_{\alpha\alpha})^2 + R (d\epsilon_{\beta\beta} - d\epsilon_{\gamma\gamma})^2 \} \right]^{1/2} \right]^n}{\sqrt{\frac{3}{2} [(R(X-K)^2 + (K-1)^2 + (1-X)^2 + 2NZ^2) / (2+R)]^{1/2}}} \quad (4.155)$$

If $\delta\epsilon_{\alpha\alpha}$, $\delta\epsilon_{\beta\beta}$, and $\delta\gamma_{\beta\alpha}$ are known, the stress ratios X, K and Z can be computed with known anisotropic material properties R and N. Afterwards the corresponding stresses can be readily computed for a yielding material with known strain-hardening properties (A, B, and n).

D-Equations of equilibrium:

α -direction

$$\frac{\delta P_{\alpha\alpha}}{\delta\alpha} + \frac{\delta P_{\beta\alpha}}{\delta\beta} + \frac{P_{\alpha\alpha} - X P_{\beta\alpha}}{r_{\beta}} - P_{\alpha\beta} \left(\frac{2}{r_{\alpha}} - \frac{1}{r_{\gamma}} \right) = 0 \quad (4.156)$$

β -direction

$$\frac{\delta P_{\beta\beta}}{\delta\beta} + \frac{\delta P_{\beta\alpha}}{\delta\alpha} + \frac{P_{\beta\beta} - (K/X)P_{\beta\beta}}{r_\gamma} - \frac{P_{\beta\beta} - P_{\beta\beta}/X}{r_\alpha} + P_{\beta\alpha} \left(\frac{2}{r_\beta} \right) = 0 \quad (4.157)$$

Starting from a point where the stress-strain state is known or already computed, these two differential equations can be solved by integration provided that the functional variations of stresses along a finite but incremental distance are specified.

$$\int_{\alpha}^{l_\alpha = \alpha + \Delta\alpha} P_{\alpha\alpha} d\alpha = - \int_{\alpha}^{\alpha + \Delta\alpha} \frac{P_{\alpha\alpha}}{r_\beta} (1-X) d\alpha - \int_{\alpha}^{\alpha + \Delta\alpha} \frac{\delta P_{\beta\alpha}}{\delta\beta} d\alpha + \int_{\alpha}^{\alpha + \Delta\alpha} P_{\alpha\beta} \left(\frac{2}{r_\alpha} - \frac{1}{r_\gamma} \right) d\alpha \quad (4.158)$$

For an increment of $\Delta\alpha$ along α -line

$$\int_{\beta}^{l_\beta = \beta + \Delta\beta} P_{\beta\beta} d\beta = - \int_{\beta}^{\beta + \Delta\beta} \frac{P_{\beta\beta}}{r_\gamma} (1 - (K/X)) - \frac{P_{\beta\beta}}{r_\alpha} (1 - (1/X)) d\beta - \int_{\beta}^{\beta + \Delta\beta} \frac{\delta P_{\beta\alpha}}{\delta\alpha} d\beta - \int_{\beta}^{\beta + \Delta\beta} \frac{2P_{\beta\alpha}}{r_\beta} d\beta \quad (4.159)$$

For an increment of $\Delta\beta$ along a β -line

If one wants to list all of the variables in the equations of plasticity that are used :

$P_{\alpha\alpha}, P_{\beta\beta}, P_{\gamma\gamma}, P_{\beta\alpha}, \bar{\epsilon}, \bar{P}, A, B, n, R, N, X, K, Z, \delta\epsilon_{\alpha\alpha}, \delta\epsilon_{\beta\beta}, \delta\epsilon_{\gamma\gamma}, \delta\epsilon_{\beta\alpha}, \Delta\alpha, \Delta\beta, r_{\gamma\alpha}, r_{\beta\gamma}, r_{\alpha\gamma}, r_{\alpha\beta}, r_{\beta\alpha}, r_{\gamma\beta}.$

Here A, B, n, R, N are material properties. The stress ratios X, K and Z can be written in terms of incremental strains. The radius of curvatures $r_{\gamma\alpha}, r_{\beta\gamma}, r_{\alpha\gamma}$ are equal to infinity.

Then the independent unknowns can be specified as follows:

Unknowns = $P_{\alpha\alpha}, P_{\beta\beta}, P_{\gamma\gamma}, P_{\beta\alpha}, \delta\epsilon_{\alpha\alpha}, \delta\epsilon_{\beta\beta}, \delta\epsilon_{\gamma\gamma}, \delta\epsilon_{\beta\alpha}, r_{\alpha\beta}, r_{\beta\alpha}, r_{\gamma\beta}$
 these eleven unknowns can not be easily solved with the given equations of plasticity. Assume that the stress and strain states are known at two points B and C after

deformation. Point A is the neighbour point whose new coordinates and the stress strain states are going to be solved as shown figure 4.11.

Let the new x and y coordinates of point A differ by amounts of du and dv respectively, from its original coordinates.

If the curvilinear α and β -lines are assumed to be parts of second order polynomials, the coefficient of the polynomials can be determined in terms of known $x_b, y_b, x_c, y_c, x_o, y_o$ and the unknowns du and dv provided that the slopes of the lines at points B and C are known. Another way of determining the polynomials is to use two or more points.

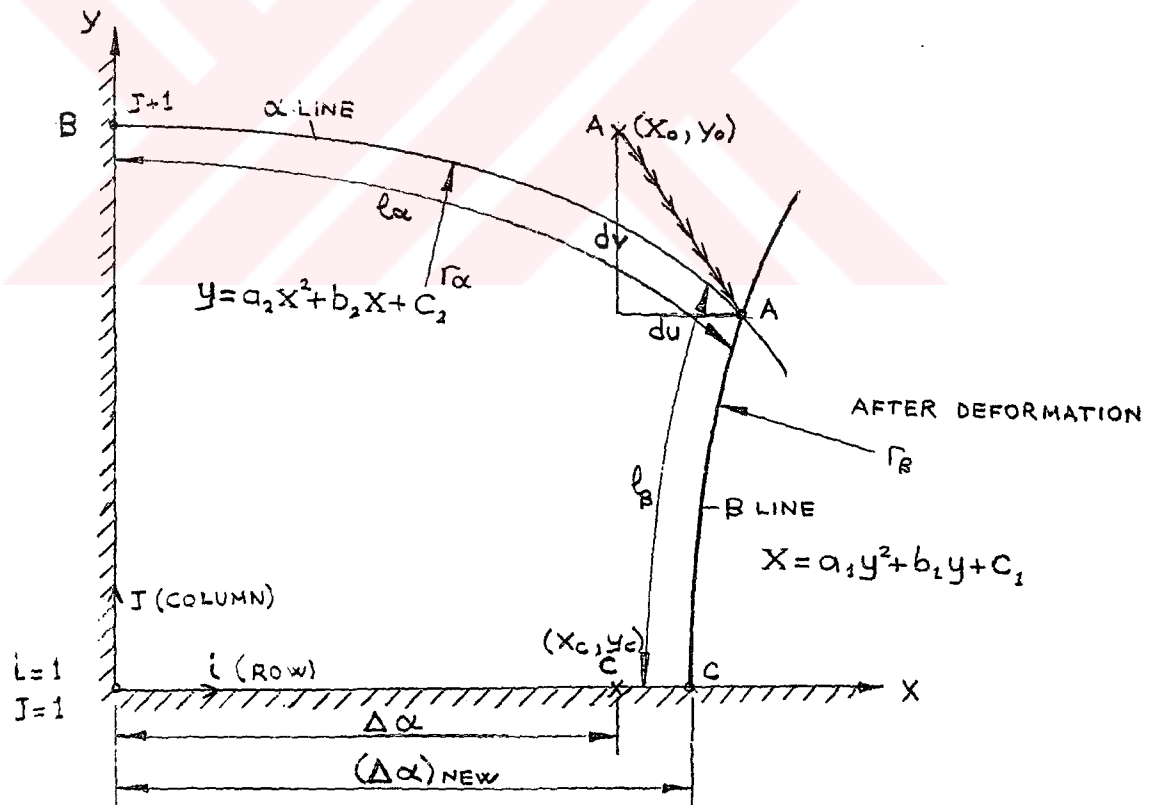


Figure.4.11 Solution along a pair of α and β -lines for the unknown point A.

After the polynomials are fitted, their curvatures can be readily determined together with appropriate signs. The arc lengths l_β and l_α can be computed by a numerical integration method where the arc length is:

$$l_\alpha = \int_{x_b}^{x_o+du} \sqrt{1 + (dy/dx)^2} dx \quad (4.160)$$

or

$$l_\alpha = \int_{x_b}^{x_o+du} \sqrt{1 + (2a_2 x + b_2)^2} dx \quad (4.161)$$

Then using equation (4.31)

$$\delta \epsilon_{\alpha\alpha}^{n+1} = \text{Ln} (l_\alpha^{n+1} / l_\alpha^n) = f_1 (du) \quad (4.162)$$

and similarly

$$\delta \epsilon_{\beta\beta}^{n+1} = \text{Ln} (l_\beta^{n+1} / l_\beta^n) = f_2 (dv) \quad (4.163)$$

with the assumption of linear variation of incremental strains over the arc lengths.

Equations 4.162 and 4.163 reduce to:

$$\delta \epsilon_{\alpha\alpha}^{n+1} \Big|_A = 2 \text{Ln} (l_\alpha^{n+1} / l_\alpha^n) - \delta \epsilon_{\alpha\alpha}^{n+1} \Big|_B = f_3 (du, dv) \quad (4.164)$$

$$\delta \epsilon_{\beta\beta}^{n+1} \Big|_A = 2 \text{Ln} (l_\beta^{n+1} / l_\beta^n) - \delta \epsilon_{\beta\beta}^{n+1} \Big|_B = f_4 (dv, du) \quad (4.165)$$

Incremental shear strains $\delta \epsilon_{\alpha\beta}^{n+1}$ can be computed by using equation 4.32.

All these manipulations indicate that the independent unknowns at point A:

Unknowns 1: $P_{\alpha\alpha}, P_{\beta\beta}, P_{\gamma\gamma}, P_{\beta\alpha}, du, dv$

This is the reduced form of unknowns where du and dv are parameters of displacement. Assuming trial values for du and dv , temporary $P_{\alpha\alpha}, P_{\beta\beta}, P_{\gamma\gamma}$ and $P_{\beta\alpha}$ values can be computed by using:

i) Swift law and Hill's generalized equivalent stress and strain relations for anisotropic work hardening material

ii) Equilibrium equation in α -direction

iii) Equilibrium equation in β -direction

iv) The last equation is convergence criteria. The convergence criterion is in fact an implicit compatibility equation.

After du and dv parameters are converged, the actual values of $P_{\alpha\alpha}$, $P_{\beta\beta}$, $P_{\gamma\gamma}$ and $P_{\beta\alpha}$ can be determined. All the other remaining variables can be solved successively.

Method of Solutions

An originally rectangular grid with a mesh size equal to L_0 and L_1 is embedded to the wire as partially shown in Figure. 4.11 whose origin is at point O. Solutions start from the boundary point where $\delta\epsilon_{\alpha\alpha}$, $\delta\epsilon_{\beta\beta}$, $\delta\epsilon_{\gamma\gamma}$, $P_{\alpha\alpha}$, $P_{\beta\beta}$, $P_{\gamma\gamma}$ and $P_{\beta\alpha}$ are known as boundary conditions. First, the next grid point along the axial-symmetry line is solved. This point corresponds to point C in Figure. 4.11. In addition to the known point C, point B is also known as it lies along the die inlet. Point A is solved by an algorithm whose outline is already given in section 4.3.2. The solution can be repeated up to the interface between wire and die, because the nature of the problem is same for every point. After the solution reaches the interface, the next point on the axial symmetry line is solved and the procedure repeats itself until the last point on the interface is solved.

i-Solution For Axial-Symmetry Line

i) Shear terms are zero along this line

$$\delta\epsilon_{\alpha\beta} = \delta\epsilon_{\beta\alpha} = 0 \quad (4.166)$$

ii) $\epsilon_{\alpha\beta} = \epsilon_{\beta\alpha} = 0 \quad (4.167)$

iii) $P_{\alpha\beta} = P_{\beta\alpha} = 0 \quad (4.168)$

iv) $y = 0 \quad (4.169)$

v) $\delta/\delta\beta = 0 \quad (4.170)$

vi) $1/r_{\alpha} = 0 \quad (4.171)$

vii) Assume incremental direct strain $\delta\epsilon_{\alpha\alpha}$.

Equilibrium equations

α -direction

$$\frac{\delta P_{\alpha\alpha}}{\delta\alpha} + \frac{P_{\alpha\alpha} - X P_{\alpha\alpha}}{r_{\beta}} = 0 \quad (4.172)$$

β -direction

$$\frac{P_{\beta\beta} - (K/X) P_{\beta\beta}}{r_{\alpha}} = 0 \quad (4.173)$$

\Rightarrow

$$K = X \quad (4.174)$$

$$\frac{d\epsilon_{\alpha\alpha}}{d\epsilon_{\beta\beta}} = \frac{2(1-X)}{(X-1)} \quad (4.175)$$

$$\Rightarrow d\epsilon_{\alpha\alpha} = -2d\epsilon_{\beta\beta} \quad (4.176.a)$$

$$d\epsilon_{\gamma\gamma} = -d\epsilon_{\alpha\alpha}/2 \quad (4.176.b)$$

$$P_{\alpha\alpha}^* = \frac{A \left[B + \sqrt{\frac{2}{3}} \left[\frac{2+R}{1+2R} \left((d\epsilon_{\gamma\gamma} - R d\epsilon_{\alpha\alpha})^2 + (d\epsilon_{\beta\beta} - d\epsilon_{\alpha\alpha})^2 + R (d\epsilon_{\beta\beta} - d\epsilon_{\gamma\gamma})^2 \right)^{1/2} \right]^n}{\sqrt{\frac{3}{2} \left[\frac{2(X-1)^2}{2+R} \right]^{1/2}}} \quad (4.177)$$

Algorithm:

Step 1. Assume incremental direct strain $\delta\epsilon_{\alpha\alpha}$.

Step 2. Assume a trial value for X

For the first trial

$$X = C - 1/C \quad (4.178)$$

where

$$C = \left(1 + \frac{1}{\mu \cot \alpha} \right) \left(1 - \left(A/A_0 \right)^{\mu \cot \alpha} \right) \quad (4.179)$$

Step 3. Using $\delta\epsilon_{\alpha\alpha}$ compute $\delta\epsilon_{\beta\beta}$ and $\delta\epsilon_{\gamma\gamma}$ by using equation (4.176.a, b)

Step 4. Determine $P_{\alpha\alpha}^*$ value by using equation 4.177 and known material properties A, B, n and R

$$\text{Step 5. } P_{\beta\beta}^* = P_{\alpha\alpha}^*/X \quad ; \quad P_{\gamma\gamma}^* = P_{\alpha\alpha}^*/K$$

Step 6. Determine $P_{\alpha\alpha}$ by integrating the equation 4.173 the initial value of $P_{\alpha\alpha}$

$$P_{\alpha\alpha} = (P_{\alpha\alpha})_1$$

If the assumed value for X is correct $P_{\alpha\alpha}$ and $P_{\alpha\alpha}^*$ will be identical. The convergence criterion for X is defined as:

$$|P_{\alpha\alpha} - P_{\alpha\alpha}^*| < \delta \quad (4.180)$$

The value of X is changed until the above condition is satisfied. Otherwise, the procedure is repeated by starting from step 2.

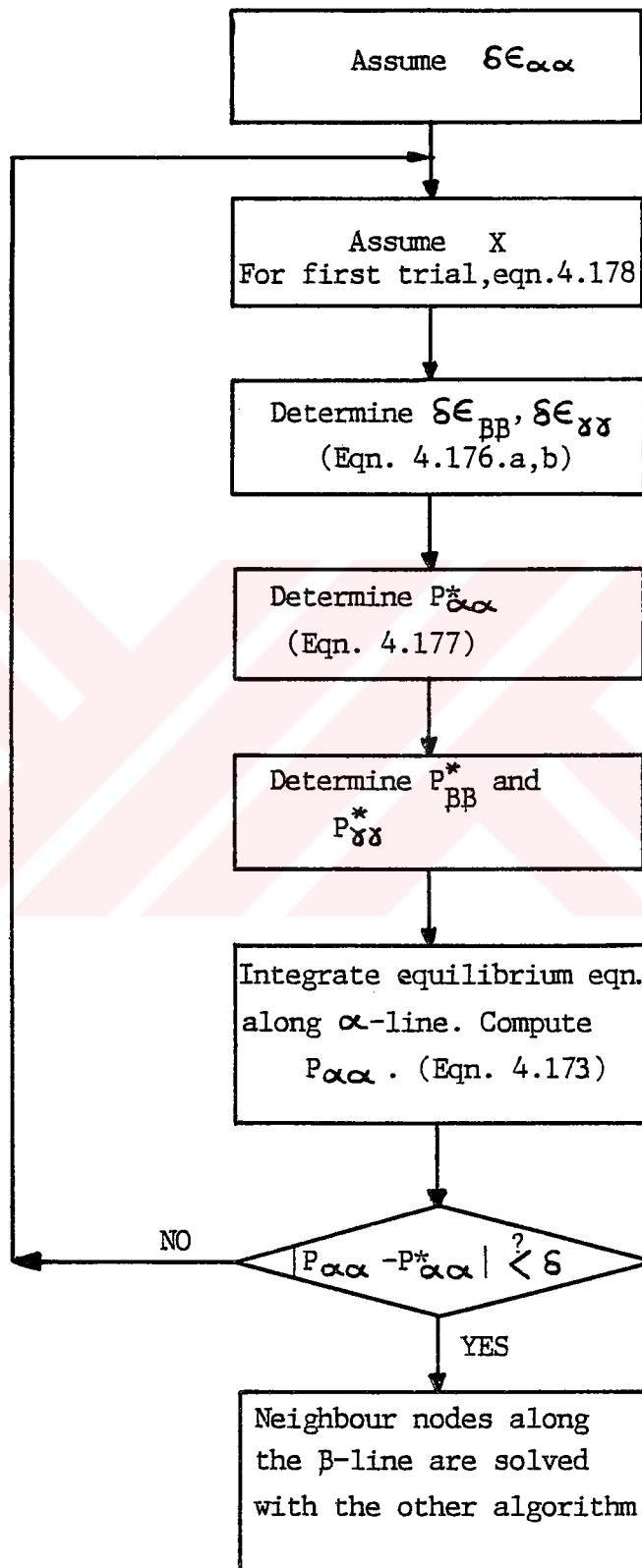


Figure.4.12. Computer program layout for axial symmetry line.

;;-Solution along a β -line:

The two independent variables are the node displacements du and dv . A double convergence scheme is used to determine the exact values of the node displacements du and dv . This fixes the new position of point A. The lines over which the conditions of equilibrium should be satisfied are the α and β -lines. The step-by step algorithm is as follows:

Step 1. Assume trial value for du (Outer loop of the convergence scheme)

Step 2. Assume trial value for dv (Inner loop of the convergence scheme)

After step 2, the trial co-ordinates of point A will be;

$$A: (x_0 + du, y_0 - dv)$$

Step 3. Fit a second order polynomial to β -line using points C and A; (Appendix A)

$$X = a_1 y^2 + b_1 y + c_1 \quad (4.181)$$

Step 4. Use a numerical integration method (Appendix C) in the limits of (x_c) and $(x_0 + du)$ to determine the new arc length of curvilinear line C-A (Equation 4.161)

Step 5. Determine the incremental direct strain $\delta \epsilon_{\beta\beta} |_A$ (Equation 4.165)

Step 6. The procedure given in steps 3 to 5 is repeated to fit a polynomial to α -line and eventually $\delta \epsilon_{\alpha\alpha} |_A$ is computed. (equation 4.164)

$$Y = a_2 x^2 + b_2 x + c_2 \quad (4.182)$$

Step 7. Compute the slopes S_β and S_α at point A:

$$S_\alpha |_A = 2a_2 (x_0 + du) + b_2 \quad (4.183. a)$$

$$S_{\beta} |_A = 2a_1 (y_0 - dv) + b_1 \quad (4.183. b)$$

Step 8. Determine $\delta\epsilon_{\alpha\beta} |_A$. This completes the determination of the temporary, incremental-orthogonal components of strain at point A. (Equation 4.32) The strain $\delta\epsilon_{\gamma\gamma} |_A$ is computed from the principle of constancy of volume. (Equation 4.35)

Step 9. X, Z and K ratios are determined. (Equation 4.43, 4.44, 4.45)

Step 10. Compute the value of $P_{\alpha\alpha}^*$ by using equation 4.61.

Step 11. Determine the values of $P_{\beta\beta}^*$, $P_{\gamma\gamma}^*$ and $P_{\beta\alpha}^*$.

Step 12. Start to integrate the equilibrium equations along β -line (Equation 4.159).

i - The initial values at point C are known.

$$P_{\alpha\alpha}, P_{\beta\beta}, P_{\gamma\gamma}, \delta\epsilon_{\alpha\alpha}, \delta\epsilon_{\beta\beta}, \delta\epsilon_{\gamma\gamma}, P_{\beta\alpha}, r_{\alpha}, r_{\beta}.$$

ii - Express the variation of $P_{\beta\alpha}$, X, K as second order polynomials.

$$P_{\beta\alpha}(y) = P_1 y^2 + P_2 y + P_3 \quad \text{in the domain } y_c, y_0 - dv \quad (4.184. a)$$

$$X(y) = X_1 y^2 + X_2 y + X_3 \quad \text{in the domain } y_c, y_0 - dv \quad (4.184. b)$$

$$K(y) = K_1 y^2 + K_2 y + K_3 \quad \text{in the domain } y_c, y_0 - dv \quad (4.184. c)$$

$$P_{\beta\alpha}(x) = P_1 X^2 + P_2 X + P_3 \quad \text{in the domain } x_c, x_0 + du \quad (4.184. d)$$

iii - The with the transformation of $\beta \equiv y$ and $\alpha \equiv x$, the piecewise numerical integration along the β -line is performed in the domain $y_c < y < y_0 - dv$ by using the fourth-order Runge-Kutta algorithm with the initial values of y_0, x_0 and $P_{\alpha\alpha} |_0$ and $P_{\beta\beta} |_0$ (Appendix D).

This integration yields the temporary value of $P_{\beta\beta}$ at point A.

Step 13. Compare the $P_{\beta\beta}$ value with $P_{\beta\beta}^*$ which is found in step 11. Computing the difference, check the validity of the assumed value

$$|P_{\beta\beta} - P_{\beta\beta}^*| < \delta \quad (4.185)$$

If this inequality holds, it means that dv is a root. Otherwise, the whole procedure is repeated by returning back to step 2, and a new trial value for dv is assumed. This is the inner loop for convergence.

Step 14. When the root is found, the equilibrium equation along α -line is integrated. (Equation 4.158)

i- The initial given values at point B are

$$P_{\alpha\alpha}, X, K, P_{\beta\alpha}, r_{\alpha} \text{ and } r_{\beta}$$

ii- Express the variations of $P_{\beta\alpha}, X, K$ along α -line with second order polynomials.

iii- Then with the transformation of $\beta \equiv y$ and $\alpha \equiv x$, the piecewise numerical integration along the α -line is performed in the domain $x_b < x < x_o + du$. This integration gives $P_{\alpha\alpha}$ value at point A (Appendix D).

Step 15. Compare this value with $P_{\alpha\alpha}$ (Equation 4.61)

$$|P_{\alpha\alpha} - P_{\alpha\alpha}^*| < \delta$$

If the inequality holds for the root du convergence requirement is satisfied. This completes the iteration on outer loop. Otherwise the complete procedure is repeated by returning step 1. After determining the permanent root which simultaneously satisfies the inequalities, the new position of point A is fixed.

$$(x_A, y_A) \equiv (x_o + du, y_o - dv) \quad (4.186)$$

Step 16. Proceed to the next grid node along the same β -line and repeat the complete procedure.

Step 17. After the interface between die and wire is reached, check

$$|\text{Beta}(I, J) - R_{di}(I, J)| < \delta \quad (4.187)$$

If this inequality is not satisfied then return to the beginning (solution for axial symmetry line) and change the assumed value of $\delta\epsilon_{\alpha\alpha}$, and repeat the complete procedure. When the inequality holds, the solution returns back to step 1, of the algorithm for the next solution along the axial symmetry line. This procedure repeats itself until all the nodal points in the drawing region are solved.



CHAPTER V

DESCRIPTION OF THE COMPUTER PROGRAM FOR THE NUMERICAL SOLUTION

A computer program is developed in order to perform the numerical procedure described in section 4.3.2. It is written in BASIC 4.0 language to be operated on HP 9816. It starts from the undeformed state by reading the initial values and boundary conditions.

5.1 Computer Algorithm

Step 1 . Read the material properties A, B, n, R, the number of intermediate stages(NS). Maximum number of iterations is also specified. Number of grid lines to be embedded in x direction namely M is given as input.

Step 2 . Coefficient of friction between wire and die, half die cone-angle, initial and final reduced wire diameter are given as input.

Step 3 . Actual grid lengths with a nominal size of L0 and L1 which are physically embedded to the specimen is computed as following.

$$L = \frac{r_f - r_{10}}{\tan \alpha} \quad (5.2)$$

$$L0 = L/M \quad (5.3)$$

$$Ny = \text{INT}(D1/2L0) \quad (5.4)$$

$$L1 = R1/Ny \quad (5.5)$$

Step 4 . This is the outermost loop for intermediate stages for multi-stage wire-drawing process. The following boundary conditions are given as input at every stage:

;-Compute the outermost grid number.

$$NG=INT(R1/L1)+1 \quad (5.6)$$

;;-The total plastic strains and stresses along β -line (die inlet) are given as boundary condition at each nodal point lying on it.

;;;-The co-ordinates (x,y) of the nodes are also specified.

Step 5 . Compute r_β values for every grid element along the inlet. The radii of curvature are determined by the subprogram by fitting a Lagrange polynomial to given three points with known co-ordinates (Appendix A):

$$X = a_1 y^2 + b_1 y + c_1 \quad (5.7)$$

and the radius of curvature is computed from the equation:

$$1/r = \pm \frac{d^2 y / dx^2}{\{1+(dy/dx)^2\}^{3/2}} \quad (5.8)$$

The appropriate sign convention for the radius r is established by the rule which is given in Figure.5.1. The straight line combines the initial and the last points. Its slope is SS . The lines shown in bold lines have a positive curvature according to the sign convention. This condition corresponds to the situation when the fitted polynomial has a larger slope (including the sign) than SS at the last point. Conversely, the broken lines indicate the condition when the radius of curvature is negative.

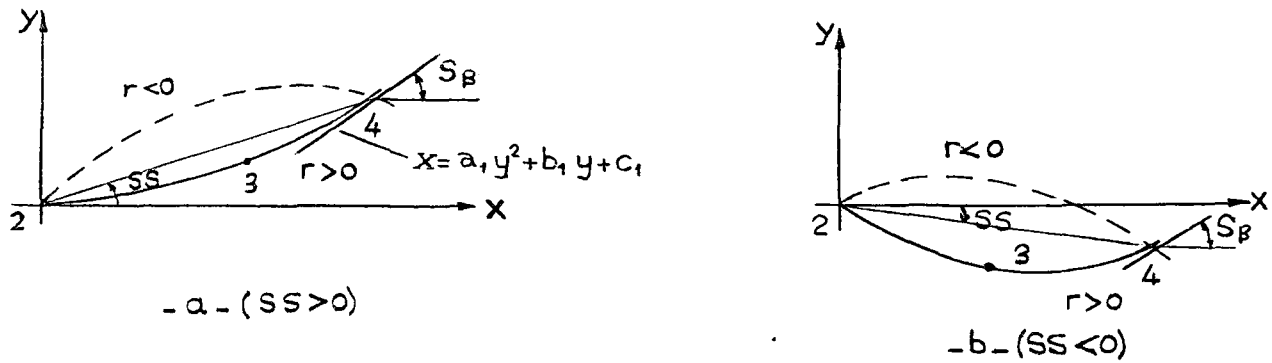


Figure.5.1 Sign convention for radius of curvature along a β -line.

Step 6 . This is the beginning of the loop corresponding to the solution along the axial-symmetry line. Here, the incremental direct strain $\delta\epsilon_{\alpha\alpha}$ is assumed and will be checked later.

Step 7 . Assume X. After X converges, $P_{\alpha\alpha}$, $P_{\beta\beta}$, $\delta\epsilon_{\alpha\alpha}$ and $\delta\epsilon_{\beta\beta}$ values are determined. The new coordinates of the point is computed from the following equation;

$$du = e^{1/2} (\delta\epsilon_{\alpha\alpha}^{i+1} + \delta\epsilon_{\alpha\alpha}^i) \Delta\alpha \quad (5.9)$$

Assuming a linear variation of the strain along the infinitesimal grid length.

Here dv is identically zero due to axial-symmetry. Then the new co-ordinates of a point such as C as shown in Figure.4.11.

New coordinates for point C = $(X_c + du, y_c)$

Step 7 . After determining the next point on axial-symmetry line neighbour nodes along the β -line are solved.

For this assume trial value for du (Outer loop of the convergence)

Step 8 . Assume trial value for dv (inner loop of the convergence)

After this the trial coordinates of the point A will be:

$$A: (x_0 + du, y_0 - dv)$$

Step 9 . Fit a second order polynomial to β -line using points C & A (Appendix A):

$$x = a_1 y^2 + b_1 y + c_1 \quad (5.10)$$

To determine the coefficients a_1, b_1 & c_1

i - The slope of the polynomial at point C. Starting from the boundary line, the slope of the β -lines are known. The slope of β -line along the axial symmetry line is zero. This establishes the sufficient number of equations to solve the coefficients of the unknown polynomial or,

ii - For further points along the β -line, the two previous known points and point A is used to determine the polynomial. The same arguments hold for α -lines also.

Step 10. Use a numerical integration method in the limits of x_c and $(x_0 + du)$ to determine the new arc length of curvilinear line C-A. (Equation 4.161)

Step 11. Determine the incremental direct strain $\delta \epsilon_{\beta\beta}^{n+1} |_A$ from Equation 4.165.

Step 12. The procedure given in steps 9 to 11 is repeated to fit a polynomial to α -line and eventually $\delta \epsilon_{\alpha\alpha}^{n+1} |$ is computed.

$$y = a_2 x^2 + b_2 x + c_2 \quad (5.11)$$

Step 13. Compute the slopes S_{β}^{n+1} and S_{α}^{n+1} at point A:

$$S_{\alpha}^{n+1} |_{A} = 2a_2(X_0 + du) + b_2 \quad (5.12.a)$$

$$S_{\beta}^{n+1} |_{A} = 2a_1(y_0 - dv) + b_1 \quad (5.12.b)$$

Then compute the shear strain using Equation 4.32

$$\delta \epsilon_{\beta\alpha} |_{A}^{n+1} = 1/2 (S_{\beta}^{n+1} |_{A} - S_{\alpha}^n |_{A})$$

Step 14. $\delta \epsilon_{\gamma\gamma}$ is computed from the principle of constancy of volume.

Step 15. X, K and Z ratios are determined (Equations 4.43, 4.44, 4.45)

Step 16. Compute the temporary value of $P_{\alpha\alpha}^*$ by using equation (4.61)

Step 17. Determine temporary values of $P_{\beta\beta}^*$, $P_{\gamma\gamma}^*$ and $P_{\beta\alpha}^*$

Step 18. Start to integrate the equilibrium equation along β -line (Equation 4.159)

i - The initial values at point C are known

$$P_{\alpha\alpha}, P_{\beta\beta}, P_{\beta\alpha}, r_{\alpha}, r_{\beta}$$

ii - Express the variation of $P_{\beta\alpha}$, X, K as second order polynomials

$$P_{\beta\alpha}(y) = P_1 y^2 + P_2 y + P_3 \quad \text{in the domain } y_b, y_0 - dv \quad (5.13.a)$$

$$X(y) = X_1 y^2 + X_2 y + X_3 \quad \text{in the domain } y_b, y_0 - dv \quad (5.13.b)$$

$$K(y) = K_1 y^2 + K_2 y + K_3 \quad \text{in the domain } y_b, y_0 - dv \quad (5.13.c)$$

$$P_{\beta\alpha}(x) = P_1 x^2 + P_2 x + P_3 \quad \text{in the domain } x_b, x_c + du \quad (5.13.d)$$

If the point is a neighbour point to axial-symmetry line, the slopes are assumed to be zero. Otherwise previous two points and the point C is used to fit the polynomials.

iii-Then with the transformation of $\beta \equiv y$ and $\alpha \equiv x$, the stepwise numerical integration along the β -line is performed in the domain $y_c < y < y_0 - dv$ by using the fourth-order Runge-Kutta algorithm with the initial values of y_0, x_0 and $P_{\alpha\alpha}|_0$ and $P_{\beta\beta}|_0$ (Appendix D)

$$C_1 = f(y_0, P_{\beta\beta}|_0) \quad \text{with } h = y_1 - y_0 \quad (5.14.a)$$

$$C_2 = f(y_0 + 1/2h, P_{\beta\beta}|_0 + 1/2C_1) \quad (5.14.b)$$

$$C_3 = f(y_0 + 1/2h, P_{\beta\beta}|_0 + 1/2C_2) \quad (5.14.c)$$

$$C_4 = f(y_0 + h, P_{\beta\beta}|_0 + 1/2C_3) \quad (5.14.d)$$

Then

$$P_{\beta\beta}|_1 = P_{\beta\beta}|_0 + 1/6 h (C_1 + 2C_2 + 2C_3 + C_4) \quad (5.14.e)$$

This integration yields the temporary value for $P_{\beta\beta}$ at point A.

Step 19. Compare this $P_{\beta\beta}$ value with $P_{\beta\beta}^*$ which is found in step 17. Computing the difference, check the validity of the assumed dv value.

$$|P_{\beta\beta} - P_{\beta\beta}^*| < \delta \quad (5.15)$$

If this inequality holds, it means that dv is a root. Otherwise, the whole procedure is repeated by returning back to step 8, and a new trial value for dv is assumed. The temporary root can be determined by the binary chapping and inverse interpolation method (Appendix B).

Step 20. When the temporary root is found, the equilibrium equation along α -line is integrated.

i-The initial given values at point B are:

$P_{\alpha\alpha}, X, K, P_{\beta\alpha}, r_{\alpha}$ and r_{β}

;;-Express the variations of $P_{\beta\alpha}, X, K$ along α -line with second order polynomials.

$$P_{\beta\alpha}(x) = P_1 x^2 + P_2 x + P_3 \quad \text{in the domain } x_b, x_o + du \quad (5.16.a)$$

$$X(x) = X_1 x^2 + X_2 x + X_3 \quad \text{in the domain } x_b, x_o + du \quad (5.16.b)$$

$$K(x) = K_1 x^2 + K_2 x + K_3 \quad \text{in the domain } x_b, x_o + du \quad (5.16.c)$$

$$P_{\beta\alpha}(y) = P_1 y^2 + P_2 y + P_3 \quad \text{in the domain } y_b, y_o - dv \quad (5.16.d)$$

;;-Then with the transformation of $\beta \equiv y$ and $\alpha \equiv x$, the piecewise numerical integration along the α -line is performed in the domain $x_b < x < x_o + du$. This integration gives $P_{\alpha\alpha}$ value at point A (Appendix D).

Step 21. Compare this value with $P_{\alpha\alpha}$ (Equation.4.61)

$$|P_{\alpha\alpha} - P_{\alpha\alpha}^*| < \delta \quad (5.17)$$

If this inequality holds for the root du convergence requirement is satisfied. This completes the iteration on outer loop. Otherwise the complete procedure is repeated by returning to step 7.

After determining the permanent root, the new position of point A is automatically fixed;

$$(x_A, y_A) \equiv (x_o + du, y_o - dv) \quad (5.18)$$

Step 22. Store the permanent values of all associated variable for point A.

Step 23. Proceed to the next grid node along the same β -line and repeat the complete procedure as given in steps 7-23.

After the interface between die and wire is reached the

assumed value for $d\epsilon$ is checked by using die geometry such that :

$$\text{Beta}(I,J) - \text{Rdi}(I,J) \leq \delta \quad 5.11$$

where:

$\text{Beta}(I,J)$: Coordinate of the node after deformation .

$\text{Rdi}(I,J)$: Radius at that node

If this inequality is not satisfied return to step 6 and repeat the whole procedure by changing the assumed value for $\delta\epsilon_{\alpha\alpha}$. If the inequality holds then the solution returns back to step 7 of the algorithm for the next solution along the axial-symmetry line. This procedure repeats itself until all the nodal points in the drawing region are solved.

Step 24. If it is multi-stage process then return to step 4 for the solution of next stage.

Step 25. Program stops after the final stage is solved.

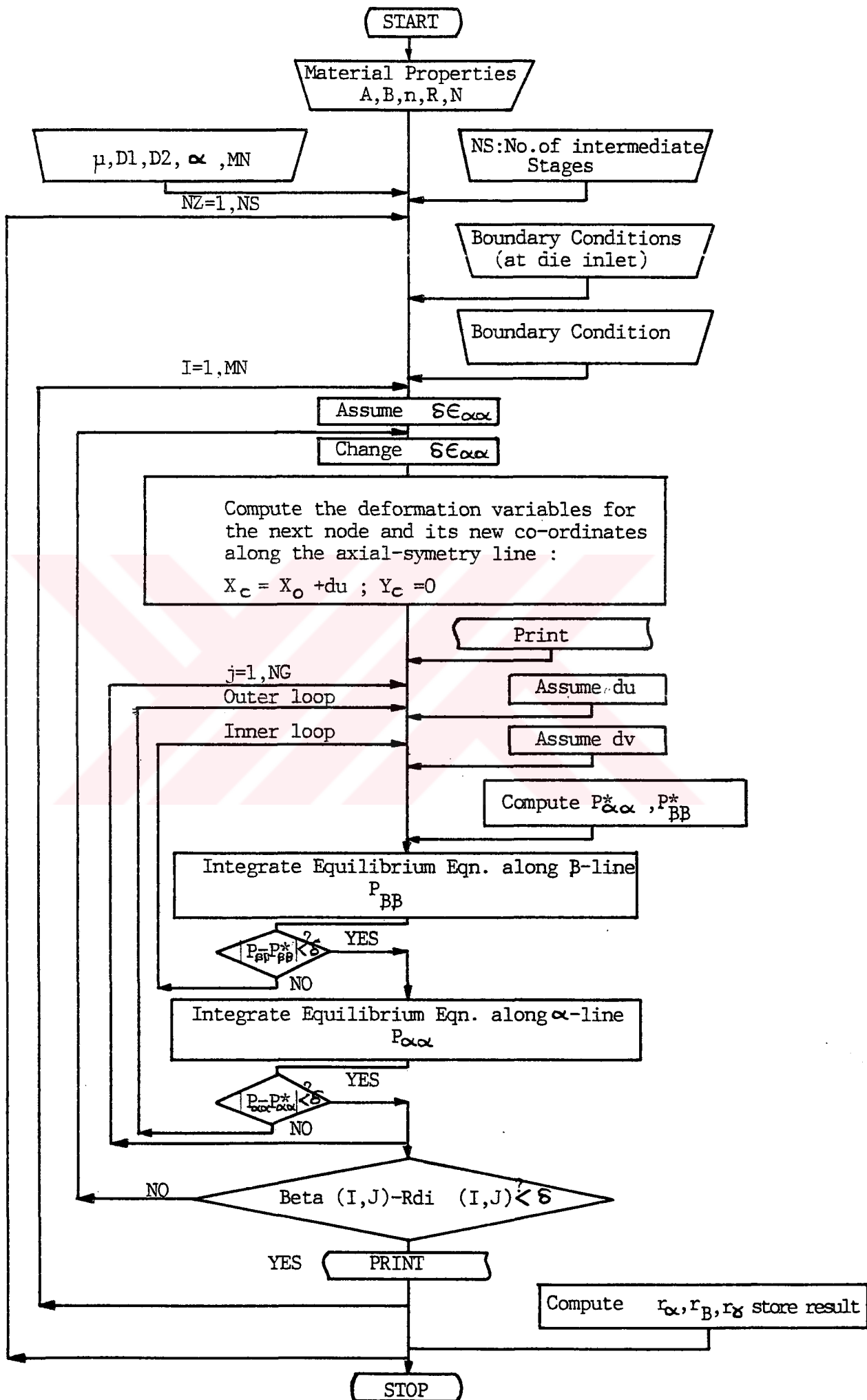


Figure.5.2. Computer program layout for numerical solution.

5.2 Sample Solution

The computer program is used to solve a case study as specified below:

i;-The drawing material has following properties:

$$A = 25 \text{ kg/mm}^2$$

$$B = 0.0122 \text{ mm/mm}$$

$$n = 0.37$$

ii;-An anisotropy ratio is taken as 1.2 and parameter characteristics of anisotropy N is taken as 1.1.

iii;-Initial and final diameters of wires are 3 and 2 mm respectively.

iv;-Coefficient of friction between wire and die is 0.05.

v;-Half die cone angle is 12° .

vi;-Drawing region is divided into five division in α -direction ($MN=5$). Also, it is calculated that there are four division in β -direction ($NG=4$).

vii;-The convergence criteria parameter δ is chosen as 0.1 kg/mm^2 .

viii;-The convergence criteria parameter δ used for equation $\text{Beta}(I, J) - \text{Rdi}(I, J) < \delta$ is chosen as 0.2 mm .

The computer program determines the stress-strain state at each deformed nodal point. Their new co-ordinates are calculated and printed. The results which are reduced and adapted for graphical representation are given in Appendix F.

5.3 Program Properties

The memory requirement of the program is about 125 K bytes. It takes about 20 iterations to converge to the root of X for the solution of a node on the axial-symmetry line. Converging rate for $P_{\alpha\alpha}$ and $P_{\beta\beta}$ values along the β -line largely depends upon the initial trial values of du and dv . Trial values are up-dated by the converged du and dv values of the previous node. The step size for variations in du and dv are taken to be 5×10^{-3} mm for each iteration. The total number of iterations in the nested loop for the solutions along the β -line is about 100 iterations after all the provisions are taken such as up-dating the trial values of du and dv . The execution time is roughly about 50 seconds for a node along the β -line. It drops approximately to 5 seconds for a node along the axial-symmetry line. The total execution time can be expressed roughly with the following formula

$$t = MN \times 5 + (NG - 1)(MN - 1) \times 50 \quad [\text{seconds}] \quad (5.19)$$

The program is composed of a main program and eight subprograms. The main program has two options. These are analytical and numerical solutions for wire-drawing process. The subprograms that are used in numerical solution are:

- 1 / Subprogram ALRUNG : It performs the integrations along the axial symmetry line.

- 2 / Subprogram COMUØ : It specifies the functional relationship

- 3 / Subprogram LANGPOL3 : It computes the radius of curvature for the given three nodal points and determines its sign (langrangian)

- 4 / Subprogram POLANG2 : It fits a polynomial to given two points and the slope of the function at the first point. It also determines the radius of curvature.
- 5 / Subprogram GENRUNG : It performs the integrations along the α and β -lines.
- 6 / Subprogram GRIDUØ : It specifies the functional relationship of the equilibrium equations along α and β -lines.
- 7 / Subprogram TRANTEG : It determines the arc lengths of the deformed grid sides.
(Trapezoidal rule)
- 8 / Subprogram BINCHAP : It finds the exact root of trial values. (Binary chapping, inverse interpolation)

CHAPTER VI

DESCRIPTION OF THE COMPUTER PROGRAM FOR THE ANALYTICAL SOLUTION

A computer program is developed in order to perform the analytical procedure described in section 4.2 by using Sachs, Siebel and Whitton empirical formula. The results of drawing stress, drawing force, mean die pressure and die splitting force for different reductions can be obtained graphically by means of this program.

6.1 Computer Algorithm

Step 1. Read the initial wire diameter, coefficient of friction, half die-cone angle and the mean yield stress of material.

Step 2. Starting from 0% percent reduction, compute the drawing stress, drawing force, mean die pressure and die splitting force by using Sachs equation (Equation 4.131) by 1% reduction increments until 50% reduction is reached.

Step 3. Repeat the same procedure by using Siebel equation (Equation 4.136)

Step 4. Repeat the same procedure by using Whitton empirical formula (Equation 4.137)

Step 5. Plot the drawing stress, drawing force, mean die pressure and die splitting force versus percentage reduction graphics by using the values obtained from Sachs, Siebel and Whitton equations.

Step 6. If you want to change one of the inputs return step 1. otherwise program stops.

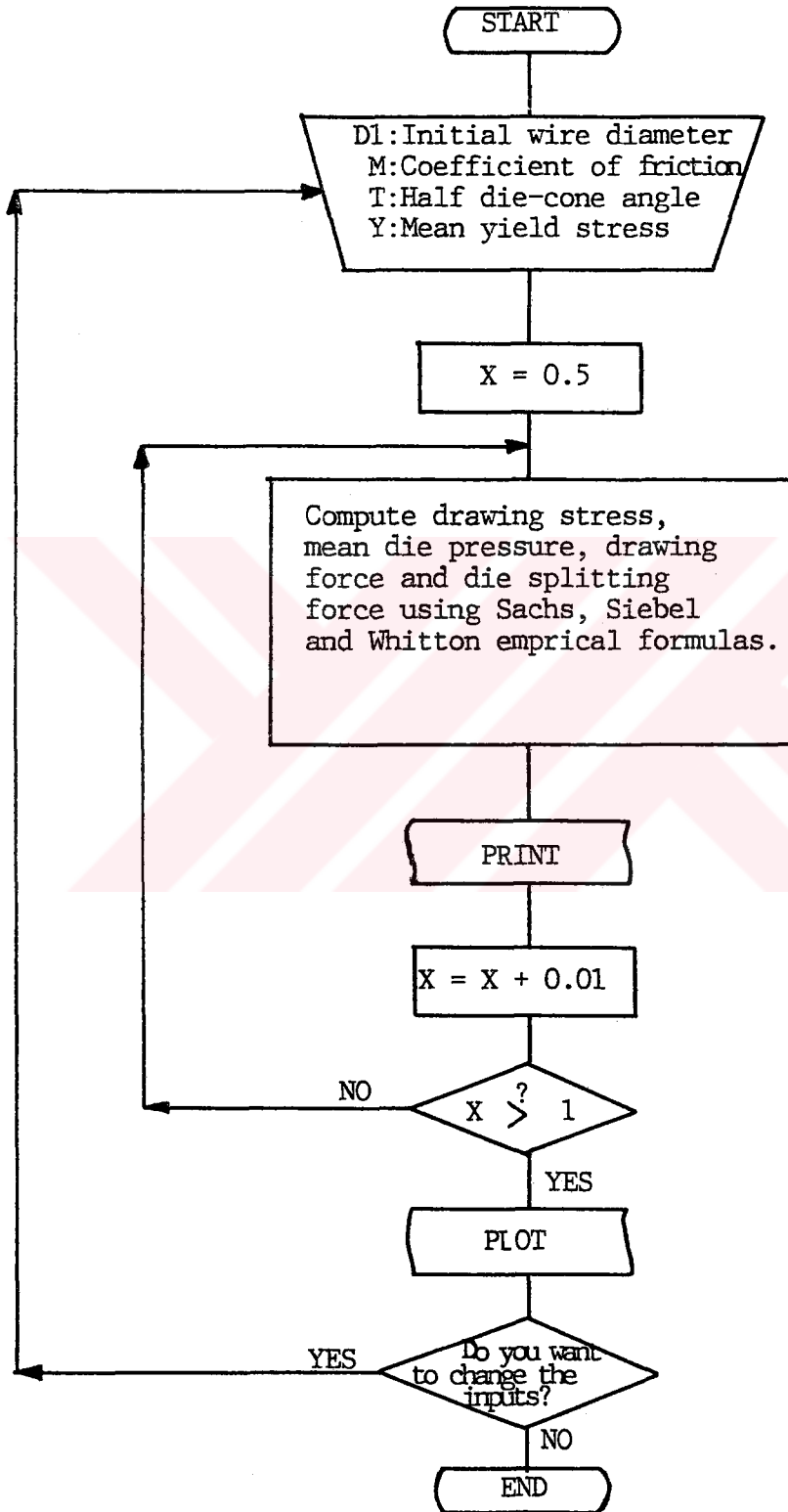


Figure.5.3. Computer program layout for analytical Solution.

6.2 Sample Solution

The computer program is used to solve a case study as specified below:

The drawing stress, drawing force, mean die pressure and die splitting forces are compared for a wire-drawing pass of 30 percent reduction on a wire initially 3 mm diameter, in a die of 12° semi cone angle, assuming a mean yield stress $Y = 25 \text{ kg/mm}^2$ and coefficient of friction=0.05 for the following cases:

i/ Siebel's theory

ii/ Sach's theory

iii/Whitton formula

The results which are reduced and adapted for graphical presentation are given in Appendix E.

CHAPTER VII

RESULTS AND DISCUSSIONS

7.1 Numerical Results

Sample computer outputs are given in Appendix F. Outputs consist of the incremental strains, namely $\delta\epsilon_{\alpha\alpha}$, $\delta\epsilon_{\beta\beta}$ and $\delta\epsilon_{\gamma\gamma}$, for each element node. Associated strains, new co-ordinates of the node and converged du and dv values are also given together with the number of iterations that it takes for convergence. Associated $P_{\alpha\alpha}$, $P_{\beta\beta}$, $P_{\gamma\gamma}$ and $P_{\alpha\beta}$ are also printed in units of kg/mm^2 . These results can be used to derive important conclusions about the wire-drawing operation and material behaviour in the drawing region. The variation of $\delta\epsilon_{\alpha\alpha}$, $\delta\epsilon_{\beta\beta}$, $\delta\epsilon_{\gamma\gamma}$, $\delta\epsilon_{\alpha\beta}$, $P_{\alpha\alpha}$, $P_{\beta\beta}$, $P_{\gamma\gamma}$, $P_{\alpha\beta}$ along the α and β -lines are also given in Appendix F. Incremental strains increase in magnitude steadily as the deformation progresses. Drawing stress increases in the drawing direction and decreases in radial direction. Radial stress increase in radial direction and decrease in drawing direction. Shear stress is slightly decrease in drawing direction and increase in radial direction.

The results obtained from analytical solution for the drawing stress is near to numerically obtained results.

7.2. Discussions

Internal stress distribution obtained in numerical analysis is generally in agreement with Shield and Siebel's distribution. In general, stresses increase in the drawing direction and decrease in radial direction. Also incremental strains increase in magnitude steadily as the deformation

progresses. Regarding the analytical analysis, when the numerical results are compared with the Sachs, Siebel and Whitton's results it can be observed that numerically obtained values for drawing stress is higher than analytical ones and close to Siebel's results.

Numerical solution depends upon the boundary conditions at the die inlet and axial symmetry line. These conditions must be derived from experimental data or numerical solution of the other regions. At axial symmetry line instead of using $\epsilon_{\alpha\alpha}$ value given as a boundary condition, solution along a β -line is started with a temporary, assumed $\epsilon_{\alpha\alpha}$ value. The solution proceeds along the β -line up to the interface between wire and die where the boundary conditions associated with this line are tested. Solution returns back to the axial symmetry line and starts with another $\epsilon_{\alpha\alpha}$ value until the boundary conditions are satisfied. A similar iterative scheme can be provisionally suggested about the boundary conditions at the die inlet. Since for very light reductions, the wire bulges prior to its entry to the die stresses are not equal to zero in fact. Solution may start with assumed boundary conditions and continue until the die exit is reached, where the corresponding boundary conditions are tested. It is obvious that such a scheme will be very elaborate, time consuming and simply impractical, therefore it is left as a personal choice to use. The computing time is already long enough for the present algorithm such that some simplifications may seem to be reasonable.

It is observed that as the mesh size and the number of iterations is increased, much more correct results can be obtained. But mesh size can not be decreased below a certain value because of the available computer memory. Drawing region can be subdivided maximum into twenty. The total number of iterations in the nested loop for the solutions

along the β -line is not increased over 100. Because the computing time is also increases and this scheme is very time consuming and simply impractical. Converging rate along the β -line largely depends upon the initial trial values of du and dv . Depending on these assumed values and the boundary conditions, in some of the nodes convergence can not be obtained with the above specified number of iterations and hence at that nodes correct results can not be obtained.

A material element with initially orthogonal sides, may transform into a completely arbitrary shape with sides intersecting obliquely. Although this non-orthogonality condition may have negligible importance at incipient modes of deformation, it can be included only by modifying the governing equations. In this case it is believed that a more comprehensive and complete method of analysis will be achieved whenever such solutions are required.

T. C.
Yükseköğretim Kurulu
Dokümantasyon Merkezi

CHAPTER VIII

CONCLUSIONS

In this thesis, a theory is developed in order to analyse the wire-drawing process using the finite difference method. An anisotropic and strain-hardening material model is used under three dimensional stress conditions. An originally embedded rectangular grid system transforms into a family of curvilinear, non-orthogonal lines as the deformation progresses. Theory encounters this situation where curvilinear, orthogonal co-ordinates are used in formulating and solving the problem. A computer program is developed to carry out the necessary calculations and to determine the strains and the associated stresses taking place during the wire-drawing operation. Results obtained by the numerical method can be compared with analytical results for the same material. This shows that the computer program can furnish users with sufficient and reliable information to make a complete and detailed analysis of the wire-drawing process. The program enables to follow the space dependence of strains, stresses, displacements throughout the wire-drawing operation.

Additional solutions are obtained using analytical equations derived by Sachs, Siebel and also Whitton's empirical equation. Analytical solutions is simple and comparable with the numerical method with respect to its simplicity and ease of application.

Polynomial representation of the deforming grids is highly adaptable to any degree of deformation. Relevant theory is also based on a similar approach. For these reasons, the philosophy and the methodology is sufficient and flexible enough to extend the field of interest to more complicated die geometries in the future.

Curvilinear, non-orthogonal co-ordinates can also be included only by modifying the governing equations. In this case it is believed that a more comprehensive and complete method of analysis will be achieved whenever such solutions are required.

Further Work: Present study on its own, is believed to be an initiation and innovation in this field with respect to the philosophy of approach, method of solutions and the results obtained. It was found out that a complete assessment of the problem is only possible if different aspects of investigations are realized. These are: theoretical analysis, experimental research and method of solutions.

The computer program can be improved further whenever a more comprehensive and complete solutions are required. A similar iterative scheme developed for axial-symmetry line can also be suggested about the boundary conditions at the die inlet. Solution may start with assumed boundary conditions and continue until the die exit is reached, where the corresponding boundary conditions are tested. In this analyse the coefficient of friction between wire and die is assumed to be constant throughout the drawing region. It may also be taken as a variable. It is obvious that such a scheme will be very time consuming.

Since polynomial representation of the deforming grids is highly adaptable to any degree of deformation, the methodology is sufficient and flexible enough to extend the field of interest to more complicated die geometries in the future.

Although non-orthogonality condition may have negligible importance at incipient modes of deformation, it can be included only by modifying the governing equations.

REFERENCES

- 1-Hugh Ford, Advanced Mechanics of Materials: New York, Wiley
London, Longmans, p. 613-625, 1963.
- 2-J. G. Wistreich, The Fundamentals of Wire-Drawing
, Metallurgical Reviews, vol. 3, no. 10, 1958.
- 3-Betzalel Avitzur, Metal Forming, Processes & Analysis, New
York, McGraw-Hill, p. 219-249, 1968.
- 4-J. I. Orbegozo, Fracture in Wire-Drawing, Annals of the
C. I. R. P., vol. XVI, p. 319-330, 1968.
- 5-Wolfgang Teller, Present State of Wire-Drawing, , Wire-World
International, vol. 18, May/June 1976.
- 6-W. Johnson and P. B. Mellor, Engineering Plasticity, John Wiley
& Sons, 1983
- 7-R. W. Gottschlich and N. N. Breyer, High-Speed Surface Removal
for Bar, Rod and Wire, Journal of Metals, May 1963.
- 8-Kilkis Birol I., Theoretical and Experimental Investigation
of the Radial-Drawing Region of Square Blanks, A Ph. D.
Thesis, 1980.
- 9-W. W. Sokolovsky, The theory of Plasticity-An outline work
of done in russia, Journal of applied Mechanics, March,
1946.
- 10-P. B. Mellor, The role of plastic anisotropy in sheet metal
forming, Annals of C. I. R. P. vol. XVIII, p. 133-138, 1970.

- 11-Jackson, L. K. , Smith, K, F and Lankford, W. T. , Metals Tech., Tech. Pub. 2440, 1948.
- 12-Hill, R. , A Theory of the yielding and plastic flow of anisotropic metals, Proc. R. Soc. , A193, p. 281, 1948.
- 13-Dorn, J. E. , Stress strain relations for anisotropic plastic flow, J. Appl. Phys. 20, 15, 1949.
- 14-Prager, W. , The stress-strain laws of the mathematical laws of placticity: A survey of recent progress, J. Appl. Mech. , Trans ASME, v. 15, p. 225-233, 1948.
- 15-Geiringer, H. Some recent results in the theory of an ideal plastic body, Advances in Applied Mechanics, ed. Dreyden, H. L. , Karman, in. von, Academic Press, v. 3, p. 197-224, 1953.
- 16-Drucker, D. C. Limit analysis and design, Appl. Mech. Rev. , v. 7, no. 10, p. 421-423, 1954.
- 17-Drucker, D. C. , Stress-Strain relations in the plastic range: A survey of theory and experiments, Office of Naval Research, Contract NTONR, 358, NR-041-032, p. 350, 1950.
- 18-Rakhmatulin, A. Kh. and Shapiro, S. G, Propogation of disturbances in non-linear elastic and inelastic media (in Russian), Izv. Akad. Nauk. S. S. S. R. , no. 2, OTN, p. 1483-1940, 1954.
- 19-Rebinder, P. A. Physico-chemical mechanics as a new domain of Science, Vestn. Akad. Nauk, S. S. S. R. , no. 10, p. 32-42, 1957.
- 20-Freudenthal, A. M. , Geiringer, H. , The mathematical theories of the inelastic continium, ed. Flugge, S. . Encycl. Physics,

Springer, v. 6, p. 229-433, 1958.

- 21-Hodge, P. G., The mathematical theory of plasticity: New York Wiley and Sons, p. 461, 1958.
- 22-Hopkins, H. G., Dynamic expansion of the cavities in metals, ed. Sneddon, I. N., and Hill, R.: Progress in Solid Mechanics, Amsterdam, North Holland Publ., v. 1, p. 83-164, 1960.
- 23-Sandin, A., The tensile test: A measure of drawability, Jeronkontorets Annalen, v. 148, p. 259-275, 1964.
- 24-Laboratory tests predict sheet metal formability, IAMI, 44-45, 1974.
- 25-Palmer, E. W., and Smith, C. S., Trans. Am. Inst. Min. Metall engrs., v. 147, p. 164, 1942.
- 26-Baldwin, W. M., Howald, T. S., and Ross, A. N., Metals Tech. Publ. no. 1808, 1945.
- 27-Kleinger, L. J., and Sachs, G. J., Experimental results for aluminium sheets for the role of anisotropy on plastic properties, J. Aero. Sci., no. 15, p. 559-562, 1943.
- 28-Mellor, P. B., The role of plastic anisotropy in sheet metal forming, Annals of the C. I. R. P. v. 18, p. 133-138, 1970.
- 29-Voce, e., The relationship between stress and strain for homogenous deformations, J. I. Metals, no. 74, p. 537, 1936.
- 30-Swift, H. W. Plastic strain in an isotropic strain-hardening material, Engineering, no. 162, p. 381, 1947.

- 31-Keeler, S. P., Determination of forming limits in automotive stampings, Proc. S. A. E., mid-year Meeting, no. 650535, 1965.
- 32-Keeler, S. P., A circular grid system: A valuable aid for evaluating sheet metal formability, Proc. S. A. E., v. 1, p. 371-379, 1968.
- 33-Brever, R. G., and Alexander, J. M., A new technique for engraving and measuring grids in experimental plasticity, J. Mech. Phys. Solids, p. 19608, 1976.
- 34-Goodwin, G. M., Application of strain analysis in sheet metal forming problems in the press shop, S. A. E. Congress, no. 680093, 1968.
- 35-Hopkins, H. G., and Prager, W., The load carrying capacities of circular plates, J. Mech. Phys. Solids, v. 2, no. 1, p. 1-13, 1953.
- 36-Markov, A. A., On variational principles on theory of plasticity, Plasticity, Prin. Mat. Mekh. no. 11, p. 339-350, 1947.
- 37-Keller, H. B., Numerical methods for two point boundary value problems: Waltham, Mass. p. 184, 1968.
- 38-Lee, E. H., Mallet, R. L., and McKeeking, R. M., stress and deformation analysis of metal forming processes, Num. Meth. of M. Processes. Symp., A. S. M. E., Winter meeting, 1977.
- 39-Spencer, A. J. M. Approximate solutions of certain problems of axially symmetric plastic flow, J. Mech. and Phys. of solids, v. 12, no. 4, p. 231-243, 1964.
- 40-Martin, H., Finite elements and the analysis of geometrical non-linear problems, recent advances in matrix methods of

- structural analysis and design, Alabama Press, p. 343-381, 1971.
- 41-Wolf, A generalized stress models for finite element analysis, Ph. D. Thesis, Institut fur Baustatic, ETH, p. 256, 1974
- 42-Gurkok, A., Akay, H. U., FELPA., -A finite element analysis program for linear, plane and axisymmetric solid elasticity problems Comp. Prog. series 76-4, METU, 1978.
- 43-Stricklin, J. A., Rieseemann von, Tillerson, W. A., and Haisler, W. E., Static geometric and material non-linear analysis, Proc. 2nd. US-Japan Symposium on recent advances in computational methods of structural analysis and design, Berkeley, 1972.
- 44-Yamada, Y., Yoshimura, N., and Sakurai, T., Plastic stress-strain matrix and its applications for the solution of elastic-plastic problems by the finite element method, Int. J. Mech, Sci, v. 10, p. 343-394, 1968.
- 45-Bruce, R. W., and Welch, R. E., Finite element analysis of transient nonlinear structural behaviour, A.S.M.E. winter meeting, 1975.
- 46-Hibbit, H. D., and et. al., A finite element formulation for problems of large strain and large displacement: Providence, Report No. 00014-000712, Brown University, 1969.
- 47-Perzyna, P., Fundamental problems in visco-plasticity: New York, Recent advances in Applied Mechanics, Acedamic Press, p. 460, 1968.

- 48-Hill, R., and Tupper, S. J., A new theory of plastic deformations in wire-drawing, J. Iron Steel Inst, No. 159, p. 353, 1948.
- 49-Ho. W. S., and Brewer, R. C., slip-line field solution for machining with discontinuous chips, Proc. Instn. Mech. Engrs., v. 180, pt. 1, No. 34, p. 791-802, 1965-66.
- 50-Tomlenov, A. D., Plastic flow in the complex drawing of sheet metals (Russian), Kuznechno, Shtampovochohol Proizvodstvo, No. 7, 1968.
- 51-Jonson, W., Sowerby, R., and Haddow, J. B., Plane-Strain slip-line fields, Theory and bibliography. New York, American Elsevier Pub. Co., 1970.
- 52-H. Majors, JR., Studies in Cold-Drawing, Transactions of the ASME, v. 78, January, p. 79, 1956.
- 53-K. B. Lewis, The Wire-Drawing Die-Part 1, Wire and Wire Products, vol. 8, 1933, p. 197-200; Part 2, p. 234, 239, 243-251, Part 3, p. 266-269; Part 4, p. 331-333.
- 54-K. B. Lewis, Notes on Die Stresses, Wire and Wire Products, vol. 13, 1938, p. 443, 476-477.
- 55-F. C. Elder, The Wire Drawing Die, Wire and Wire Products, vol. 19, 1944, p. 25-29, 32, 33.
- 56-E. A. Davis and S. J. Dokos, Theory of Wire-Drawing, Journal of Applied Mechanics, December, 1944.
- 57-F. C. Thompson and E. L. Francis, Iron and Steel Institute, Studies of the Wire-Drawing Process, vol. 20, 1931, p. 87-124.

- 58-E. L. Francis and F. C. Thompson, The Drawing of non-ferrous wires, Journal of the Institute of Metals, vol. 46, 1931, p. 313-351
- 59-F. C. Thompson, The effect of a backward pull open the tension required to draw wire, Journal of the Iron and Steel Institute, vol. 128, 1933, p. 369-382.
- 60-F. C. Thompson, Lubrication in Wire-Drawing, The Metal Industry, London, vol. 51, 1937, p. 409-411.
- 61-G. Sachs, Plasticity problems in metals, Trans. Faraday Society, vol. 24, 1928, p. 84-92.
- 62-R. W. Lunt and G. D. S. Maclellan, An extension of Wire-Drawing Theory with special reference to the contributions of K. B. Lewis, Journal of the Institute of metals, vol. 72, 1946, p. 65-96.
- 63-G. D. S. Maclellan, A critical survey of the Wire-Drawing Theory, Journal of the Iron and Steel Institute, vol. 158, 1948, p. 347-356.
- 64-J. G. Wistreich, Investigations of the Mechanics of Wire Drawing, Proc. Inst. mech. Eng. , 1955, 169, p. 654-670.
- 65-C. T. Yang, On the Mechanics of Wire-Drawing, Journal of Engineering for Industry, November, 1961, p. 523-530.
- 66-F. C. Thompson and J. Barton, Studies of the Wire-Drawing process, Iron and steel Institute, vol. 19, 1930, p. 39-78.
- 67-J. M. Alexander, Manufacturing Properties of Materials, London, New York, D. van Nostrand, 489 pp, 1963.



APPENDICES

APPENDIX A

POLYNOMIAL FIT TO DISCRETE NODAL POINTS

For a given $(j+1)$ discrete points where the relationship between the variables x and y are given, it is possible to approximate this relationship analytically with a unique polynomial of degree not greater than (j) . Lagrange postulated the following general polynomial:

$$y = \left\{ \frac{X-X_1}{X_0-X_1} \cdot \frac{X-X_2}{X_0-X_2} \dots \frac{X-X_j}{X_0-X_j} \right\} y_0 + \left\{ \frac{X-X_0}{X_1-X_0} \cdot \frac{X-X_2}{X_1-X_2} \dots \frac{X-X_j}{X_1-X_j} \right\} y_1 + \dots \quad (A-1)$$

In the present study; usually three consecutive points at unequal intervals are available. Then a polynomial of second degree can approximate the functional relationship:

$$y = \frac{(X-X_1) \cdot (X-X_2)}{(X_0-X_1) \cdot (X_0-X_2)} y_0 + \frac{(X-X_0) \cdot (X-X_2)}{(X_1-X_0) \cdot (X_1-X_2)} y_1 + \frac{(X-X_0) \cdot (X-X_1)}{(X_2-X_0) \cdot (X_2-X_1)} y_2 \quad (A-2)$$

For the set of points 1, 2, 3 with co-ordinates (x_0, y_0) ; (x_1, y_1) ; (x_2, y_2) respectively. Expressing equation (A-2) in a more compact form:

Let

$$O = \frac{y_0}{(X_0-X_1) \cdot (X_0-X_2)} \quad (A-3. b)$$

$$P = \frac{y_1}{(X_1 - X_0) \cdot (X_1 - X_2)} \quad (A-3.c)$$

$$Q = \frac{y_2}{(X_2 - X_0) \cdot (X_2 - X_1)} \quad (A-3.c)$$

Then

$$y = (O+P+Q)X^2 + \{-O \cdot (X_2+X_1) - P(X_0+X_2) - Q(X_0+X_1)\} \cdot X + O \cdot X_1 \cdot X_2 + P \cdot X_0 \cdot X_2 + Q \cdot X_0 \cdot X_1 \quad (A-4)$$

or simply;

$$y \equiv a_1 X^2 + b_1 + c_1 \quad (A-5)$$

The constants of this second order polynomial can be determined by using the definitions given in Equations A-3, A-4 and the given three points. For a nodal point along β -direction which is neighbour to the axial-symmetry line, the polynomial can not be readily fitted, because there are only two points available for the fit. The first point can be fictitiously selected as a mirror image of the last point of the two; with respect to the axial symmetry line. In this case the co-ordinates of the first fictitious nodal point will be:

$$X_0 = X$$

$$y_0 = -y_2$$

This argument holds true only for a β -line, because there is no any such symmetry for the α -lines originating from the

die-inlet, and there remains only two points for the polynomial fit. In this case, the slope of the functional variable at the die inlet is used as the third information whenever available.

i. e.

If (x_1, y_1) , (x_2, y_2) and $(dy/dx)_{x_1}$ are given, then after certain manipulations:

$$y = \frac{(2 \cdot X_1 - X - X_2) \cdot (X - X_2)}{(X_1 - X_2)} y_1 + \frac{(X - X_1) \cdot (X - X_2)}{(X_1 - X_2)} (dy/dx)_{x_1} + \frac{(X - X_1)}{(X_2 - X_1)} y_2 \quad (A-6)$$

With a similar approach, the polynomial constants a_1 , b_1 , and c_1 can be determined for the first case also. Usually the slopes of the polynomials at the last point are required to compute the shear strains. (See Equation 4.31). In this case:

$$(dy/dx)_{x_2} = 2 \cdot X_2 \cdot (O + P + Q) - \{O \cdot (X_2 + X_1) - P(X_0 + X_2) - Q(X_0 + X_1)\} , \quad (A-7)$$

when three points are given

or:

$$(dy/dx)_{x_2} = 2 \cdot (y_1 - y_2) / (X_1 - X_2) - (dy/dx)_{x_1} , \quad (A-8)$$

when two points and the slope at first point is given.

The above methodology can be equivalently applied to any functional relationship apart from physical curves associated with the grid. For example, if one wants to obtain the functional dependance of $P_\beta \alpha$ on β -direction between the axial-symmetry line and the next neighbour point on the β -line:

$$P_{\beta\alpha}|_1 = 0 \quad (\text{No shear stress along axial-symmetry line})$$

$$\beta_1 = 0 \quad .$$

Also

$$\delta(P_{\beta\alpha})/\delta\beta = 0 \quad (\text{Due to axial symmetry})$$

and, if the value of $P_{\beta\alpha}$ associated with the trial position of this next point is given:

$$P_{\beta\alpha}|_2 = C_2$$

Where;

$$\beta_2 = X_2 + du$$

Then:

$$P_{\beta\alpha}(\beta) = 0 \cdot \beta^2 + (P_{\beta\alpha}|_2 / \beta_2^2) \cdot \beta + 0 \equiv (P_{\beta\alpha}|_2 / \beta_2^2) \cdot \beta \quad (\text{A-9})$$

In this specific case , the relationship comes out to be linear function.

APPENDIX B

BINARY CHAPPING AND INVERSE INTERPOLATION METHOD TO DETERMINE THE ROOT OF A FUNCTION

When a function is computed at a set of discrete points of the argument, the root of this function can be determined provided that the function changes its sign within the region of interest. Figure. shows such a relationship.

Assume that any stepwise solution algorithm associated with the variables x and y starts from point D and it is required to find the root. In this case the solution is allowed to iterate until the sign of the functional variable changes. Let points A and B are the two last consecutive points where:

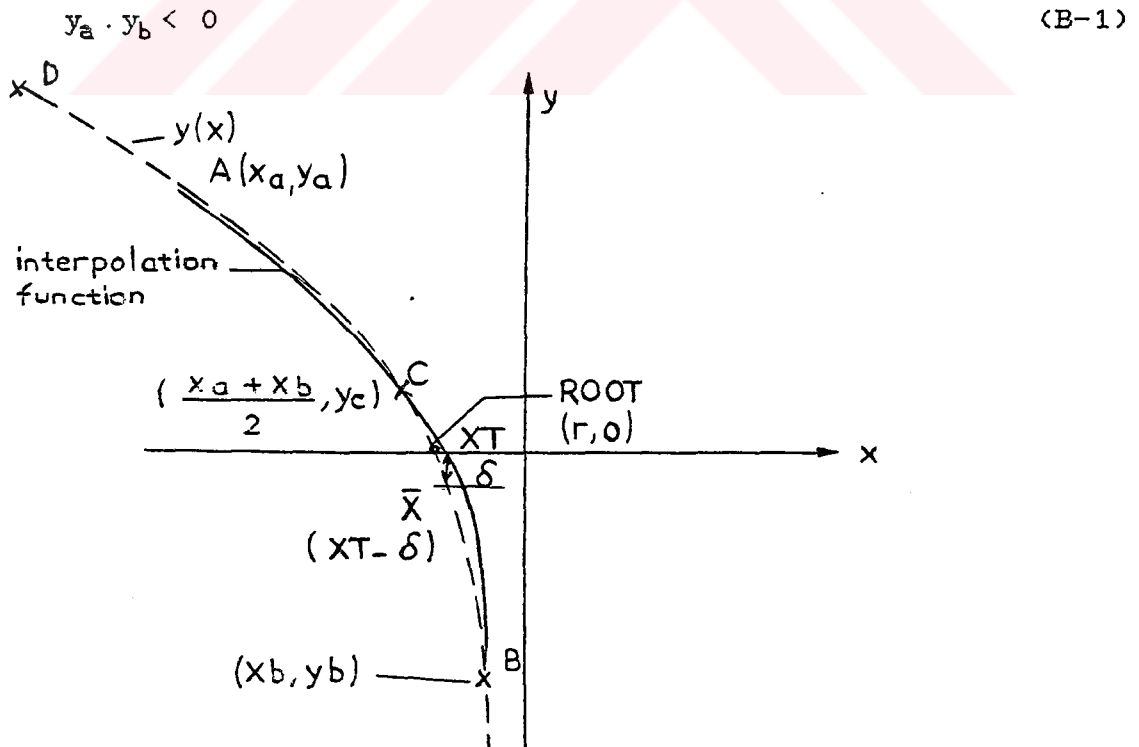


Figure.B.1 Determination of the root of a function

If the steps are held sufficiently small and the function is not ill conditioned and highly unstable, the root will likely be in between the points A and B:

$$X_a < r < X_b \quad (B-2)$$

The actual functional relationship given a discrete points is shown with a broken line. A third point C is defined on this line with its abscissa to:

$$X_c = \frac{X_a + X_b}{2} \quad (B-3)$$

The ordinate of this point is found by the same functional relationship $y(x)$:

$$y_c = y(x_c) \quad (B-4)$$

Now a second degree polynomial interpolation is made to the three points A, B and C:

$$y = \frac{(X_b - X) \cdot y_{ac} - (X_a - X) \cdot y_{bc}}{X_b - X_a} \quad (B-5)$$

where

$$y_{ac} = \frac{(X_c - X) \cdot y_a - (X_a - X) \cdot y_c}{X_c - X_a} \quad (B-6)$$

and

$$y_{bc} = \frac{(X_b - X) \cdot y_c - (X_c - X) \cdot y_b}{X_b - X_c} \quad (B-7)$$

This polynomial is shown with a bold line which passes through points A, B and C, and the approximates the discrete functional relationship with a continuous function in this domain. The approximate root will correspond to the condition where y_{bc} will equal to zero. Let this approximate root be denoted by XT. Then:

$$0 = \frac{(X_b - XT) \cdot y_{ac} - (X_a - XT) \cdot y_{bc}}{X_b - X_a} \quad (B-8)$$

It is difficult to solve XT directly from equation B-8 . The inverse interpolation can be effected by interchanging the given x's with the corresponding y's and carrying out the calculation as for direct interpolation:

$$XT = \frac{(y_b - 0) \cdot X_{ac} - (y_a - 0) \cdot X_{bc}}{y_b - y_a} \quad (B-9)$$

where

$$X_{ac} = \frac{(y_c - 0) \cdot X_a - (y_a - 0) \cdot X_c}{y_c - y_a} \quad (B-10)$$

and

$$X_{bc} = \frac{(y_b - 0) \cdot X_c - (y_c - 0) \cdot X_b}{y_b - y_c} \quad (B-11)$$

This XT value will of course will not correspond to the exact root r on the actual functional relationship. The corresponding y value for XT is denoted by δ , and this new point is shown by X. Depending upon the sign of δ , either point A or point B is deleted(chopped). By this elimination

method of the worst point. XT value is converged to the actual root r:

if $\delta < 0$ delete point B.

if $\delta > 0$ delete point A.

Substituting this new point X instead of A or B, the interpolation algorithm is repeated until δ value becomes negligibly small:

If $\delta < \text{EPS}$ the interpolation iteration is stopped after some more iteration to make sure that the solution converges to the actual root. Here EPS is a specified small number denoting the degree of accuracy.

APPENDIX C

NUMERICAL INTEGRATION

The Trapezoidal Method

Consider an integrable function $f(x)$ on the interval $a \leq x \leq b$. We wish to calculate the integral

$$I(x) = \int_a^x f(x) \cdot dx \quad (C-1)$$

If x_j is located at the dividing line between two panels, then $I(x_j)$ is the area under $f(x)$ from $x=a$ to this dividing line. The quantity $I(x_{j+1})$ is then composed of this area plus the area of one more panel. Assuming that $I(x)$ is an analytic function in the area of interest, then $I(x_{j+1})$ can be obtained from the Taylor series expansion about x_j as

$$\begin{aligned} I(x_{j+1}) &= I(x_j + \Delta x) \\ &= I(x_j) + (\Delta x) I'(x_j) + ((\Delta x)^2 / 2!) I''(x_j) + \\ &\quad + ((\Delta x)^3 / 3!) I'''(x_j) + O(\Delta x)^4 \end{aligned} \quad (C-2)$$

But since

$$I(x) = \int_a^x f(x) dx, \text{ then } I'(x_j) = f(x_j),$$
$$I''(x_j) = f'(x_j), \text{ etc.}$$

$$\begin{aligned} \Rightarrow I(x_{j+1}) &= I(x_j) + (\Delta x) f(x_j) + ((\Delta x)^2 / 2!) f'(x_j) + \\ &\quad + ((\Delta x)^3 / 3!) f''(x_j) + O(\Delta x)^4 \end{aligned} \quad (C-3)$$

The first derivative $f'(x_j)$ will now be replaced by the simple forward difference representation :

$$\frac{f(x_j+\Delta x)-f(x_j)}{\Delta x} = \frac{\Delta x}{2} f''(x_j) + O(\Delta x)^2 \quad (C-4)$$

$$\Rightarrow I(x_{j+1}) = I(x_j) + (\Delta x/2)[f(x_{j+1}) + f(x_j)] - (\Delta x)^3/12 f''(x_j) + O(\Delta x)^4 \quad (C-5)$$

$$\Rightarrow S_{j+1} = I(x_{j+1}) - I(x_j) = (\Delta x/2)[f(x_{j+1}) + f(x_j)] - (\Delta x)^3/12 f''(x_j) + O(\Delta x)^4 \quad (C-6)$$

The term $(\Delta x/2)[f(x_{j+1}) + f(x_j)]$ is the trapezoidal approximation for a single panel. The remaining term then represents the error. In order to evaluate the integral over the entire interval, the contributions of each panel must be added. Thus,

$$I = \sum_{j=1}^n S_j \quad (C-7)$$

or

$$I = (\Delta x/2)[f(a) + f(b) + 2 \sum_{j=1}^{n-1} f(x_j)] - (\Delta x)^3/12 \sum f''(x_j) + \text{higher order terms} \quad (C-8)$$

The dominant error term can be recast into a more understandable form. We apply the mean value theorem to the summation:

$$\sum_{j=0}^{n-1} f''(x_j) = n f''(\bar{x}), \quad a \leq \bar{x} \leq b \quad (C-9)$$

So the dominant error term becomes

$$-\frac{(\Delta x)^3}{12} \frac{(b-a)}{\Delta x} f''(\bar{x}) = -\frac{(\Delta x)^2}{12} (b-a) f''(\bar{x}) \quad (C-10)$$

$$I = (\Delta x/2) (f_0 + f_n + 2 \sum_{j=1}^{n-1} f_j) + O(\Delta x)^2 \quad (C-11)$$

For most reasonably well-behaved functions, it is possible to obtain a much improved integration technique by estimating the error term. Using simple differences, $f''(\bar{x})$ can be estimated as

$$f''(\bar{x}) \approx \frac{f'(b) - f'(a)}{b - a} \quad (C-12)$$

If this estimate is employed, then

$$I \approx (\Delta x/2) (f_0 + f_n + 2 \sum_{j=1}^{n-1} f_j) - ((\Delta x)^2 / 12) [f'(b) - f'(a)] \quad (C-13)$$

where :

$$\tilde{E} = -((\Delta x)^2 / 12) [f'(b) - f'(a)]$$

: Asymptotic error estimate

APPENDIX D

THE NUMERICAL SOLUTION OF ORDINARY DIFFERENTIAL EQUATION

Runge-Kutta Methods

The Runge-Kutta methods are among the most widely used formula for the numerical solution of ordinary differential equations. We will study only the fourth order formula which is the most popular:

$$y_{n+1} = y_n + 1/6 (k_1 + 2k_2 + 2k_3 + k_4), \quad n \geq 0, \quad (D-1)$$

$$k_1 = h f(y_n, t_n), \quad (D-2.a)$$

$$k_2 = h f(y_n + 1/2h, t_n + 1/2k_1), \quad (D-2.b)$$

$$k_3 = h f(y_n + 1/2h, t_n + 1/2k_2), \quad (D-2.c)$$

$$k_4 = h f(y_n + h, t_n + k_3), \quad (D-2.d)$$

APPENDIX E
SAMPLE OUTPUTS FOR ANALYTICAL SOLUTION

ANALYTICAL ANALYSIS OF WIRE DRAWING

BY MEANS OF THIS PROGRAM THE VARIATION OF MEAN DIE PRESSURE, DRAWING STRESS
AND DRAWING FORCE WITH PERCENTAGE REDUCTION OF AREA FOR DIFFERANT DIE ANGLES
CAN BE PLOTTED BY USING THE THEORIES OF SIEBEL, SACHS & AND ALSO WHITTON
EMPRICAL FORMULA.

NOMENCLATURE

Y IS THE MEAN YIELD STRESS IN (KG/MM²)
D1 IS THE INITIAL DIAMETER OF WIRE IN (MM)
D2 IS THE FINAL DIAMETER OF WIRE IN (MM)
M IS THE COEFFICIENT OF FRICTION BETWEEN WIRE AND DIE WHICH WAS ASSUMED CONSTANT
T IS THE SEMI ANGLE OF DIE CONE IN (DEGREE)

L IS THE LENGTH OF WIRE IN CONTACT WITH DIE IN (MM)
Q IS THE MEAN DIE PRESSURE IN (KG/MM²)
K IS THE DRAWING STRESS IN (KG/MM²)
P IS THE DRAWING FORCE IN (KG)
S IS THE SPLITTING FORCE BETWEEN THE HALVES OF DIE IN (KG)
R IS THE PERCENTAGE REDUCTION IN AREA

PLEASE WAIT
R= .3 REDUCTION IN AREA

KSS(21)= 10.5649983778 KG/MM^2 (SACHS)

KLL(21)= 14.5362788676 KG/MM^2 (SIEBEL)

KWW(21)= 10.6332326798 KG/MM^2 (WHITTON)

R= .3 REDUCTION IN AREA

PSS(21)= 52.2757010301 KG (SACHS)

PLL(21)= 71.9256303692 KG (SIEBEL)

PWW(21)= 52.6133249317 KG (WHITTON)

R= .3 REDUCTION IN AREA

QSS(21)= 19.9571195944 KG/MM^2 (SACHS)

QLL(21)= 27.4588074172 KG/MM^2 (SIEBEL)

QWW(21)= 20.0860131425 KG/MM^2 (WHITTON)

R= .3 REDUCTION IN AREA

SSS(21)= 62.7027815898 KG (SACHS)

SLL(21)= 86.2721494478 KG (SIEBEL)

SWW(21)= 63.1077490479 KG (WHITTON)

PLEASE WAIT

KMAX:MAXIMUM DRAWING STRESSES W.R.T. SACHS,SIEBEL & WHITTON

KMAX= 19.750992823 KG/MM^2 (SACHS)

KMAX= 24.9562555208 KG/MM^2 (SIEBEL)

KMAX= 19.7802360953 KG/MM^2 (WHITTON)

PMAX:MAXIMUM DRAWING FORCES W.R.T. SACHS,SIEBEL & WHITTON

PMAX= 69.805770698 KG (SACHS)

PMAX= 88.2026876311 KG (SIEBEL)

PMAX= 69.9091249536 KG (WHITTON)

QMAX:MAXIMUM MEAN DIE PRESSURES W.R.T. SACHS,SIEBEL & WHITTON

QMAX= 24.8452007047 KG/MM^2 (SACHS)

QMAX= 304.710607126 KG/MM^2 (SIEBEL)

QMAX= 256.877261527 KG/MM^2 (WHITTON)

SMAX:MAXIMUM SPLITTING FORCES W.R.T. SACHS,SIEBEL & WHITTON

SMAX= 83.7294557039 KG (SACHS)

SMAX= 105.795881245 KG (SIEBEL)

SMAX= 83.8534253339 KG (WHITTON)

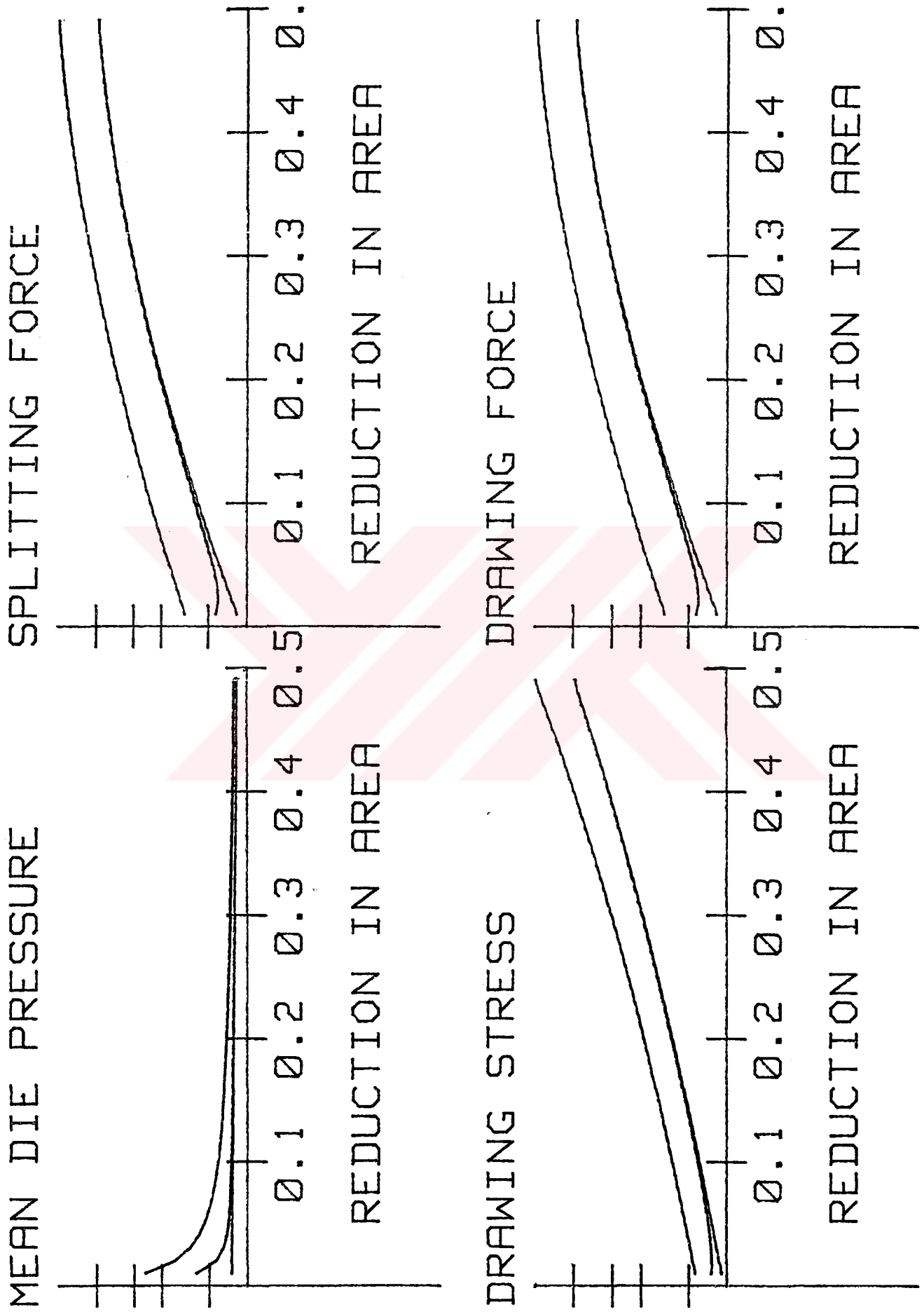


Figure .E.1. Variation of drawing stress, mean die pressure, splitting force and drawing force with reduction.

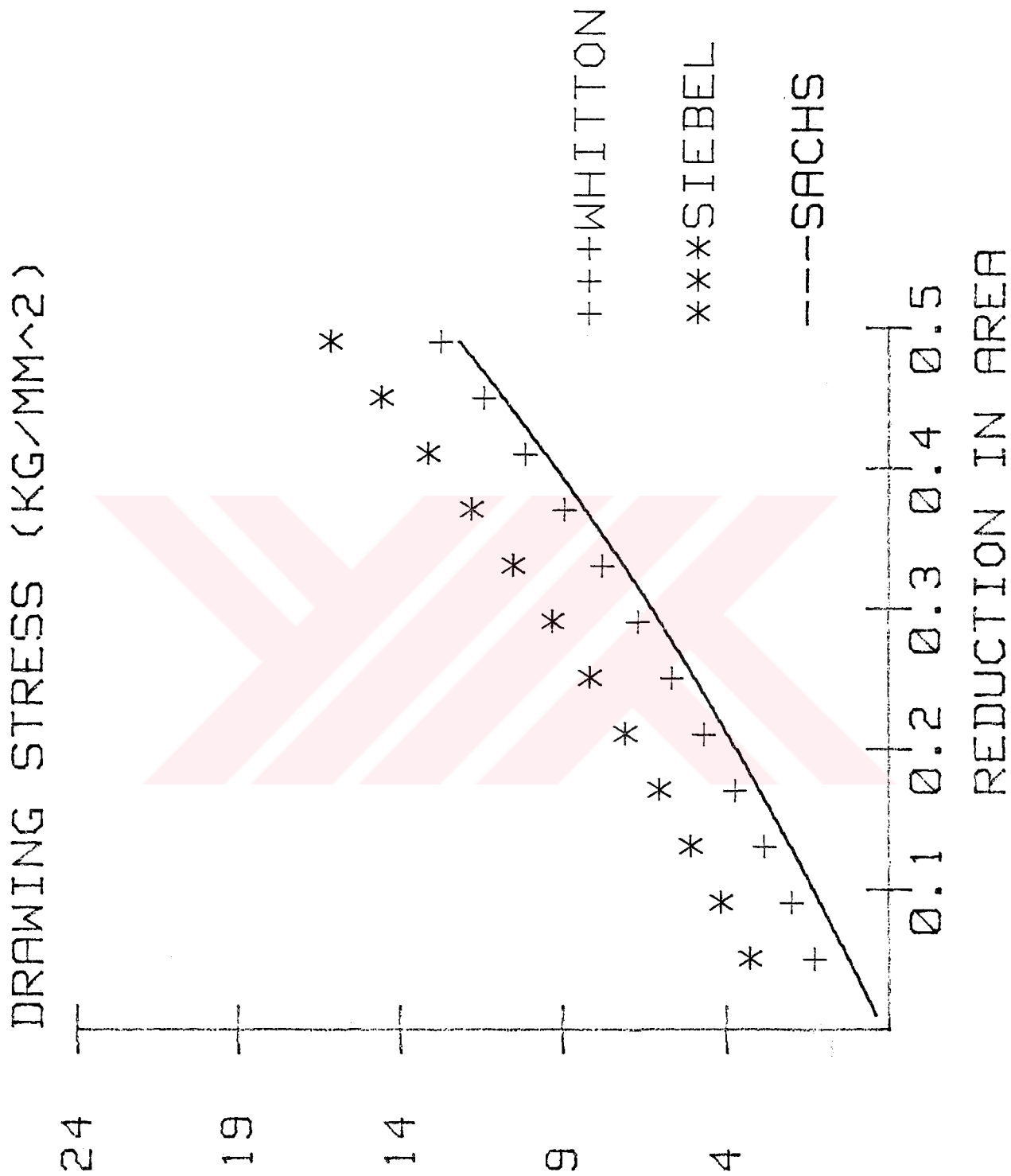


Figure.E.2. Variation of drawing stress with reduction.

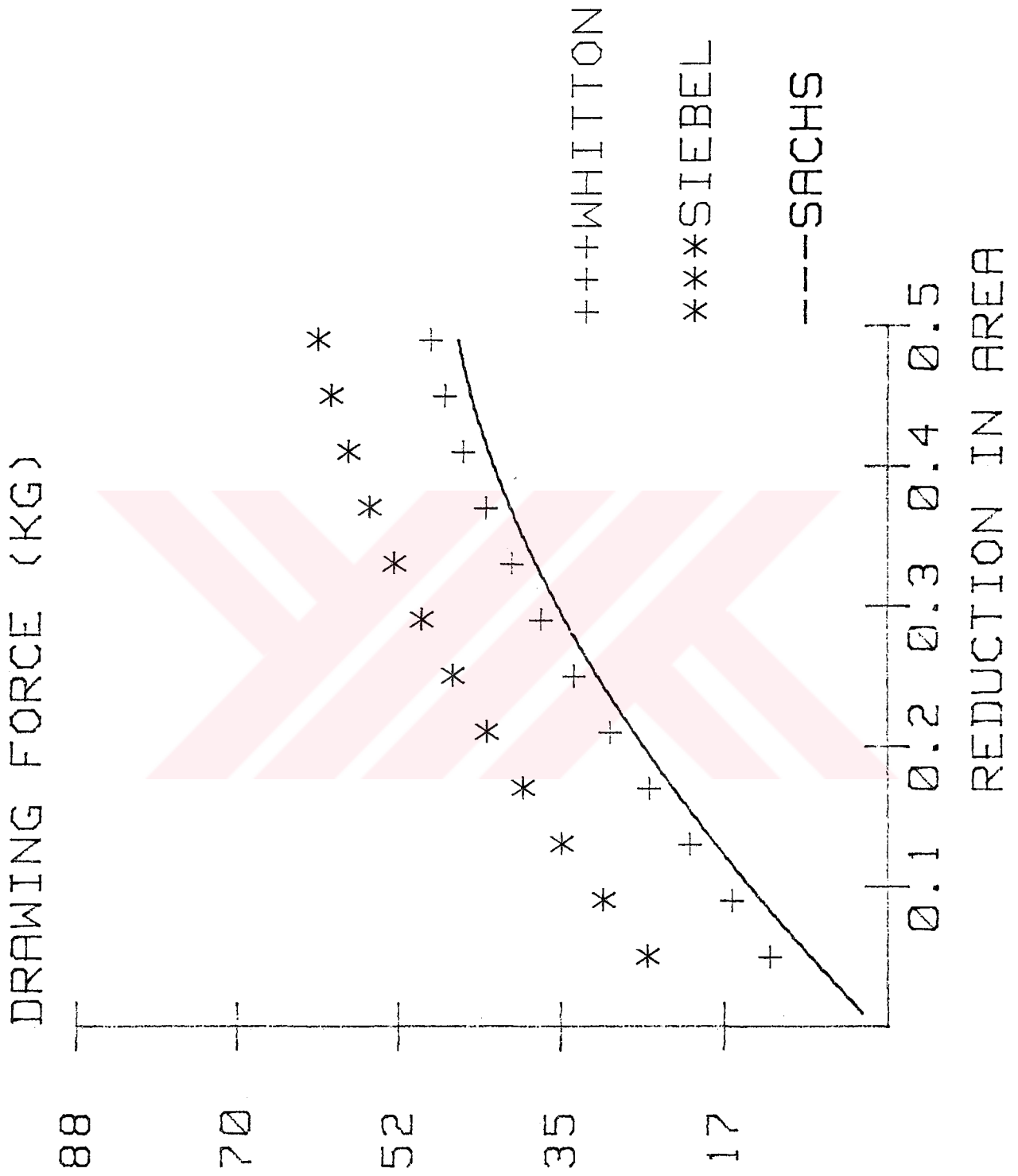


Figure.E.3. Variation of drawing force with reduction.

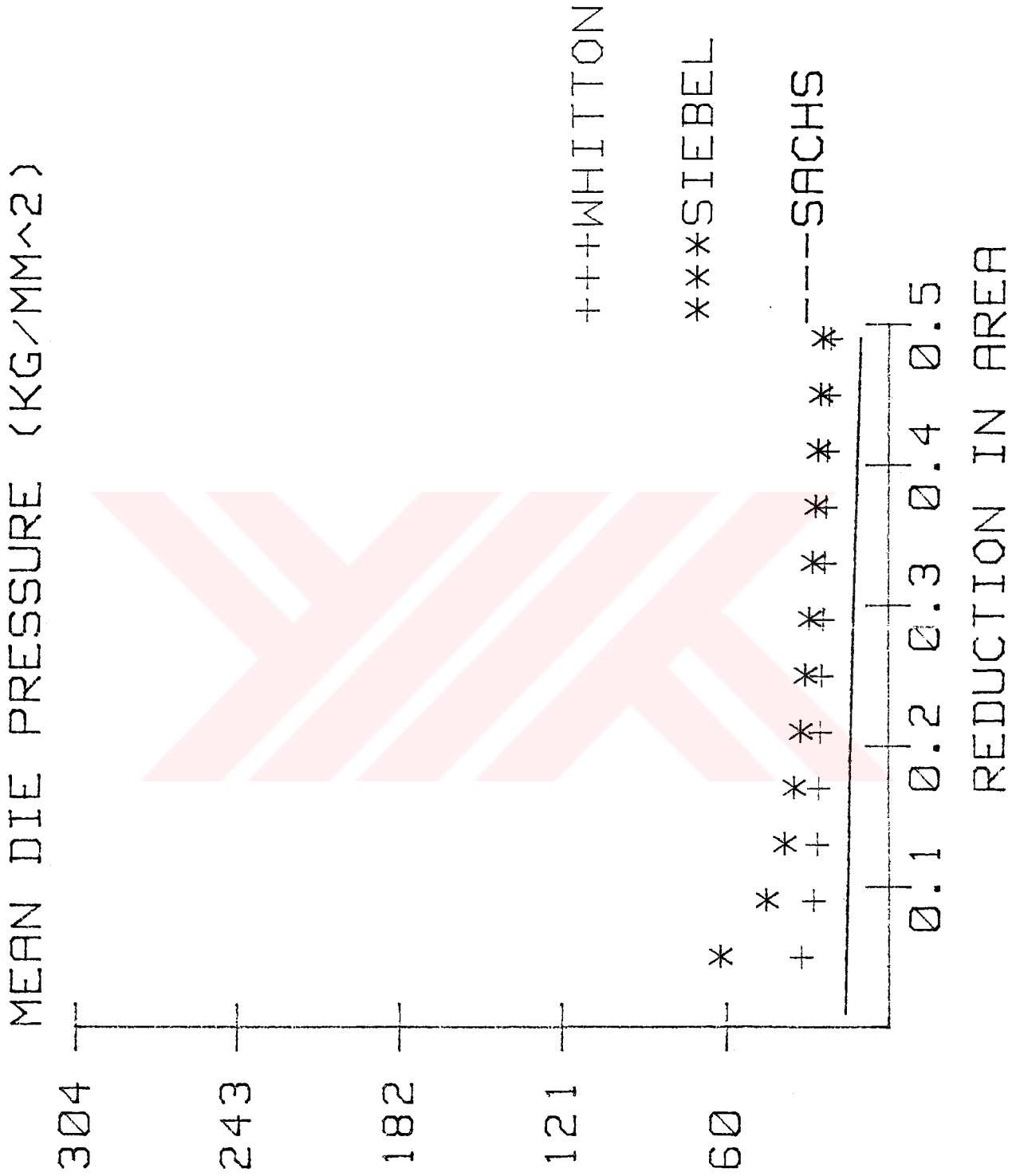


Figure.E.4. Variation of mean die pressure with reduction.

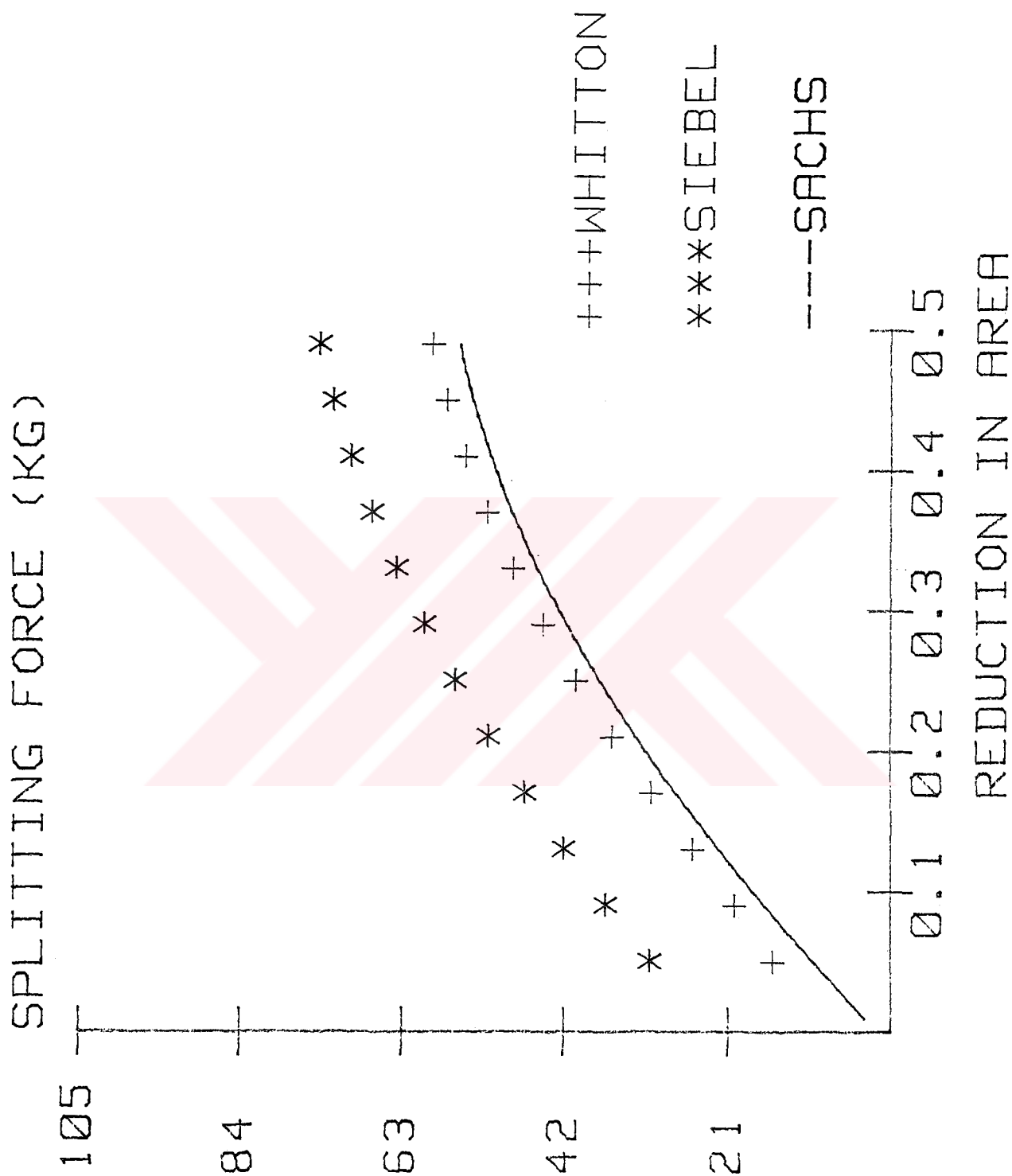


Figure.E.5. Variation of splitting force with reduction.

APPENDIX F
SAMPLE OUTPUTS FOR NUMERICAL SOLUTION

NOMENCLATURE

SAA, SAB, SAG: CURRENT STRAINS IN ALFA, BETA, GAMA DIRECTIONS

SSA : SHEAR STRAIN IN ALFA-BETA PLANE

SEA, SEB, SEG: CURRENT STRESSES IN ALFA, BETA, GAMA DIRECTIONS

SSE : SHEAR STRESS IN ALFA-BETA PLANE

XS : STRESS RATIO (SEB/SEA)

KS : STRESS RATIO (SEG/SEA)

YS : STRESS RATIO (SSE/SEA)

DA, DB : GRID LENGTHS IN ALFA AND BETA LINES FOR STRAIGHT LINES ONLY

H : STEP LENGTH IN RUNGA-KUTTA ALGORITHM

RA, RB, RG : RADII OF CURVATURE ON ALFA, BETA AND GAMA LINES

ALFA, BETA : CURRENT COORDINATES OF GRID NODES

OGA, OGB : ORIGINAL INSCRIBED GRID COORDINATES IN ALFA, BETA DIRECTIONS

SA : SLOPE OF ALFA LINE AT THE GRID NODE (MEASURED FROM ALFA AXIS)

SB : SLOPE OF BETA LINE AT THE GRID NODE (MEASURED FROM BETA AXIS)

AK, AJ : SHEAR ANGLES ON ALFA AND BETA LINES AT A GIVEN NODE

AA, AB : ARC LENGTHS OF ALFA AND BETA LINES BETWEEN SUCCESSIVE
NODES (THEY ARE COMPUTED BY POLYNOMIALS FITTED TO
DEFORMED GRID NODES)

AAN, ABN : NEW ARC LENGTHS OF THE ALFA AND BETA LINES BETWEEN SUCCESSIVE NODES

DSSA : INCREMENTAL SHEAR STRAIN IN ALFA-BETA PLANE

Q : (Q) APPEARING AT THE BEGINNING OR END OF ANY TERM
INDICATES THAT THIS TERM BELONGS TO PREVIOUS STAGE

NUMERICAL ANALYSIS OF WIRE DRAWING

ORIGINAL GRID COORDINATES

GRID PATTERN : 5 * 4

ALFA DIRECTION

DGA(1)= 0
DGA(2)= .47046301094E
DGA(3)= .940926021E96
DGA(4)= 1.4113890328A
DGA(5)= 1.86185204379

BETA DIRECTION

D (1)= 0
D (2)= .5
D (3)= 1
D (4)= 1.5

SOLUTION FOR 1 .TH STAGE

OUTERMOST GRID POINT= 4

BOUNDARY CONDITIONS

(A):DIE INLET

ALFA STRAIN	BETA STRAIN	GAMA STRAIN
0	0	0
0	0	0
0	0	0
0	0	0

ALFA STRESS	BETA STRESS	SHEAR STRESS
0	0	0
0	0	0
0	0	0
0	0	0

CURRENT COORDINATES OF GRID NODES AT DIE INLET

ALFA(1	1)=	0
BETA(1	1)=	0
ALFA(1	2)=	0
BETA(1	2)=	.5
ALFA(1	3)=	0
BETA(1	3)=	1
ALFA(1	4)=	0
BETA(1	4)=	1.5

STRESSES AT DIE INLET

SEa(1	1)=	0
SEB(1	1)=	0
SSE(1	1)=	0

STRESSES AT DIE INLET

SEa(1	2)=	0
SEB(1	2)=	0
SSE(1	2)=	0

STRESSES AT DIE INLET

SEa(1	3)=	0
SEB(1	3)=	0
SSE(1	3)=	0

STRESSES AT DIE INLET

SEa(1	4)=	0
SEB(1	4)=	0
SSE(1	4)=	0

SOLUTIONS AT NODE NUMBER = 2 , 1

INCREMENTAL ALFA STRAIN (mm/mm)= .12
INCREMENTAL BETA STRAIN (mm/mm)= -.06
INCREMENTAL GAMA STRAIN (mm/mm)= -.06
ALFA STRESS (kg/mm^2)= 0.0
BETA STRESS (kg/mm^2)= 0.0
GAMA STRESS (kg/mm^2)= 0.0
SHEAR STRESS (kg/mm^2)= 0.0
NEW COORDINATES:

ALFA(I,J) = .50
BETA(I,J) = 0.00
DU = .500
DV = 0.000
TOTAL NUMBER OF ITERATIONS = 20

PLEASE WAIT

SOLUTIONS AT NODE NUMBER= 2 , 2

INCREMENTAL ALFA STRAIN (mm/mm)= .28
INCREMENTAL BETA STRAIN (mm/mm)= -.13
INCREMENTAL GAMA STRAIN (mm/mm)= -.15
INCREMENTAL SHEAR STRAIN (mm/mm)= -0.00
ALFA STRESS (kg/mm^2)= 1.6
BETA STRESS (kg/mm^2)= -.1
GAMA STRESS (kg/mm^2)= -.1
SHEAR STRESS (kg/mm^2)= -0.0
DU (mm)= .059
DV (mm)= -.048
NEW COORDINATES:

ALFA(2 2) (mm)= .529554818822
BETA(2 2) (mm)= .451666666667
TOTAL NUMBER OF ITERATIONS= 3

PLEASE WAIT

SOLUTIONS AT NODE NUMBER= 2 , 3

INCREMENTAL ALFA STRAIN (mm/mm)= .59
INCREMENTAL BETA STRAIN (mm/mm)= 1.33
INCREMENTAL GAMA STRAIN (mm/mm)= -1.91
INCREMENTAL SHEAR STRAIN (mm/mm)= -.03
ALFA STRESS (kg/mm^2)= 1.3
BETA STRESS (kg/mm^2)= .6
GAMA STRESS (kg/mm^2)= 4.0
SHEAR STRESS (kg/mm^2)= 0.0
DU (mm)= .139
DV (mm)= -.102
NEW COORDINATES:

ALFA(2 3) (mm)= .609554818822
BETA(2 3) (mm)= .898333333333
TOTAL NUMBER OF ITERATIONS= 7

PLEASE WAIT

SOLUTIONS AT NODE NUMBER= 2 , 4

INCREMENTAL ALFA STRAIN (mm/mm)= .89
INCREMENTAL BETA STRAIN (mm/mm)= .72
INCREMENTAL GAMA STRAIN (mm/mm)= -1.61
INCREMENTAL SHEAR STRAIN (mm/mm)= -.05
ALFA STRESS (kg/mm²)= .8
BETA STRESS (kg/mm²)= 1.2
GAMA STRESS (kg/mm²)= 3.9
SHEAR STRESS (kg/mm²)= .1
DIE SPLITTING FORCE (kgf)= .7
DU (mm)= .239
DV (mm)= -.130
NEW COORDINATES:

ALFA(2 4) (mm)= .709554818822
BETA(2 4) (mm)= 1.37
TOTAL NUMBER OF ITERATIONS= 6

PLEASE WAIT

SOLUTIONS AT NODE NUMBER = 3 , 1

INCREMENTAL ALFA STRAIN (mm/mm)= .18
INCREMENTAL BETA STRAIN (mm/mm)= -.09
INCREMENTAL GAMA STRAIN (mm/mm)= -.09
ALFA STRESS (kg/mm²)= 0.0
BETA STRESS (kg/mm²)= 0.0
GAMA STRESS (kg/mm²)= 0.0
SHEAR STRESS (kg/mm²)= 0.0
NEW COORDINATES:

ALFA(I,J) = 1.05
BETA(I,J) = 0.00
DU = .547
DV = 0.000
TOTAL NUMBER OF ITERATIONS = 20.

PLEASE WAIT

SOLUTIONS AT NODE NUMBER= 3 , 2

INCREMENTAL ALFA STRAIN (mm/mm)= 1.47
INCREMENTAL BETA STRAIN (mm/mm)= -.64
INCREMENTAL GAMA STRAIN (mm/mm)= -.83
INCREMENTAL SHEAR STRAIN (mm/mm)= .08
ALFA STRESS (kg/mm²)= 4.9
BETA STRESS (kg/mm²)= 2.0
GAMA STRESS (kg/mm²)= 1.8
SHEAR STRESS (kg/mm²)= .1
DU (mm)= .165
DV (mm)= -.167
NEW COORDINATES:

ALFA(3 2) (mm)= 1.10615485488
BETA(3 2) (mm)= .333333333333
TOTAL NUMBER OF ITERATIONS= 20

PLEASE WAIT

SOLUTIONS AT NODE NUMBER= 3 , 3

INCREMENTAL ALFA STRAIN (mm/mm)= 1.16
INCREMENTAL BETA STRAIN (mm/mm)= 1.74
INCREMENTAL GAMA STRAIN (mm/mm)= -2.90
INCREMENTAL SHEAR STRAIN (mm/mm)= -.05
ALFA STRESS (kg/mm^2)= 1.2
BETA STRESS (kg/mm^2)= .9
GAMA STRESS (kg/mm^2)= 4.6
SHEAR STRESS (kg/mm^2)= 0.0
DU (mm)= .175
DV (mm)= -.133
NEW COORDINATES:

ALFA(3 3) (mm)= 1.11615485488
BETA(3 3) (mm)= .866666666667
TOTAL NUMBER OF ITERATIONS= 1

PLEASE WAIT

SOLUTIONS AT NODE NUMBER= 3 , 4

INCREMENTAL ALFA STRAIN (mm/mm)= .94
INCREMENTAL BETA STRAIN (mm/mm)= .17
INCREMENTAL GAMA STRAIN (mm/mm)= -1.11
INCREMENTAL SHEAR STRAIN (mm/mm)= -.02
ALFA STRESS (kg/mm^2)= .8
BETA STRESS (kg/mm^2)= -.5
GAMA STRESS (kg/mm^2)= -2.3
SHEAR STRESS (kg/mm^2)= -0.0
DIE SPLITTING FORCE (kgf)= -.6
DU (mm)= .215
DV (mm)= -.200
NEW COORDINATES:

ALFA(3 4) (mm)= 1.15615485488
BETA(3 4) (mm)= 1.3
TOTAL NUMBER OF ITERATIONS= 1

PLEASE WAIT

SOLUTIONS AT NODE NUMBER = 4 , 1

INCREMENTAL ALFA STRAIN (mm/mm)= .24
INCREMENTAL BETA STRAIN (mm/mm)= -.12
INCREMENTAL GAMA STRAIN (mm/mm)= -.12
ALFA STRESS (kg/mm^2)= 0.0
BETA STRESS (kg/mm^2)= 0.0
GAMA STRESS (kg/mm^2)= 0.0
SHEAR STRESS (kg/mm^2)= 0.0
NEW COORDINATES:

ALFA(I,J) = 1.63
BETA(I,J) = 0.00
DU = .580
DV = 0.000
TOTAL NUMBER OF ITERATIONS = 20

PLEASE WAIT

SOLUTIONS AT NODE NUMBER= 4 , 2

INCREMENTAL ALFA STRAIN (mm/mm)= 1.18
INCREMENTAL BETA STRAIN (mm/mm)= -.74
INCREMENTAL GAMA STRAIN (mm/mm)= -.45
INCREMENTAL SHEAR STRAIN (mm/mm)= .35
ALFA STRESS (kg/mm²)= 12.4
BETA STRESS (kg/mm²)= 9.4
GAMA STRESS (kg/mm²)= 9.8
SHEAR STRESS (kg/mm²)= .5
DU (mm)= .305
DV (mm)= -.200
NEW COORDINATES:

ALFA(4 2) (mm)= 1.71655474951
BETA(4 2) (mm)= .3
TOTAL NUMBER OF ITERATIONS= 20

PLEASE WAIT

SOLUTIONS AT NODE NUMBER= 4 , 3

INCREMENTAL ALFA STRAIN (mm/mm)= 1.54
INCREMENTAL BETA STRAIN (mm/mm)= 1.48
INCREMENTAL GAMA STRAIN (mm/mm)= -3.02
INCREMENTAL SHEAR STRAIN (mm/mm)= -.12
ALFA STRESS (kg/mm²)= 1.6
BETA STRESS (kg/mm²)= 1.9
GAMA STRESS (kg/mm²)= 5.5
SHEAR STRESS (kg/mm²)= .1
DU (mm)= .375
DV (mm)= -.300
NEW COORDINATES:

ALFA(4 3) (mm)= 1.78655474951
BETA(4 3) (mm)= .7
TOTAL NUMBER OF ITERATIONS= 20

PLEASE WAIT

SOLUTIONS AT NODE NUMBER= 4 , 4

INCREMENTAL ALFA STRAIN (mm/mm)= 1.73
INCREMENTAL BETA STRAIN (mm/mm)= .30
INCREMENTAL GAMA STRAIN (mm/mm)= -2.04
INCREMENTAL SHEAR STRAIN (mm/mm)= -.17
ALFA STRESS (kg/mm²)= 1.5
BETA STRESS (kg/mm²)= 3.2
GAMA STRESS (kg/mm²)= 5.5
SHEAR STRESS (kg/mm²)= .2
DIE SPLITTING FORCE (kgf)= 5.8
DU (mm)= .355
DV (mm)= -.300
NEW COORDINATES:

ALFA(4 4) (mm)= 1.76655474951
BETA(4 4) (mm)= 1.2
TOTAL NUMBER OF ITERATIONS= 1

PLEASE WAIT

SOLUTIONS AT NODE NUMBER = 5 , 1

INCREMENTAL ALFA STRAIN (mm/mm)= .30
INCREMENTAL BETA STRAIN (mm/mm)= -.15
INCREMENTAL GAMA STRAIN (mm/mm)= -.15
ALFA STRESS (kg/mm^2)= 0.0
BETA STRESS (kg/mm^2)= 0.0
GAMA STRESS (kg/mm^2)= 0.0
SHEAR STRESS (kg/mm^2)= 0.0
NEW COORDINATES:

ALFA(I,J) = 2.24
BETA(I,J) = 0.00
DU = .616
DV = 0.000
TOTAL NUMBER OF ITERATIONS = 20

PLEASE WAIT

SOLUTIONS AT NODE NUMBER= 5 , 2

INCREMENTAL ALFA STRAIN (mm/mm)= 2.15
INCREMENTAL BETA STRAIN (mm/mm)= -.12
INCREMENTAL GAMA STRAIN (mm/mm)= -2.04
INCREMENTAL SHEAR STRAIN (mm/mm)= .69
ALFA STRESS (kg/mm^2)= 14.4
BETA STRESS (kg/mm^2)= 12.0
GAMA STRESS (kg/mm^2)= 10.4
SHEAR STRESS (kg/mm^2)= .6
DRAWING FORCE (kgf)= 54.8
DU (mm)= .581
DV (mm)= -.133
NEW COORDINATES:

ALFA(5 2) (mm)= 2.46284456923
BETA(5 2) (mm)= .3666666666667
TOTAL NUMBER OF ITERATIONS= 1

PLEASE WAIT

SOLUTIONS AT NODE NUMBER= 5 , 3

INCREMENTAL ALFA STRAIN (mm/mm)= 1.81
INCREMENTAL BETA STRAIN (mm/mm)= .85
INCREMENTAL GAMA STRAIN (mm/mm)= -2.66
INCREMENTAL SHEAR STRAIN (mm/mm)= -.36
ALFA STRESS (kg/mm^2)= 4.8
BETA STRESS (kg/mm^2)= 5.9
GAMA STRESS (kg/mm^2)= 8.9
SHEAR STRESS (kg/mm^2)= .3
DRAWING FORCE (kgf)= 18.3
DU (mm)= .501
DV (mm)= -.367
NEW COORDINATES:

ALFA(5 3) (mm)= 2.38284456923
BETA(5 3) (mm)= .633333333333

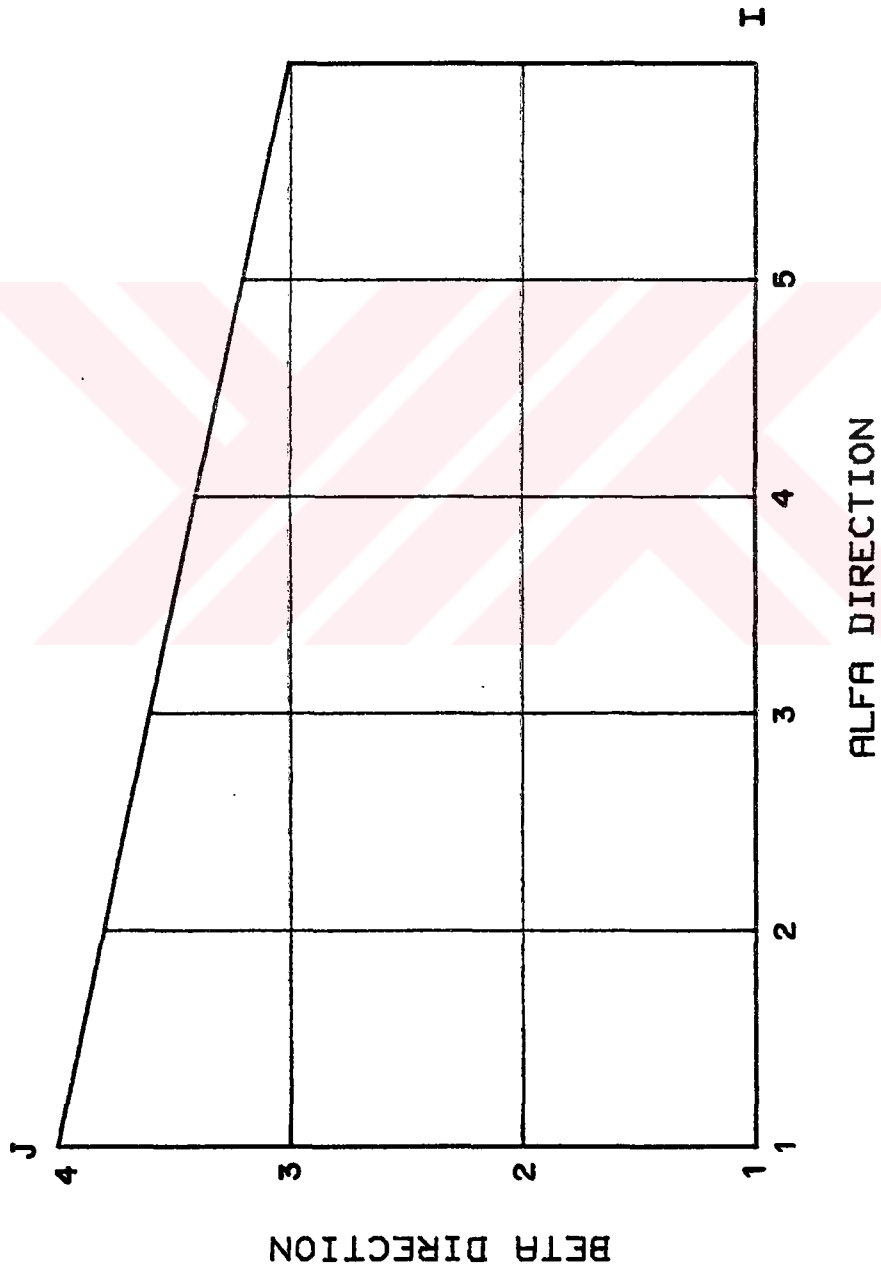
PLEASE WAIT

SOLUTIONS AT NODE NUMBER= 5 , 4

INCREMENTAL ALFA STRAIN (mm/mm)= 1.62
INCREMENTAL BETA STRAIN (mm/mm)= .92
INCREMENTAL GAMA STRAIN (mm/mm)= -2.54
INCREMENTAL SHEAR STRAIN (mm/mm)= .20
ALFA STRESS (kg/mm²)= 4.4
BETA STRESS (kg/mm²)= 3.5
GAMA STRESS (kg/mm²)= .5
SHEAR STRESS (kg/mm²)= .2
DRAWING FORCE (kgf)= 16.8
DIE SPLITTING FORCE (kgf)= 8.5
DU (mm)= .601
DV (mm)= -.400
NEW COORDINATES:

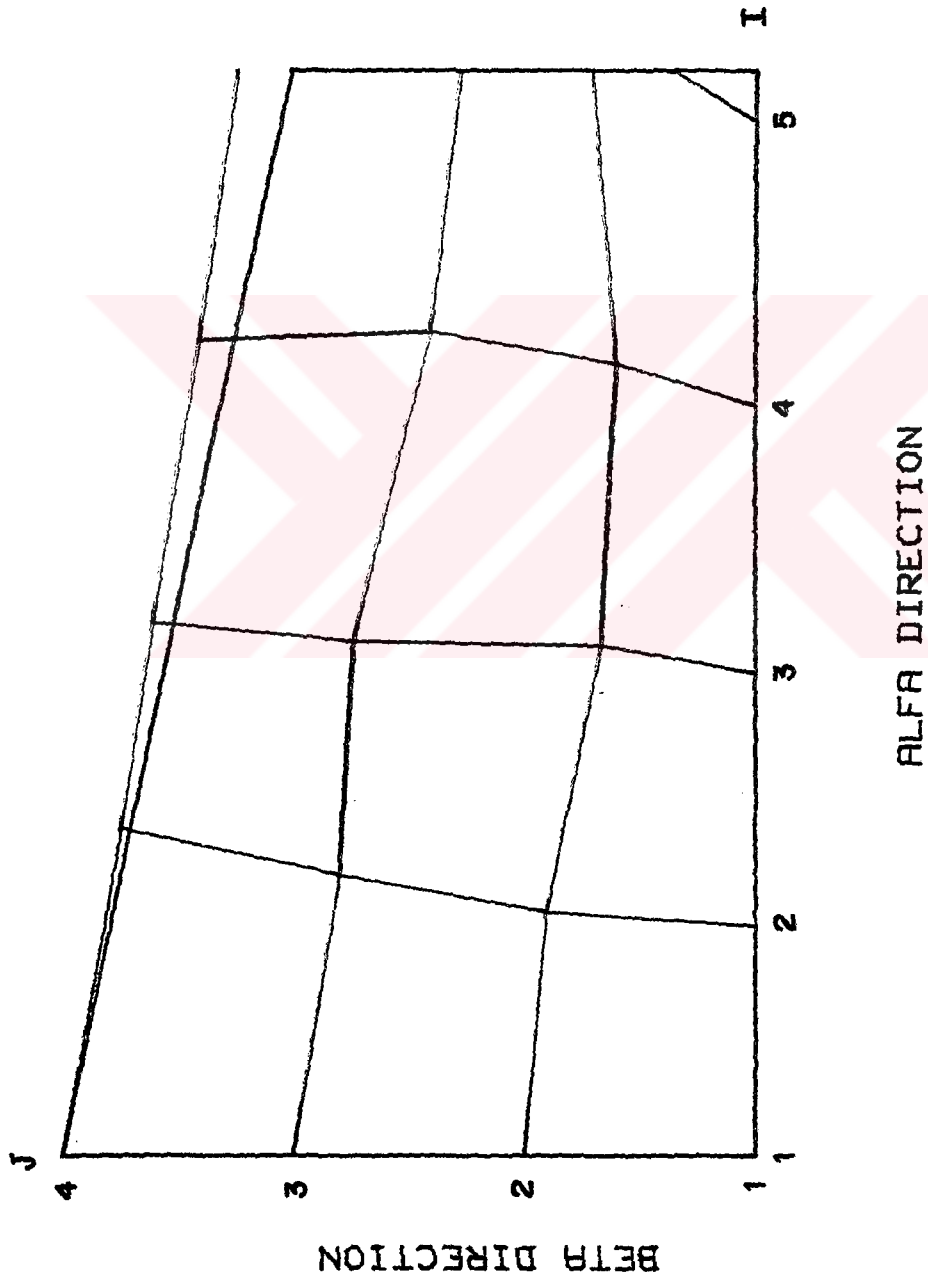
ALFA(5 4) (mm)= 2.48284456923
BETA(5 4) (mm)= 1.1
TOTAL NUMBER OF ITERATIONS= 1





ORIGINAL GRID LINES

Figure.F.1. Original grid lines along α and β -lines



GRID LINES AFTER DEFORMATION

Figure.F.2. Grid lines after deformation

J= 2

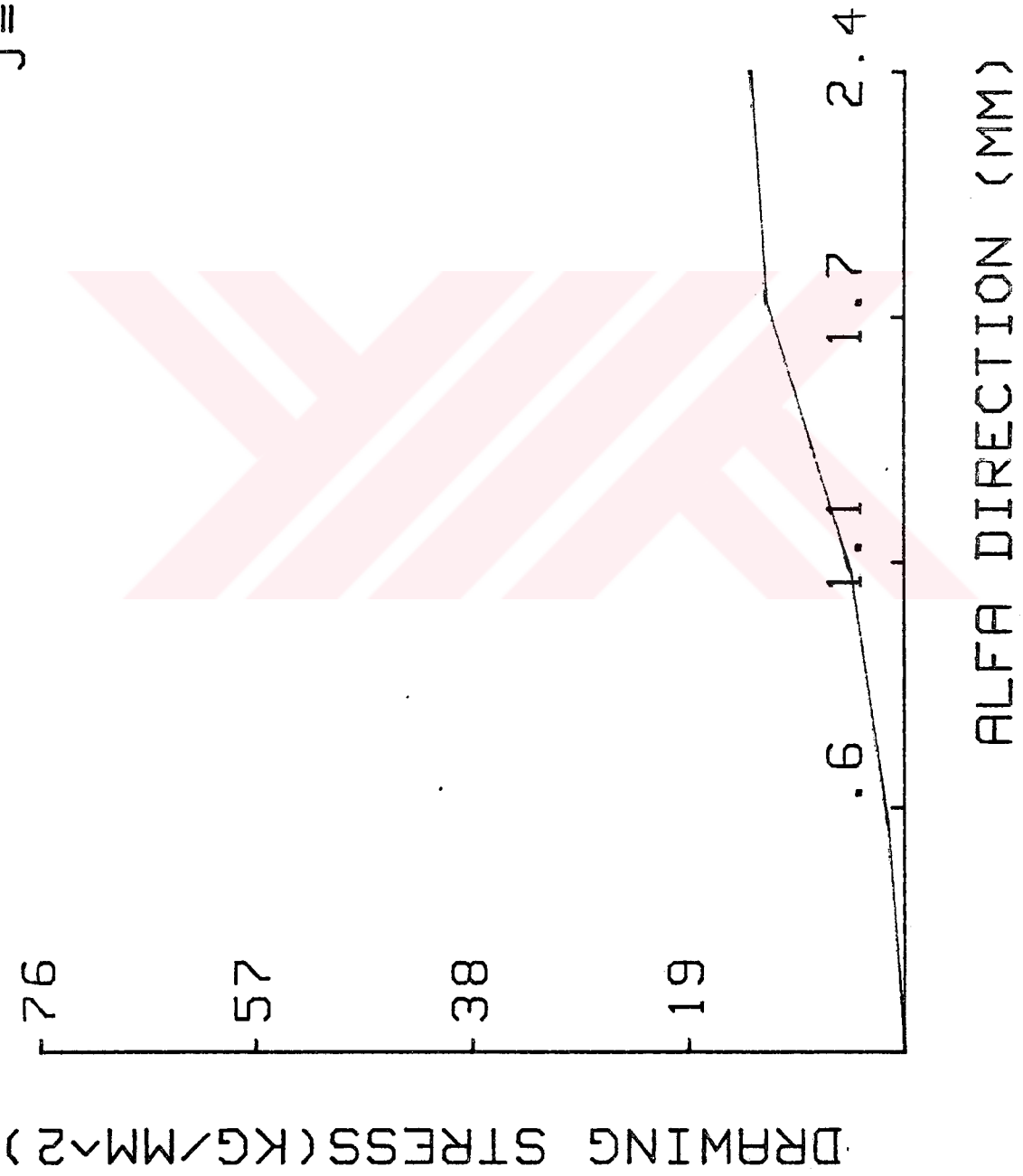


Figure.F.3. Variation of drawing stress along α -direction

J= 2

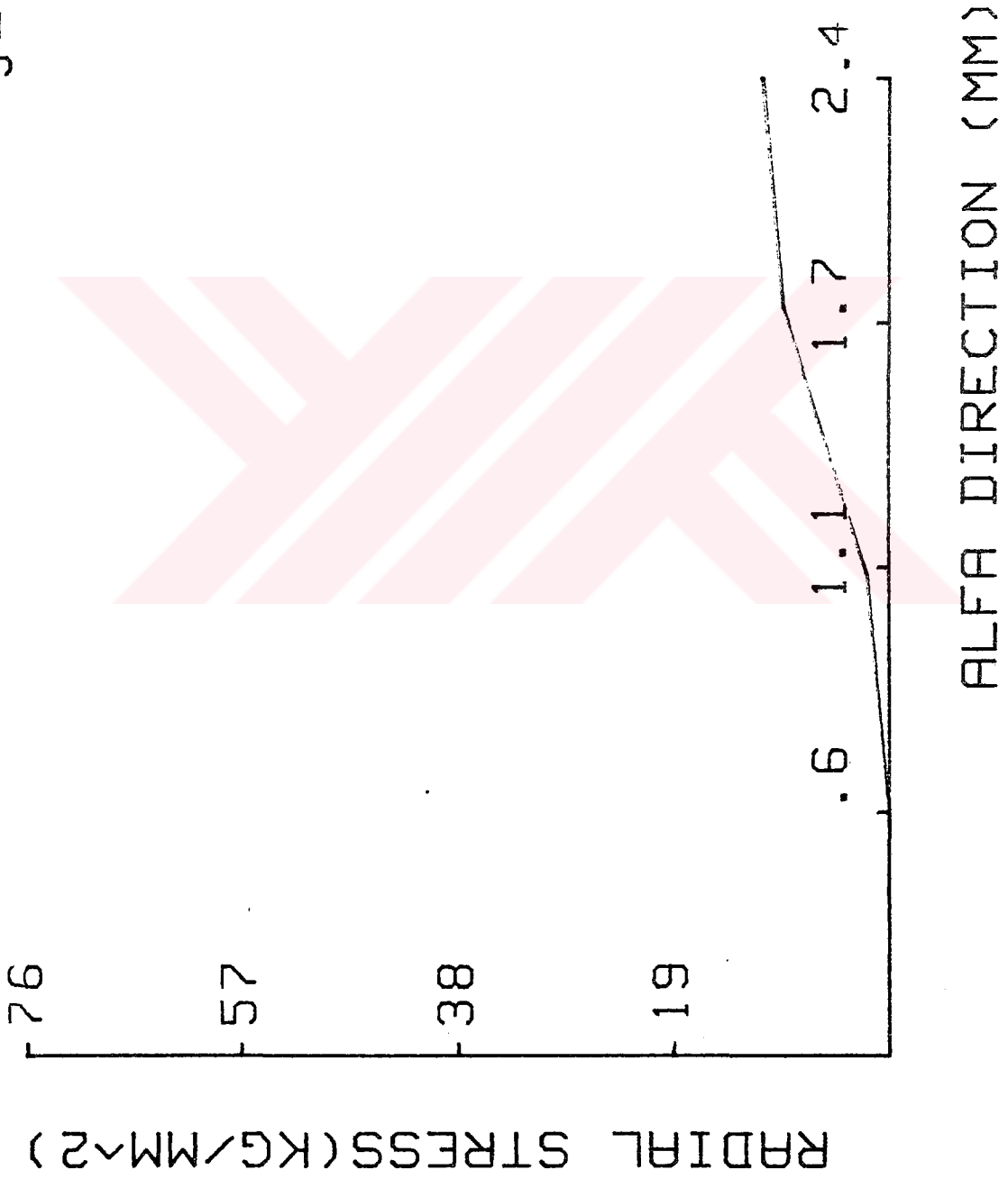


Figure.F.4. Variation of radial stress along α -direction

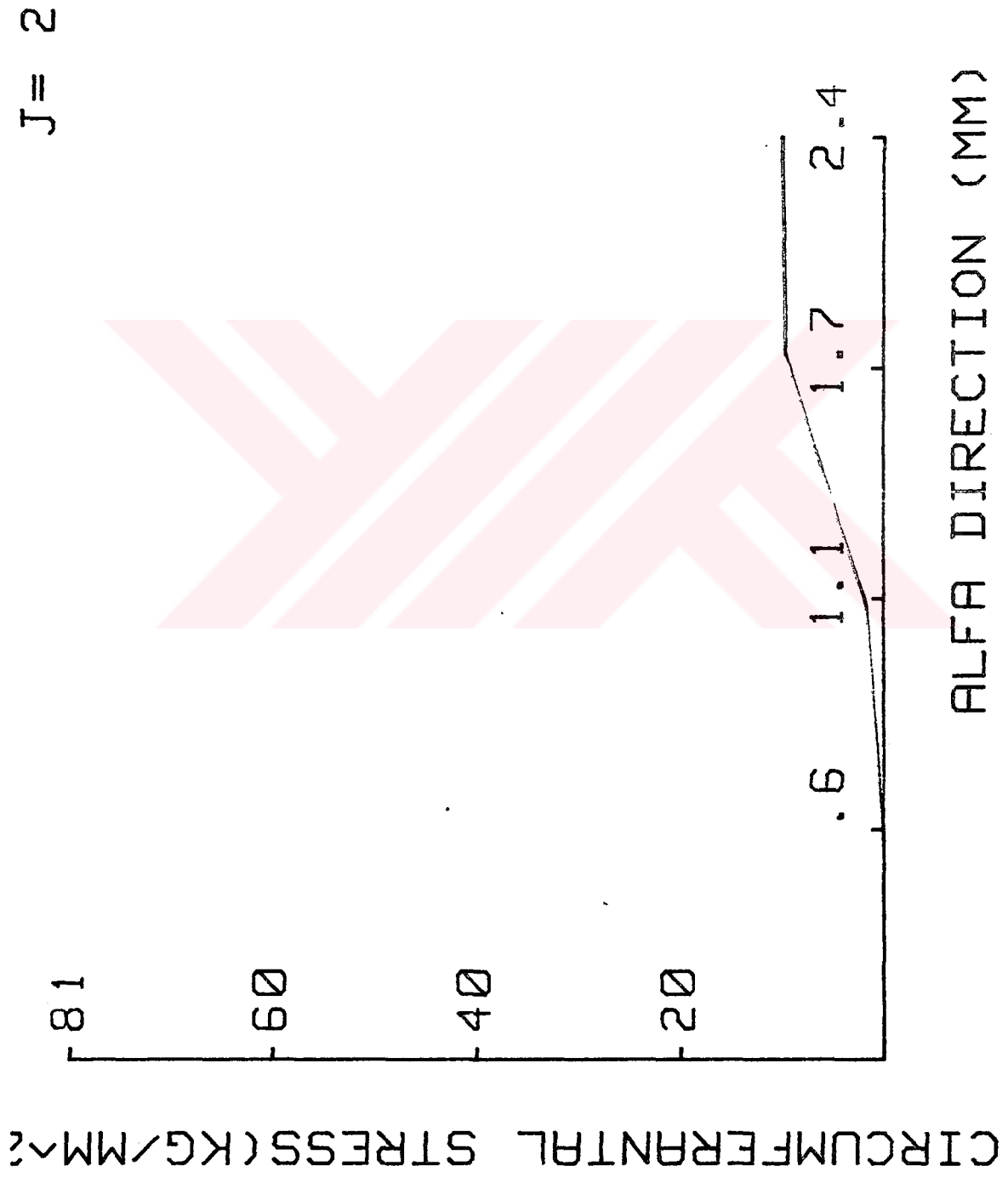


Figure.F.5. Variation of circumferential stress along α -direction

J= 2

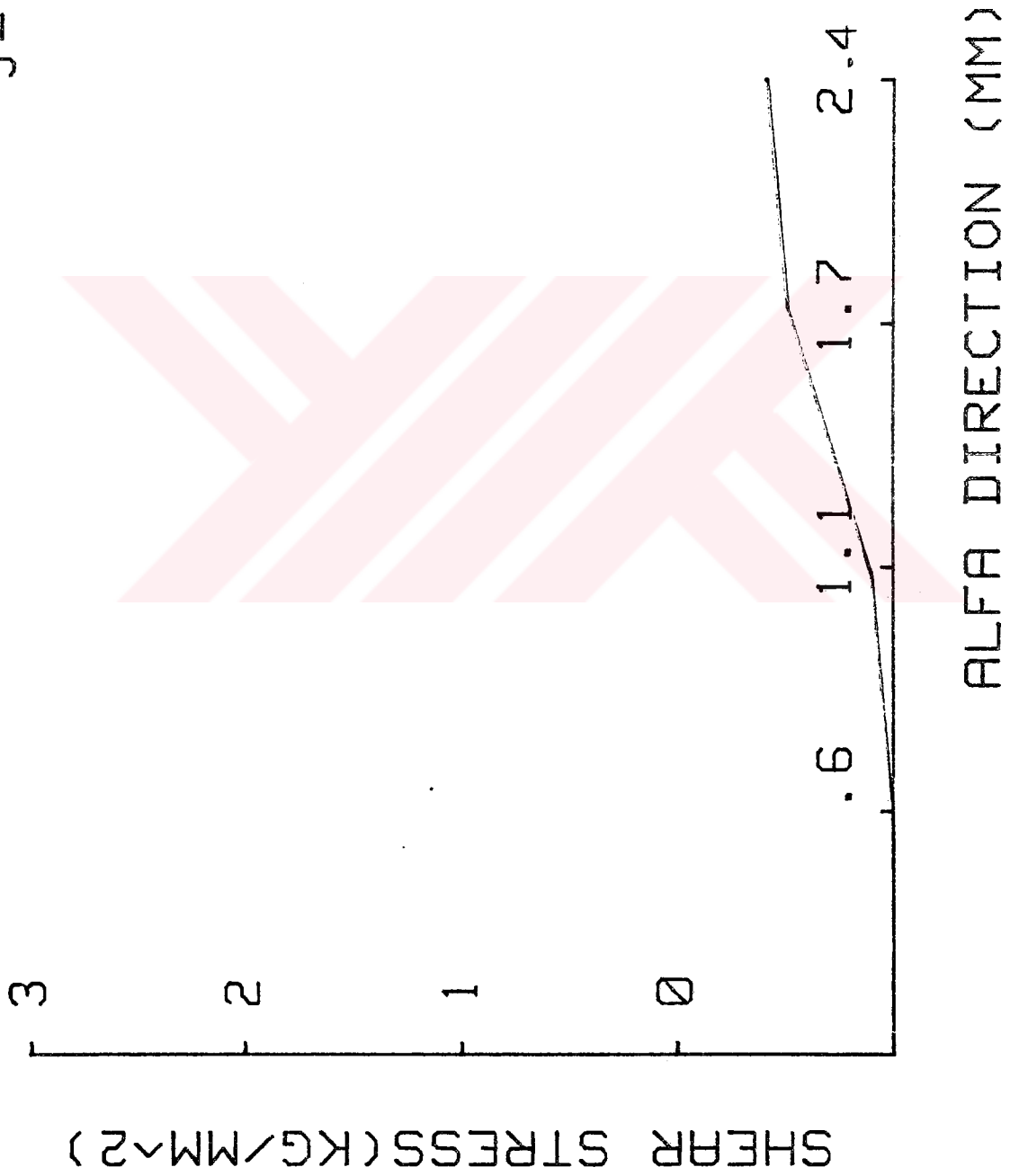


Figure.F.6. Variation of shear stress along α -direction

I = 5

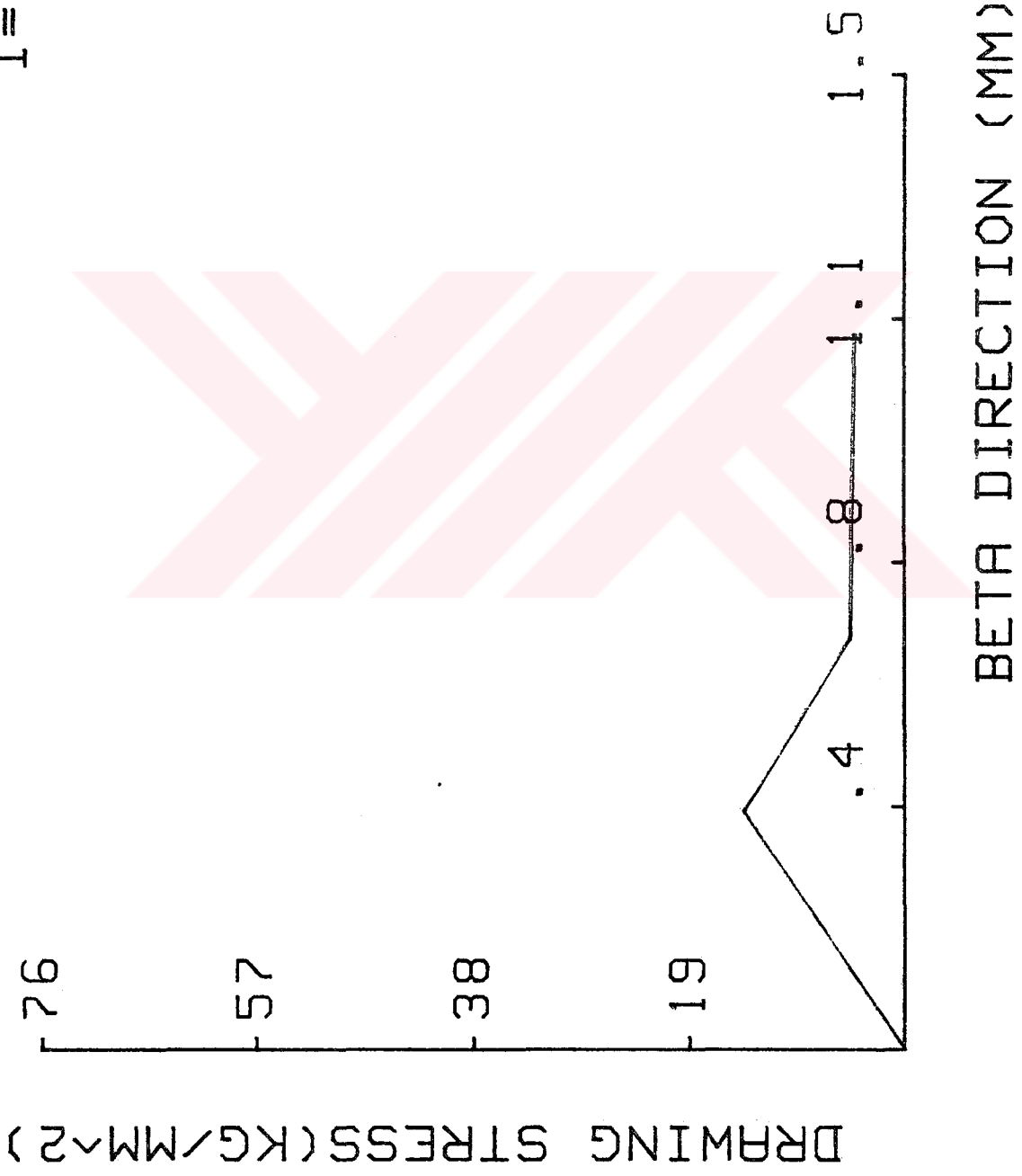


Figure.F.7. Variation of drawing stress along B-direction

I = 5

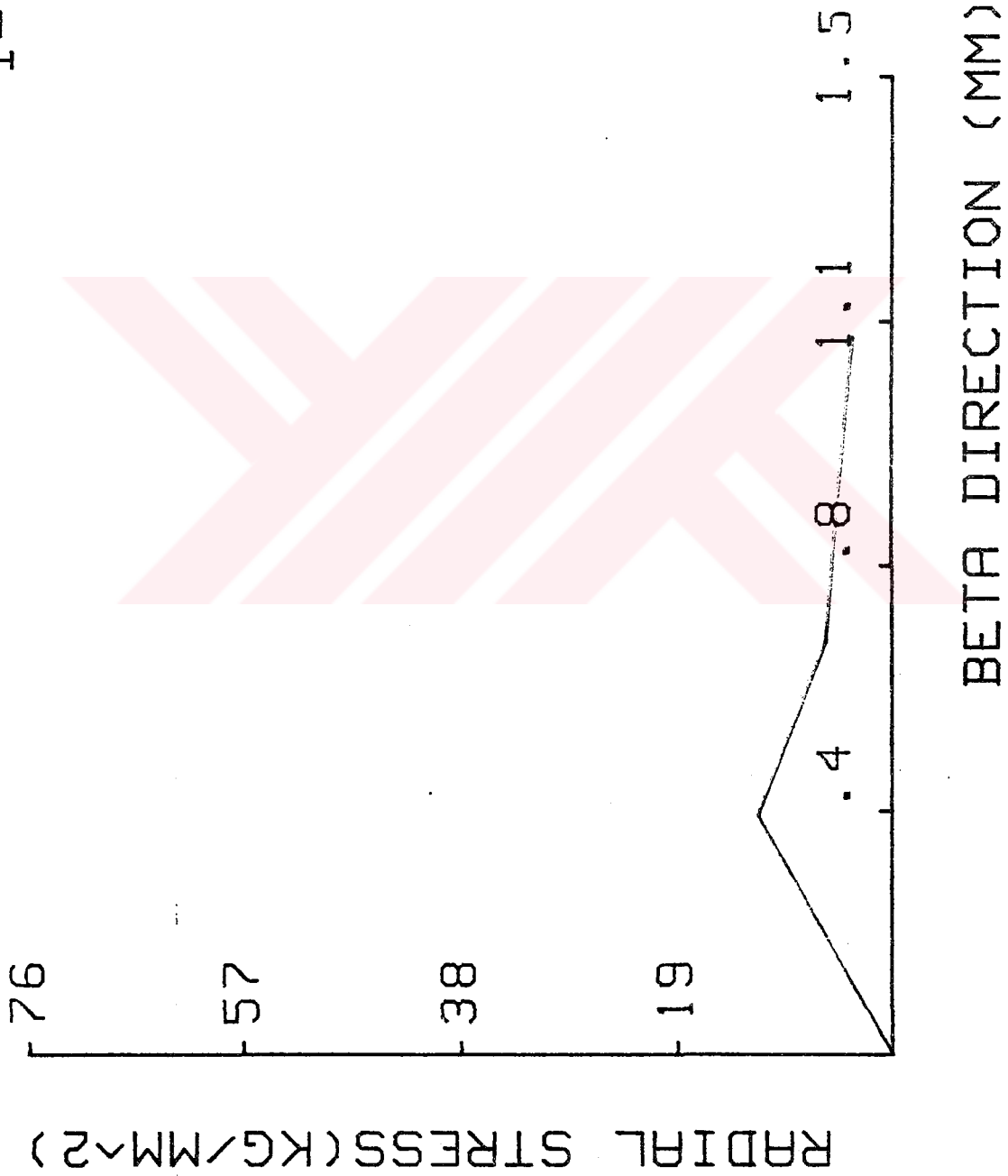


Figure.F.8. Variation of radial stress along B-direction

I = 5

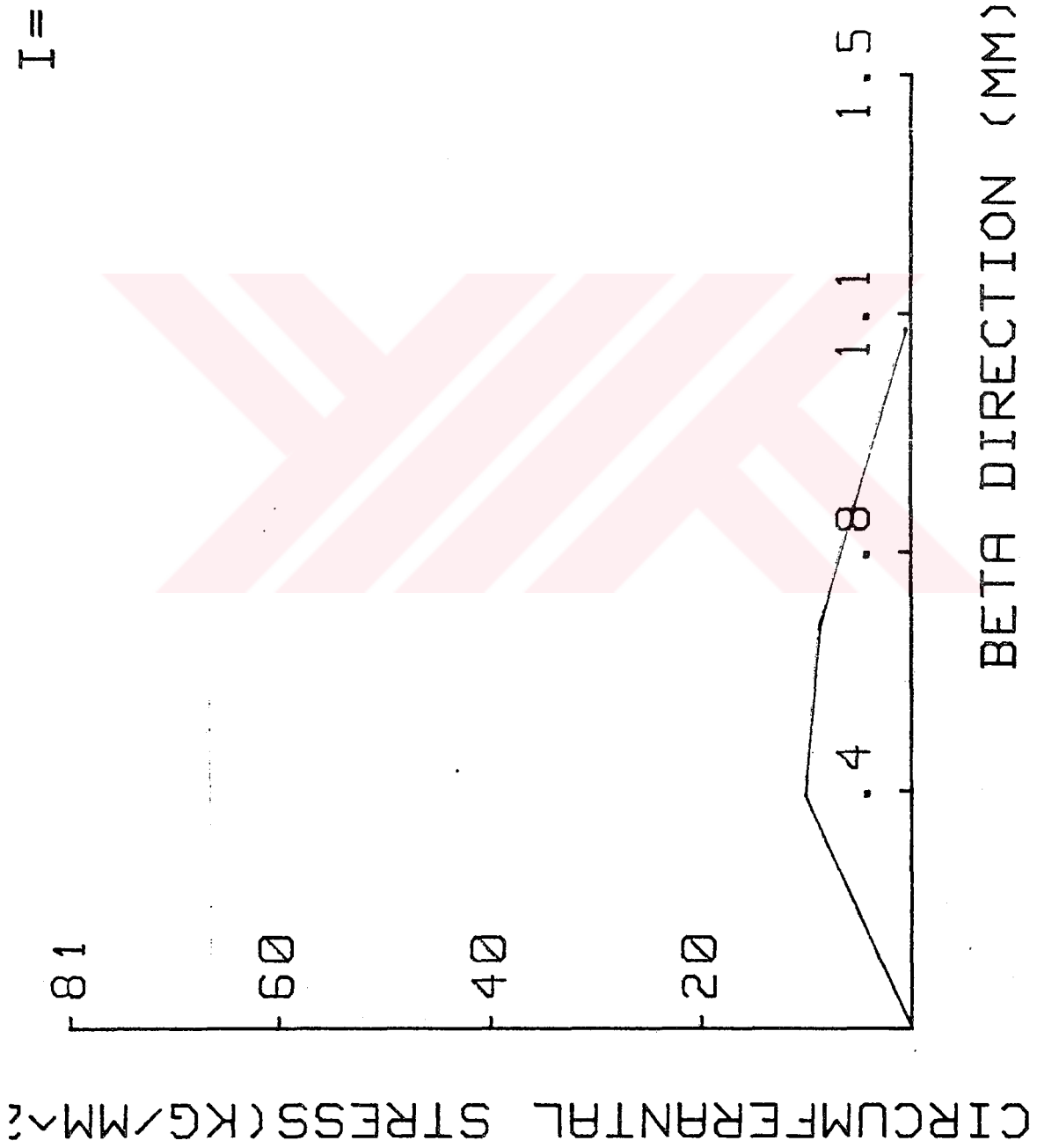


Figure.F.9. Variation of circumferential stress along β -direction

I = 5

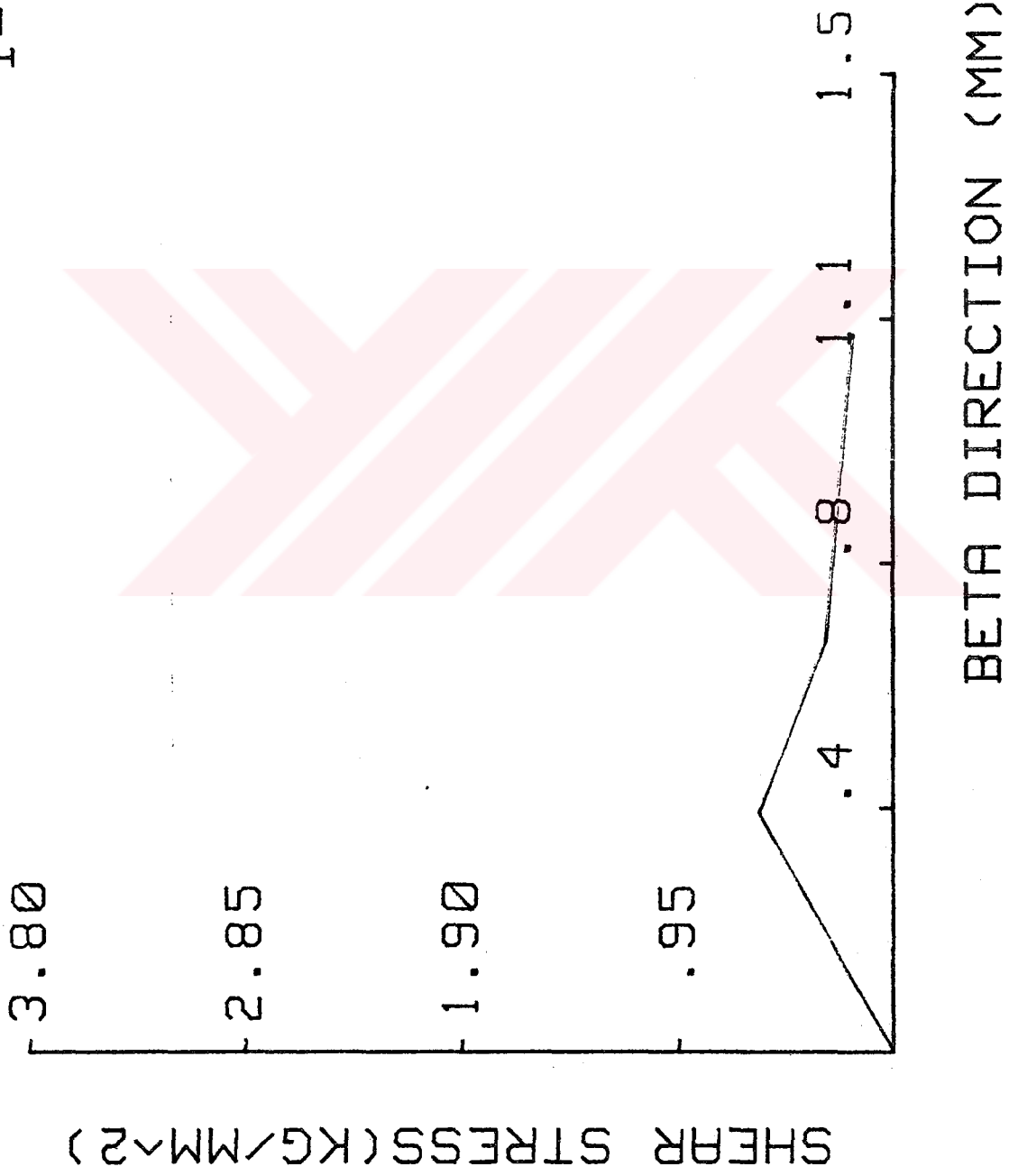


Figure.F.10. Variation of shear stress along B-direction.

J= 3

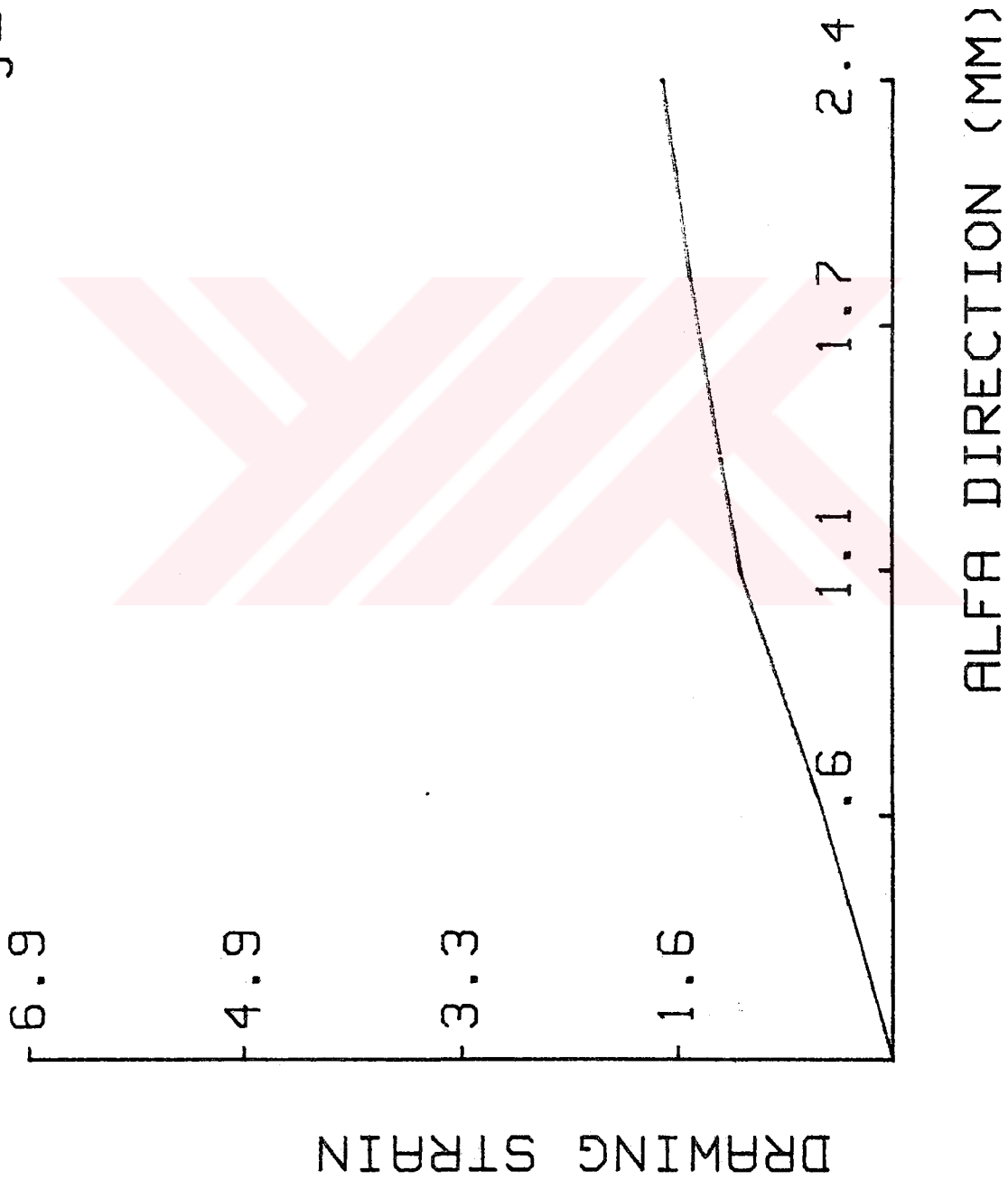


Figure.F.11. Variation of drawing strain along α -direction

J= 3



Figure.F.12. Variation of radial strain along α -direction

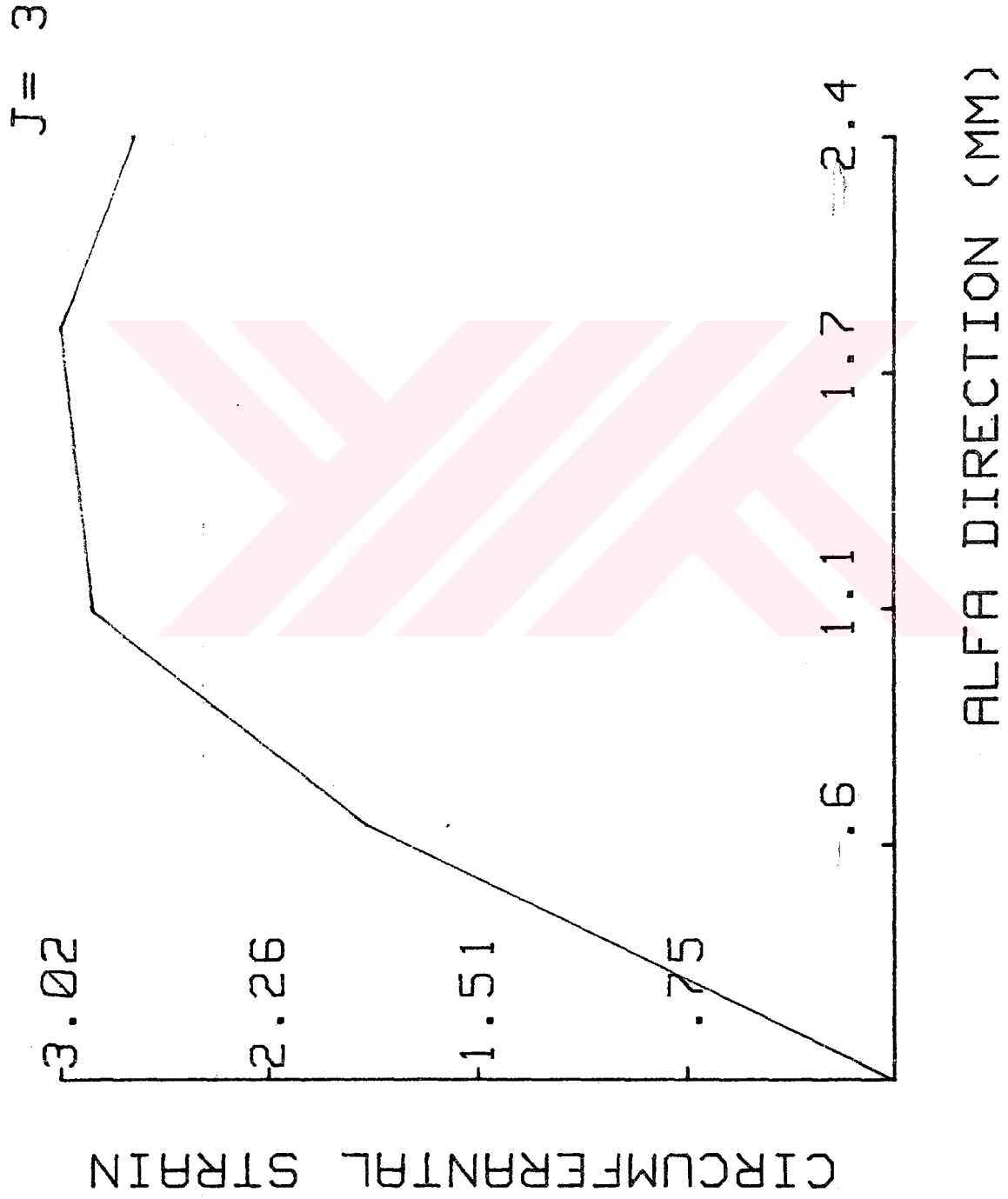


Figure.F.13. Variation of circumferential strain along α -direction

J= 2

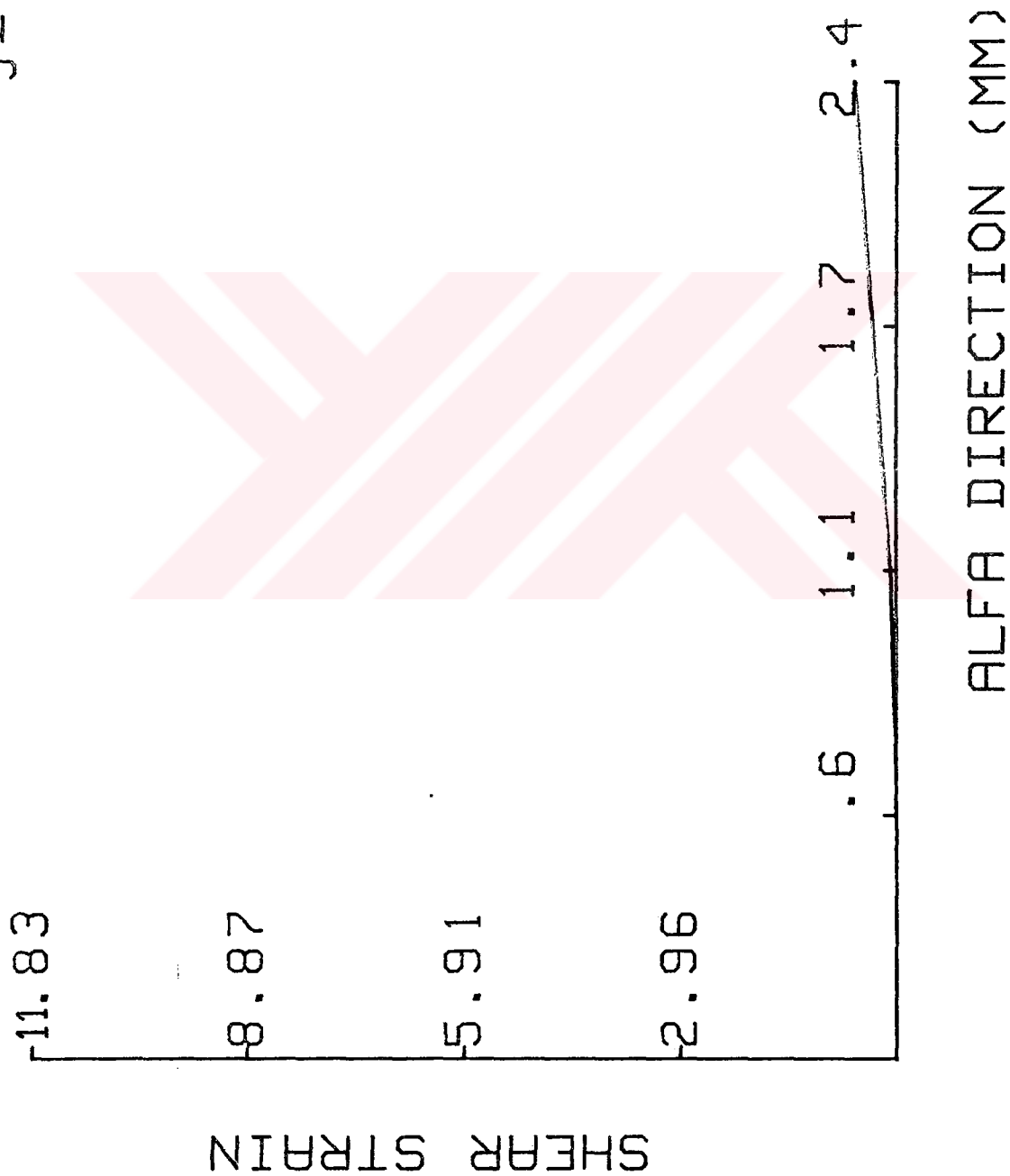


Figure.F.14. Variation of shear strain along α -direction

I = 5

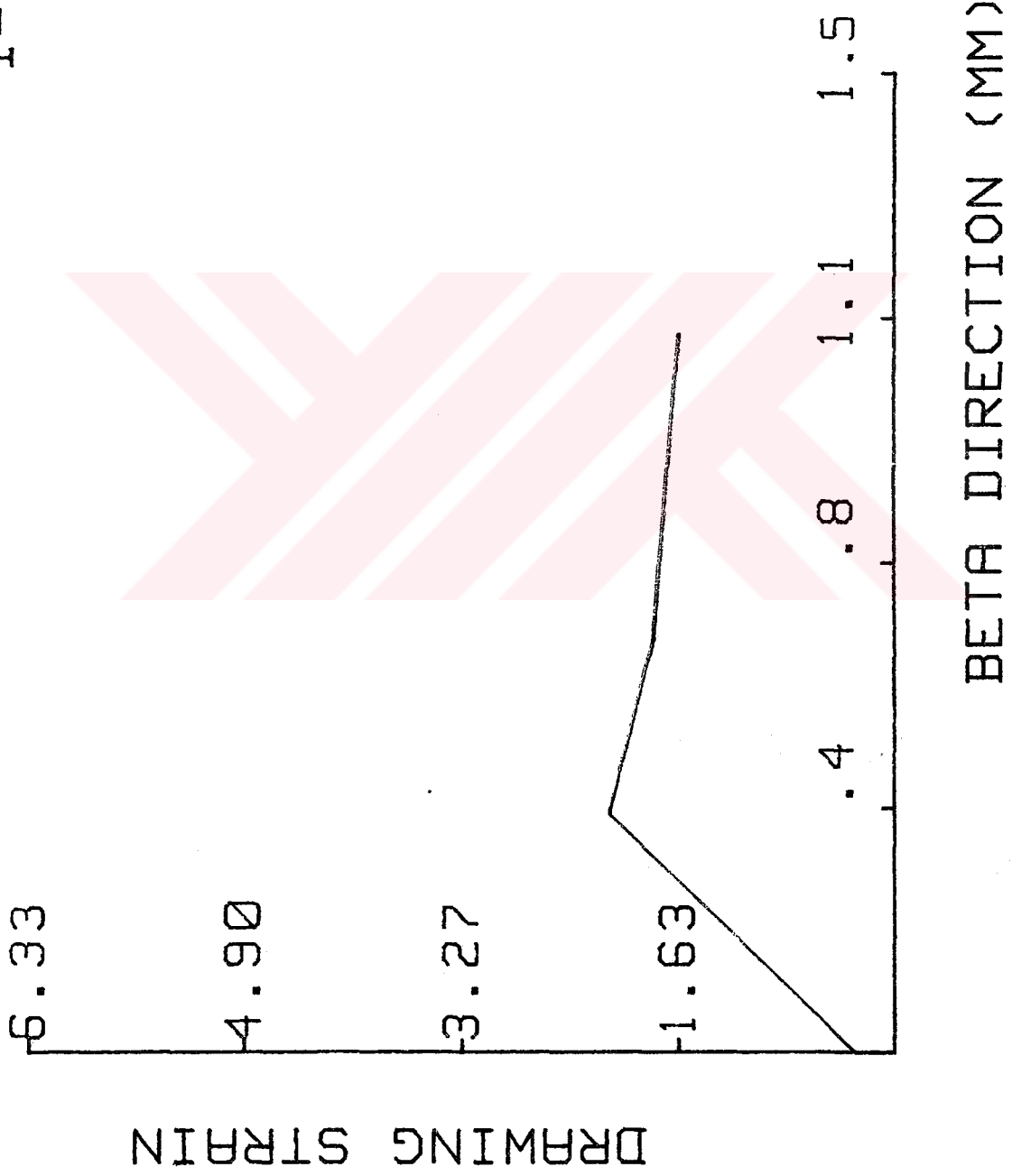


Figure.F.15. Variation of drawing strain along β -direction

I = 5

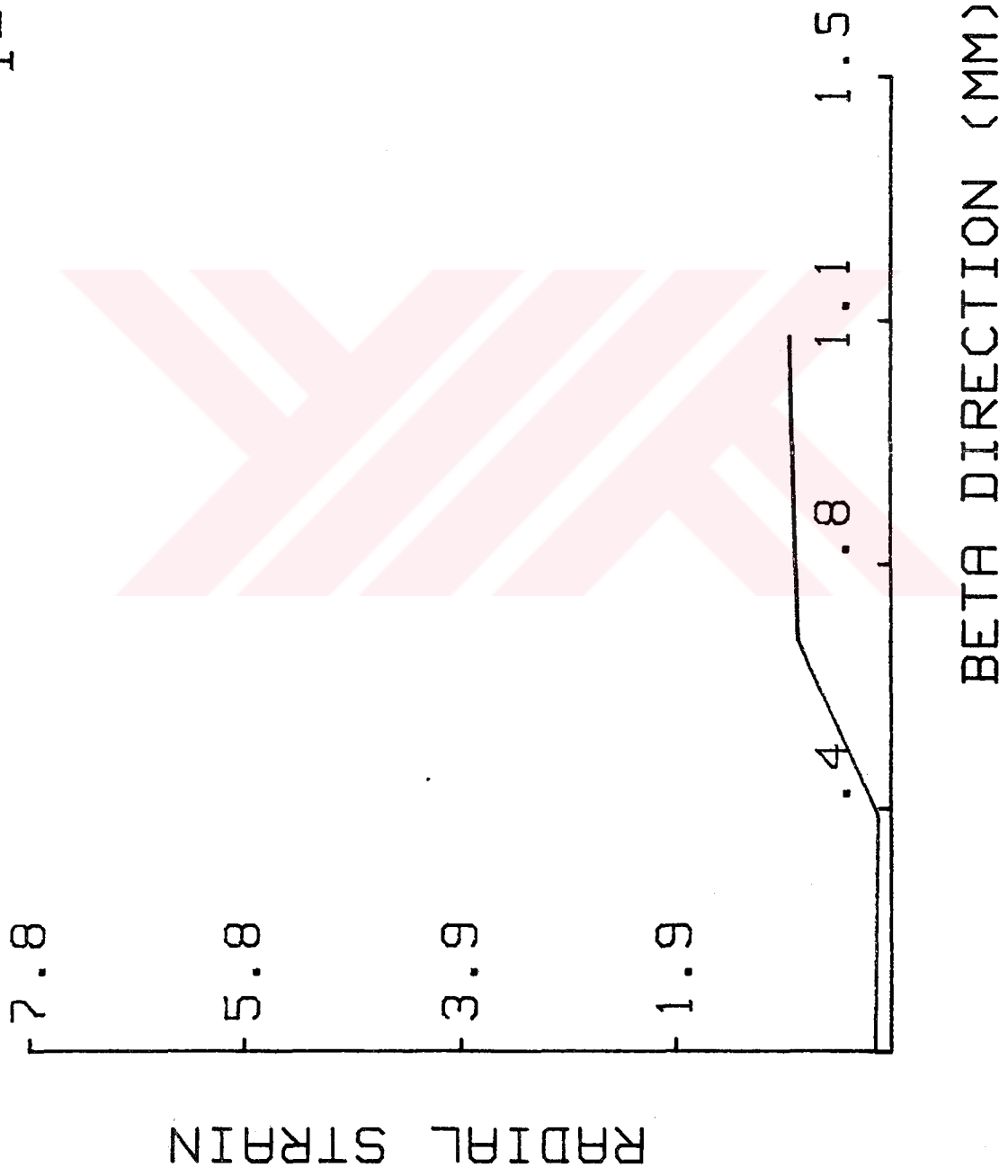


Figure.F.16. Variation of radial strain along β -direction

I = 5

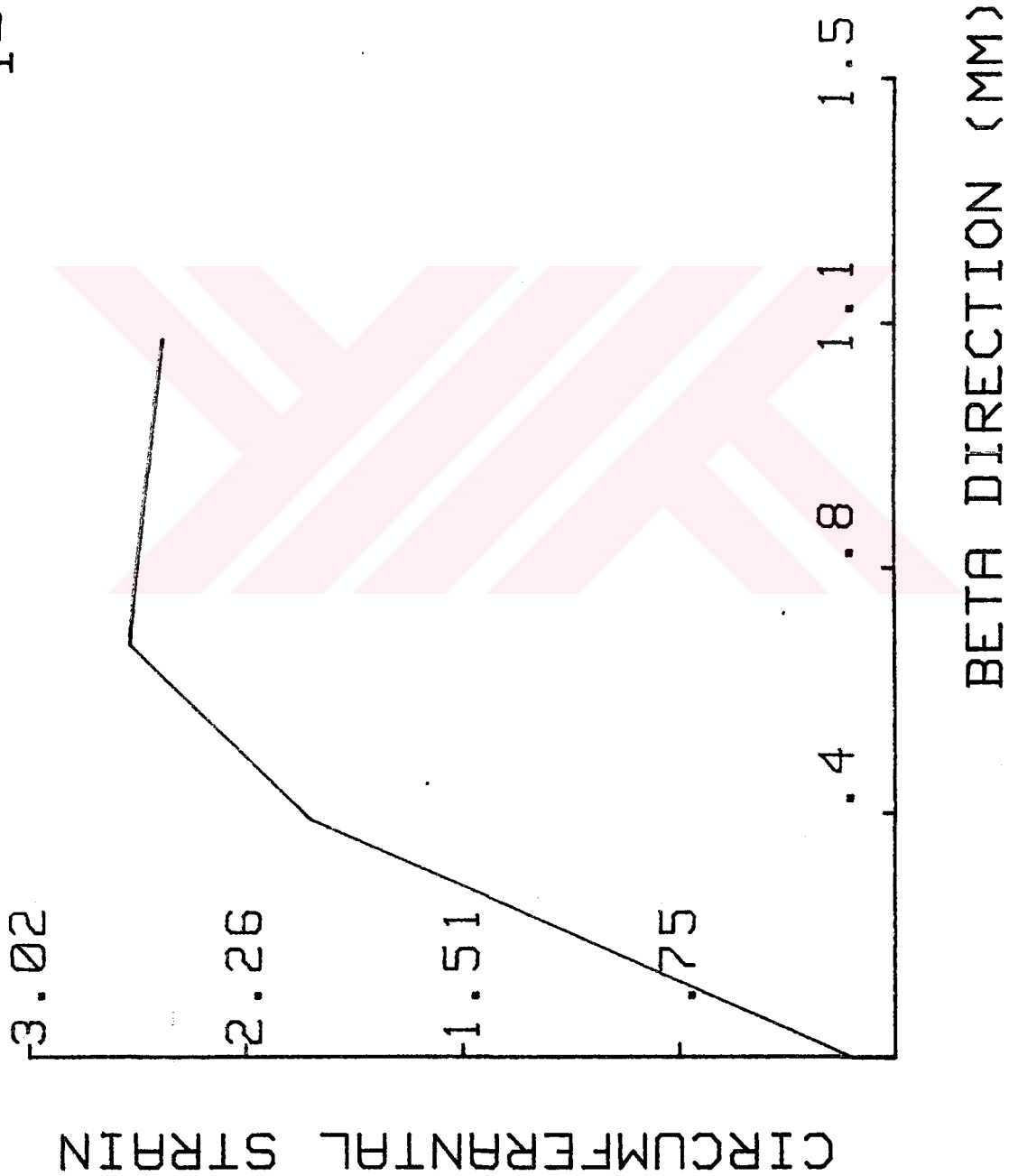


Figure.F.17. Variation of circumferential strain along β -direction

I = 5

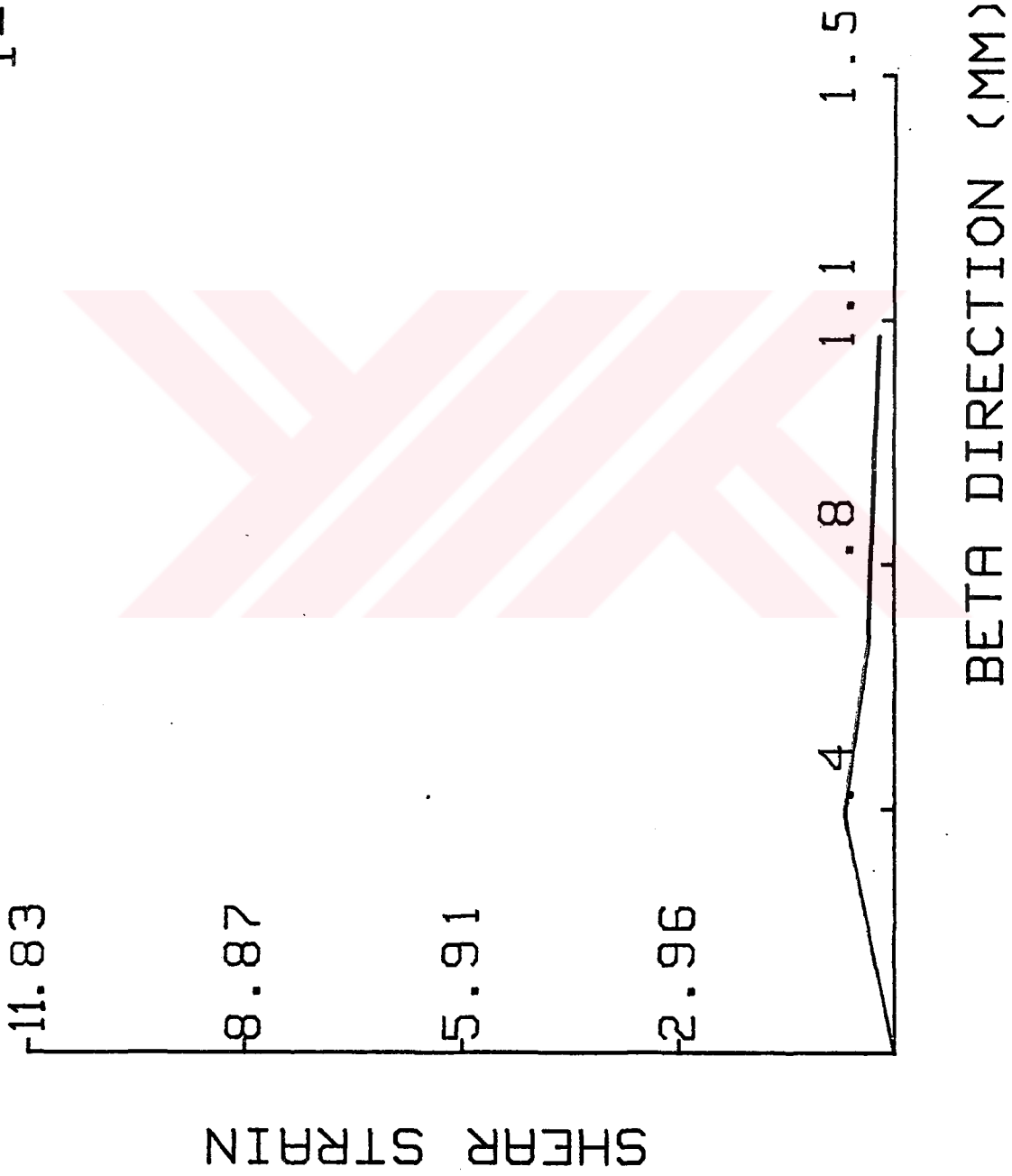


Figure.F.18. Variation of shear strain along B-direction

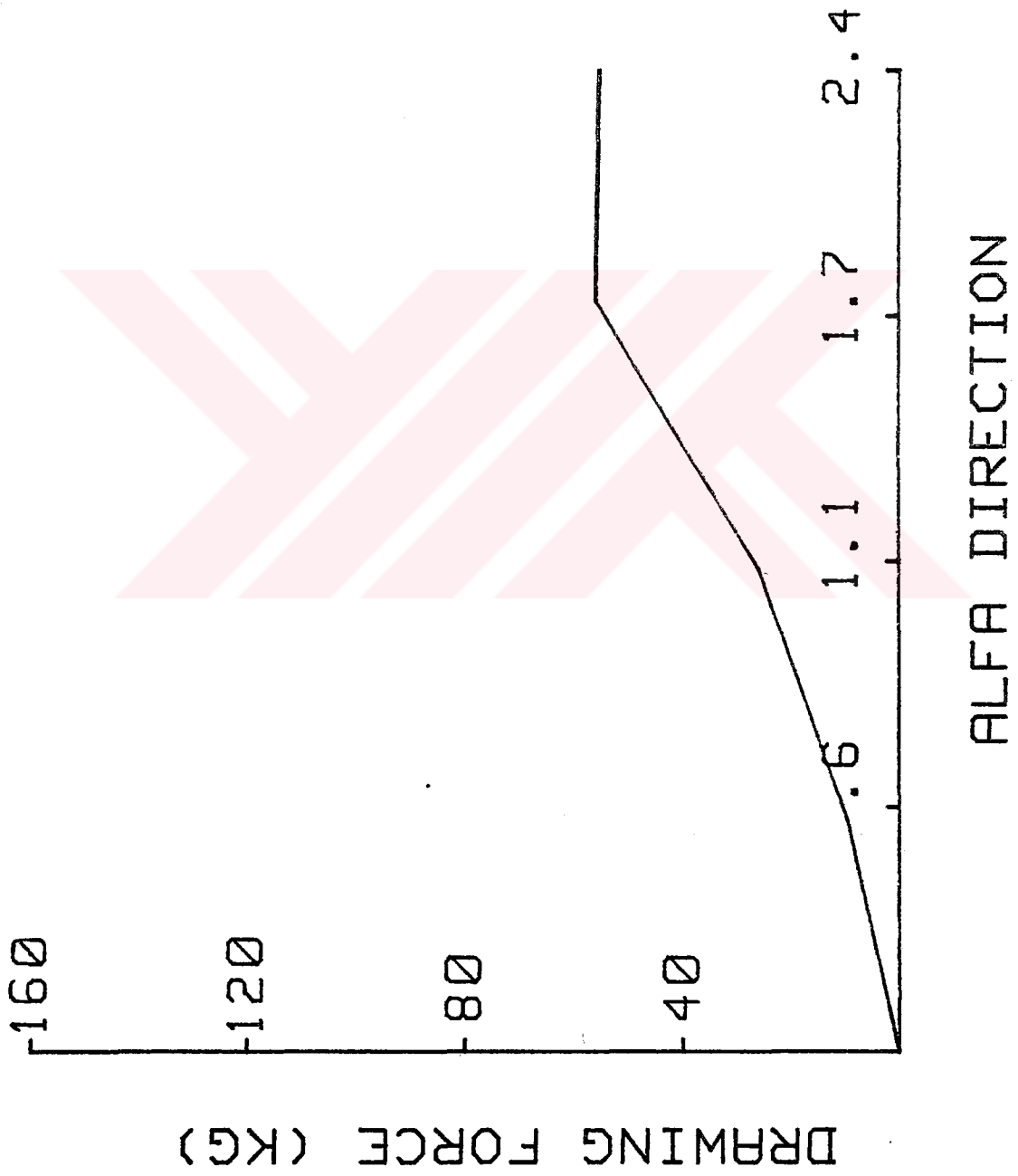


Figure.F.19. Variation of drawing force along α -direction

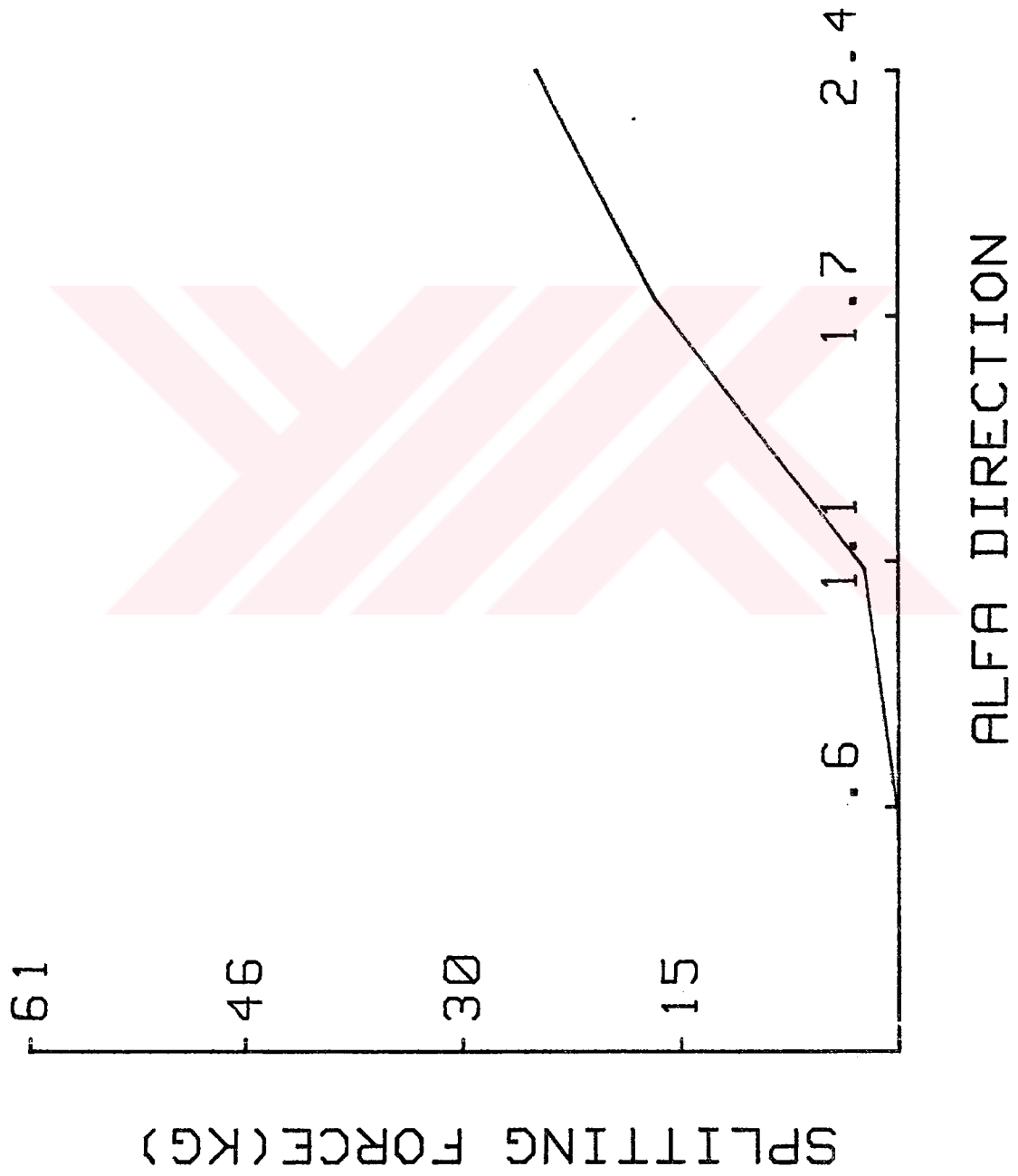


Figure.F.20. Variation of die splitting force along α -direction

Doc. No. 1000
Date: 10/10/2000
Page: 10/10